AD NUMBER

**AD476361**

LIMITATION CHANGES

TO:

**Approved for public release; distribution is unlimited.**

FROM:

**Distribution authorized to U.S. Gov't. agencies and their contractors;
Administrative/Operational Use; AUG 1960. Other requests shall be referred to Bureau of Ships, Washington, DC.**

AUTHORITY

**USNSSC notice 26 Mar 1970**

GENERAL ENGINEERING LABORATORY

# PROPELLER SHAFT THRUST BEARING ANALYSIS PHASE - II

BY

E. B. ARWAS

B. STERNLICHT

REPORT NO. 60GL181

AUGUST 1, 1960



GENERAL ELECTRIC

The information contained in this report has been prepared for use by the General Electric Company and its employees. No distribution should be made outside the Company except when indicated below:

# General Engineering Laboratory

PROPELLER SHAFT THRUST BEARING ANALYSIS - PHASE II

by

E. B. Arwas
B. Sternlicht

Report No. 60GL181

August 1, 1960

GENERAL ELECTRIC
SCHENECTADY, NEW YORK

# TABLE OF CONTENTS


| | |
|---|---|
| Table of Contents | (i) |
| Acknowledgements | (ii) |
| List of Figures | (iii) |
| Background and Scope | 1 |
| I - Introduction | 2 |
| II - Analysis and Method of Calculation | 4 |
| III - Results | 7 |
| IV - Design Charts | 8 |
| V - Discussion | 10 |
| VI - Summary and Principal Conclusions | 16 |
| VII - Recommendations | 18 |
| Appendix I - Method of Solution of the Elasticity Equation | 19 |
| Appendix II - Input Data | 28 |
| Appendix III - Estimate of Errors | 30 |
| References | 31 |
| Tables | |
| Figures | |
| Symbols | |

## ACKNOWLEDGEMENT

The procedure for numerical integration of the Elasticity Equation ( Appendix I of this report) is due to Mr. G. K. Carter (Electric Utility Analytical Engineering Operation, General Electric Company). Mr. Carter and Miss M. A. Havill (also of Electric Utility Analytical Engineering Operation) in addition programmed the numerical integration of the bearing equations and conducted the calculations reported here, using the I. B. M. 704 computer at David Taylor Model Basin.

The authors would also like to acknowledge the assistance of:

Mr. J. C. Reid, Jr. (Bureau of Ships) who furnished considerable technical guidance and assistance essential to the completion of this investigation.

Mr. L. J. Collins (Medium Steam Turbine, Generator and Gear Dept., General Electric Company) who helped and encouraged the performance of the investigation.

## LIST OF FIGURES


| Fig. No. | Caption |
|---|---|
| Text 1 | Average Temperature Chart |
| 2 | Maximum Temperature Chart - 6 pads; $h_{min}$ = 0.0014 in. |
| 3 | Maximum Temperature Chart - 6 pads; $h_{min}$ = 0.0010 in. |
| 4 | Maximum Temperature Chart - 6 pads; $h_{min}$ = 0.0005 in. |
| 5 | Maximum Temperature Chart - 8 pads; $h_{min}$ = 0.0014 in. |
| 6 | Maximum Temperature Chart - 8 pads; $h_{min}$ = 0.0010 in. |
| 7 | Maximum Temperature Chart - 8 pads; $h_{min}$ = 0.0005 in. |
| 8 | Maximum Temperature Chart -10 pads; $h_{min}$ = 0.0014 in. |
| 9 | Maximum Temperature Chart -10 pads; $h_{min}$ = 0.0010 in. |
| 10 | Maximum Temperature Chart -10 pads; $h_{min}$ = 0.0005 in. |
| 11 | Unit Loading Chart - 6 pads; $h_{min}$ = 0.0014 in. |
| 12 | Unit Loading Chart - 6 pads; $h_{min}$ = 0.0010 in. |
| 13 | Unit Loading Chart - 6 pads; $h_{min}$ = 0.0005 in. |
| 14 | Unit Loading Chart - 8 pads; $h_{min}$ = 0.0014 in. |
| 15 | Unit Loading Chart - 8 pads; $h_{min}$ = 0.0010 in. |
| 16 | Unit Loading Chart - 8 pads; $h_{min}$ = 0.0005 in. |
| 17 | Unit Loading Chart - 10 pads; $h_{min}$ = 0.0014 in. |
| 18 | Unit Loading Chart - 10 pads; $h_{min}$ = 0.0010 in. |
| 19 | Unit Loading Chart - 10 pads; $h_{min}$ = 0.0005 in. |
| 20 | Chart of Hydrodynamic Oil Flow - 6 pads |
| 21 | Chart of Hydrodynamic Oil Flow - 8 pads |
| 22 | Chart of Hydrodynamic Oil Flow -10 pads |
| 23 | Chart of Horsepower Loss - 6 pads |
| 24 | Chart of Horsepower Loss - 8 pads |
| 25 | Chart of Horsepower Loss -10 pads |

LIST OF FIGURES - Cont'd.


| | |
|---|---|
| 26 | Oil Temperature vs. Unit Loading |
| 27 | Influence of Groove Mixing Temperature |
| 28 | Comparison of Analytical Results - Minimum Film Thickness vs. Unit Loading |
| 29 | Comparison of Analytical Results - Maximum Temperature vs. Unit Loading |
| 30 | Contour Lines - Thermal Deflections Neglected. |
| 31 | Contour Lines - Thermal Deflections Included. |
| 32 | Influence of Pad Thickness |
| 33 | Influence of L/R Ratio |


Appendixes


| | |
|---|---|
| A-1 | Co-ordinate System |
| A-2 | Pad Geometry and dimensions of 31 in. O.D., 8 pad bearing |
| A-3 | Pad dimensions - 25 in. O.D. x12 1/2 in. I.D. - 6 pads |
| A-4 | Pad dimensions - 25 in. O.D. x12 1/2 in. I.D. - 8 pads |
| A-5 | Pad dimensions - 25 in. O.D. x12 1/2 in. I.D. -10 pads |
| A-6 | Pad dimensions - 31 in. O.D. x15 1/2 in. I.D. - 6 pads |
| A-7 | Pad dimensions - 31 in. O.D. x15 1/2 in. I.D. - 8 pads |
| A-8 | Pad dimensions - 31 in. O.D. x15 1/2 in. I.D. -10 pads |
| A-9 | Pad dimensions - 41 in. O.D. x20 1/2 in. I.D. - 6 pads |
| A-10 | Pad dimensions - 41 in. O.D. x20 1/2 in. I.D. - 8 pads |
| A-11 | Pad dimensions - 41 in. O.D. x20 1/2 in. I.D. -10 pads |
| A-12 | Pad dimensions - 50 in. O.D. x25 in. I.D. - 6 pads |
| A-13 | Pad dimensions - 50 in. O.D. x25 in. I.D. - 8 pads |
| A-14 | Pad dimensions - 50 in. O.D. x25 in. I.D. -10 pads |
| A-15 | Pad dimensions - 31 in. O.D. x16 1/2 in. I.D. - Ahead Bearing of DD 933 |
| A-16 | Pad dimensions - 26 in. O.D. x17 3/4 in. I.D. - Astern Bearing of DD 933 |

## LIST OF FIGURES - Cont'd.

A-17 Pad dimensions - 31 in. O.D. x 15 1/2 in. I.D. - 8 pads ($\frac{t}{t_{std}} = 0.7$)

A-18 Pad dimensions - 31 in. O.D. x 15 1/2 in. I.D. - 8 pads ($\frac{t}{t_{std}} = 1.3$)

A-19 Groove Temperature Vs. Unit Loading

A-20 Properties of 2190T Oil

## BACKGROUND AND SCOPE

In 1958 the General Engineering Laboratory made a study of propeller shaft thrust bearing operation and reported its findings in Reference 1. Following this study a comprehensive analytical and experimental program was undertaken, for the purpose of extending present understanding of these bearings and in order to provide a body of design information for use in bearing design and selection. This program, like the preceding introductory study, was performed under a contract awarded by the Bureau of Ships to General Electric Company's Medium Steam Turbine, Generator and Gear Department.

The program was divided into three phases as follows:

Phase I: Investigate analytically the performance of propeller shaft thrust bearings using the existing Reynolds-Energy Method of solution to provide data necessary in design and selection of these bearings.

This phase was completed and a final report on it was issued in May 1959.

Phase II: Extend existing analytical techniques for propeller shaft thrust bearings by including a numerical method of solution of the Elasticity Equation. Review, and where necessary, modify the design data obtained in Phase I, so as to include the effects of pad distortion caused by pressure distribution and thermal gradients.

This phase has also been completed and the following is our final report on it.

Phase III: Instrument thrust bearings on two U.S. Navy ships and obtain experimental data on the performance of these bearings. This data is to be obtained in tests carried out at the time of scheduled sea trials. The thrust bearing performance measurements obtained in these sea trials is to be used for correlation with the design data obtained analytically in Phases I and II.

Sea trials were made during 1959 on the U.S.S. Barry, and a final report on these tests is presently being prepared. The second ship for the sea trial tests has not yet been selected.

A fourth phase which included the building of a thrust bearing test stand was contemplated but was not included in the present program, since the findings of the program could be used to determine the features of the stand.

## I. INTRODUCTION:

The need for greater accuracy in predicting the performance of tilting pad thrust bearings was discussed in References 1 and 2. In Reference 2, various performance calculation methods were described and it was shown that the load capacity of thrust bearing pads is significantly influenced by their elastic deflections, particularly in the case of centrally pivoted pads. An approximate method of calculating the pad deflections and including them in the film shape equation was worked at in Reference 2 and it formed the basis of the design charts and other calculation results given there. While this method of calculation gave results that corresponded more closely with field evidence than did results obtained by previous methods, it suffered from several limitations the principal ones being:

1. Only deflections due to load were considered. No allowance was made for deflections due to thermal gradients.

2. The effects of cut-outs and ring supports were not considered. An average pad thickness was used in each calculation and point support was assumed.

3. It was assumed that initially flat, pivoted pads assume a spherically crowned shape under load, the magnitude of the crown being proportional to the load.

In the study which is reported here, a more complete analysis is made in which the elastic deflections of the pads are calculated from numerical solution of the Elasticity Equation. The above three limitations of Reference 2 are eliminated here. Deflections due both to load and to thermal gradients are calculated and, in each case, the actual pad geometry, including cut-outs and support ring is used in the computations. Finally, simple crowning of the pads is not assumed; instead, the more complex deflected shape of the pads is described by series expansions in r and $\theta$, whose coefficients are calculated in each case to satisfy the minimum energy principle.

The analysis and calculations described in this report had the following objectives:

1. To derive a general and accurate method for calculating the performance of tilting pad bearings of any geometry.

2. To calculate and plot design charts for bearings with standard geometry pads within the range of sizes and speeds used in today's marine main propulsion units.

3. To calculate the effect of varying (from the standard) several of the geometrical parameters of tilting pads. This serves, at least, to point out the direction in which these parameters should be changed in order to achieve more nearly optimum configurations.

To meet these objectives an IBM 704 digital computer program was written which allows simultaneous solution of the Reynolds, Energy and Elasticity Equations for sector shaped pads of arbitrary geometry. Since we are concerned with tilting pads, the program includes a section which calculates at each operating condition the circumferential and radial pad inclinations which satisfy moment equilibrium.

This program was then used to calculate several bearing configurations at a number of operating conditions, as follows:

1. Four bearings with standard geometry pads, scanning the size range 25" O.D. to 50" O.D. were analyzed at speeds up to 320 RPM. The results of these calculations were used to prepare the design charts.

2. The ahead and astern bearings of the DD 933 were analyzed to permit direct comparison of theoretical prediction with the field data obtained under Phase III. (Performance data obtained with instrumented thrust shoes, during the sea trials of the DD 933.)

3. As in Reference 2, the 31" O.D. bearing was selected to study the effect of varying bearing geometry and oil inlet temperatures. Calculations were made varying the following parameters one at a time:

    a.) Pad thickness

    b.) Groove temperature

    c.) Diameter ratio (O.D./I.D.)

    d.) Number of pads

4. In order to checkout the effect of the assumptions made in Reference 2, some additional calculations were made to evaluate the effects of thermal distortion of the pads and of the ring support and of the cut-outs in the pads.

In the succeeding sections of this report the method of analysis and the calculation results are presented and discussed.

## II. ANALYSIS AND METHOD OF CALCULATION

The following assumptions are made in the analysis:

1. Steady state conditions prevail in the film.
2. Lubricant is Newtonian and incompressible.
3. Flow in clearance spaces is laminar and adiabatic.
4. Lubricant inertia forces are neglected.
5. Pressure and shear effects on viscosity are neglected.
6. Variations of the specific heat of the lubricant with pressure and temperature are neglected.

When the first four assumptions listed above are valid, the hydrodynamic pressures (which are generated in the fluid film that separates the bearing pads from the runner) may be calculated by integrating Equation 1 (Reynolds Equation):

$$\frac{\partial}{\partial r}\left(\frac{rh^3}{\mu}\frac{\partial p}{\partial r}\right) + \frac{\partial}{\partial \theta}\left(\frac{h^3}{\mu r}\frac{\partial p}{\partial \theta}\right) = 6\omega r \frac{\partial h}{\partial \theta} \qquad (1)$$

In order to integrate Eq. (1) for any given geometry and speed, the viscosity and film thickness need to be known as functions of position. For petroleum oil, in the range of present day thrust bearing practice, shear and pressure effects on viscosity are very small (Ref. 3). The local viscosity values are then functions only of the local film temperatures and the viscosity-temperature characteristics of the oil. In the present analysis, adiabatic conditions are assumed and the temperature distribution is obtained by integrating Eq. 2 (Energy Equation, Ref. 4) simultaneously with Eq. 1.

$$\frac{\mu}{h}(\omega r)^2 + \frac{h^3}{12\mu}\left[\left(\frac{\partial p}{r\partial \theta}\right)^2 + \left(\frac{\partial p}{\partial r}\right)^2\right] - C_p \rho g J \left[\left(\frac{r\omega h}{2} - \frac{h^3}{12\mu}\frac{\partial p}{r\partial \theta}\right)\frac{\partial T}{r\partial \theta} - \frac{h^3}{12\mu}\frac{\partial p}{\partial r}\frac{\partial T}{\partial r}\right] = 0 \qquad (2)$$

The film shape, for pivoted pads, is determined by the tilt of the pads, radially and circumferentially and by the deflections which result from the hydrodynamic pressures over the pads and the temperature gradients across the pads. In the present analysis, the pad deflections are calculated from the

integration of Eq. 3 (Elasticity Equation, Refs. 5 and 6).

$$\nabla^2 ( \nabla^2 w) = \frac{12(1 - \nu^2)p}{Et^3} + \frac{(1 + \nu)}{t} \nabla^2 ( \alpha \Delta T)$$

$$\text{where: } \nabla^2 = \left( \frac{\partial^2}{\partial r^2} + \frac{1}{r} \frac{\partial}{\partial r} + \frac{1}{r^2} \frac{\partial^2}{\partial \theta^2} \right) \tag{3}$$

Eq. (3) is integrated for both the pad and support plate. Local values of pad thickness are used so that the effects of changes in geometry are considered.

The boundary conditions used with the above equations are:

a.) Pressures fall to zero around the pad perimeter.

b.) Pad inlet oil is at groove mixing temperature.

c.) Radial temperature gradients are zero along the inner and outer circumferences of the pads, because of the cooling effect of the surrounding oil.

d.) Shear and bending moments are zero around the pad perimeter.

Since pad deformations under high loads may produce diverging film thicknesses (and hence breakdown of the film) near the trailing edges of the pads, an additional condition is imposed. This states that the hydrodynamic pressures over the pads are nowhere smaller than atmospheric.

The above three equations are integrated simultaneously, using numerical methods and an iterative procedure. Finite differences are used for the integration of the Reynolds and Energy Equations, as described in Refs. 7 and 8. The Elasticity Equation is integrated using the minimum energy principle, as described in Appendix 1.

The iterative procedure used for the simultaneous solution of the equations is, briefly, as follows:

1. For a given geometry, speed and minimum film thickness, integrate the Reynolds and Energy Equations, using a preliminary estimate of the deflections. This integration is carried out (as described in Refs. 7 and 8 ) and the pad inclinations are obtained as those values which yield a pressure profile whose center of pressure passes through the axis of the pivot.
2. The Elasticity Equation is then integrated for the pressure and temperature profiles obtained in step 1.

3. Reynolds and Energy Equations are integrated once again, but this time for a pad which has the elastic deflections calculated in step 2.

The above procedure is repeated until the differences between two successive iterations fall within a specified small limit.

From the final values of the film thickness, pressure and temperature profiles obtained as described above, the remaining items of interest such as total load carried on the pads, oil flow and horsepower loss are calculated in the same manner as in Ref. 2. The input data necessary for the calculations described in Appendix 2. The estimated accuracy of the calculations is discussed in Appendix 3.

## III. RESULTS

The method of Analysis outlined in the previous section was used to determine thrust bearing performance in the range of sizes, speeds and configuration outlined in the introduction to this report. The cases calculated are listed in Table I and the results are summarized in Tables II through XVII.

## IV. Design Charts

The results of the calculations made for the bearings with standard geometry pads (Tables II through V) were plotted as a set of design charts for ready use.

The average film temperature was found from the calculation results to be independent of size and speed. It is plotted versus unit load in Figure 1.

The maximum film temperature is plotted versus speed in Figures 2 through 10, for the investigated range of bearing sizes. Separate charts were made for 6, 8 and 10 pad bearings and at three values of the minimum film thickness (0.0014 in., 0.0010 in. and 0.0005 in.).

The unit loading is similarly plotted versus speed in Figures 11 through 19, for the range of bearing sizes. Once again, separate charts have been made for 6, 8, and 10 pad bearings and for the same three values of the minimum film thickness (0.0014 in., 0.0010 in., 0.0005 in.).

The hydrodynamic oil flow and the horsepower loss in the fluid film are plotted in dimensionless form in Figures 20 through 22 and 23 through 25 respectively. Separate charts are again given for 6, 8, and 10 pad bearings.

The use of the charts is illustrated in the following examples:

Example: Calculate the minimum film thickness, maximum film temperature, hydrodynamic oil flow and the fluid film horsepower loss in a 43 in. O.D. x 21 1/2 in. I.D., 8 pad thrust bearing running at 280 RPM and carrying a unit load of 610 psi.

$P_{avg}$ at $h_{min}$ = 0.0014 in. (per Figure 14) 507 psi

$P_{avg}$ at $h_{min}$ = 0.0010 in. (per Figure 15) 665 psi

| | |
|---|---|
| $p_{avg}$ at $h_{min}$ = 0.0005 in. (per Figure 16) | 848 psi |
| $p_{avg}$ at $h_{min}$ = 610 psi (by interpolation) | 0.00114 in. |
| $T_{max}$ at $h_{min}$ = 0.0014 in. (per Figure 5) | 199°F |
| $T_{max}$ at $h_{min}$ = 0.0010 in. (per Figure 6) | 223°F |
| $T_{max}$ at $h_{min}$ = 0.0005 in. (per Figure 7) | 286°F |
| $T_{max}$ at $h_{min}$ = 0.00114 in. (by interpolation) | 214°F |
| $T_{avg}$ at 610 psi (per Figure 1) | 175°F |
| $\mu_{avg}$ at $T_{avg}$ = 175°F (per Figure A-20) | $2.2 \times 10^{-6}$ lb sec/in$^2$ |
| $U_{avg} = \pi (D-L) N$ = | 473 in/sec |
| $B_{avg} = 1/2 (D-L) \theta_{TOT}$ = | 10.77 in. |
| $\frac{\mu_{avg} U_{avg}}{p_{avg} B_{avg}}$ = | $0.158 \times 10^{-6}$ |
| $\frac{Q}{B_{avg} L U_{avg}}$ (per Figure 21) | $30.0 \times 10^{-6}$ |
| Q per pad | 1.64 G.P.M. |
| $Q_{Total}$ | 13.1 G.P.M. |
| $\frac{6600 HP}{B_{avg} L p_{avg} U_{avg}}$ (per Figure 24) | $1.0 \times 10^{-3}$ |
| H. P. per pad | 5.06 H. P. |
| H. P. Total | 40.5 H. P. |

## V. Discussion

The two limiting criteria of thrust bearing performance are the maximum film temperature and the minimum film thickness. Generally, however, the main emphasis in the literature, as well as in design practice, has been on film thickness with little attention devoted to maximum temperature. This is because isothermal bearing analysis was used almost exclusively in the past. The results of the more complete study described in this report, in which the effects of temperature ( and hence viscosity) variations in the film and of the elastic deflections of the pads induced by the thermal gradients were both included, has convinced the authors that maximum temperature is the governing limitation on bearing performance. Thus, the design charts of the previous section were prepared so that both maximum film temperature and minimum film thickness can be readily obtained for any operating point within the range studied. In the subsequent discussion we will attempt to show the importance of temperature in determining thrust bearing performance. It will also be shown that when the film and groove temperatures are known, either analytically or experimentally, the minimum film thickness also is automatically defined.

### 1. Maximum and Average Temperatures

To illustrate the large temperature variation in the film, consider a 31 in. O.D. thrust bearing whose pad dimensions are given in Figure A-2. The performance data for this bearing are given in Table III and the temperature data has been summarized on Figure 26. This figure shows that while the average film temperature and the average pad outlet temperatures are comparable, they are considerably below the maximum film temperature, particularly at high loads. In addition note that the slope of the maximum film temperature increases with load. It is clear therefore that:

(a) The bearing oil drain temperature, which is often used to monitor the condition of a bearing, is in fact a very poor indicator of impending bearing failure.

b.) With a heavily loaded bearing, even a moderate increase in load may raise the maximum temperature to a dangerous level.

2. Influence of Groove Temperature

A key point of this report is brought out in Figure 27, which shows the relation between the minimum film thickness and the maximum temperature, for a range of groove temperatures and unit loads. This figure shows that for the given bearing geometry and speed, the maximum temperature can be used to predict the minimum film thickness with an accuracy of better than $\pm 0.0001$ in. If, in addition, the groove temperature is also known, then the minimum film thickness can be predicted even more closely. Thus, maximum temperature can be employed to measure minimum film thickness. This is quite significant for such temperature measurements are, in general, much easier to make than direct measurements of film thickness with presently available indicators. Also, based on the above, their potential accuracy in determining minimum film thickness appear to be superior to presently available, direct indicators of film thickness.

Fig. 27 also shows the very important influence of groove temperature on bearing performance. To illustrate this point note the gain that can be achieved by a 30°F reduction in groove temperature when the bearing is operating under 700 psi load (data from Fig. 27):

| $p_{avg}$ -psi | $T_{GR}$ - °F | $h_{min}$ - in | $T_{max}$ - °F |
|---|---|---|---|
| 700 | 160 | 0.00063 | 240 |
| 700 | 130 | 0.00093 | 197 |

3. Influence of Thermal Distortion

The influence of thermal distortion of the pads on bearing performance is shown in Figs. 28 and 29. In these figures, the minimum film thickness and maximum temperature are plotted versus unit load from the results obtained using three methods of analysis:

a.) Present analysis - complete solution, including the thermal distortion.

b.) Present analysis, but neglecting thermal distortion.

c.) Simplified analysis of Ref. 2 (In this method thermal deflections were neglected and it was assumed that the pads deform to a spherical shape under load. Using a simplified representation of the pads, the radius of curvature of the deformed pad ($R_c$), was related to the load (W), the average pad thickness (t) and the modulus (E) by the expression:

$R_c = \frac{2.23\ Et^3}{W}$ .)

The calculations were made in all three cases for the following pad geometry and operating conditions:

R = 15.5in.

L = 6.75 in.

t = 2.2 in. (uniform thickness)

N = 5.33 rps

Oil = 2190 T

$T_{GR}$ = per plot of groove mixing temperature in Fig. A-20.

Note in Figures 28 and 29 that at least at loads up to 600 psi, the results obtained using the simplified analysis of Ref. 2, were reasonably close to those obtained using the present analysis, but neglecting thermal distortion. When, however, thermal distortion is introduced in the analysis, the situation is drastically different at high loads. Thus, at unit loads greater than 600 psi the complete analysis, including thermal deformations, predicts much smaller minimum film thickness and higher maximum temperatures. Thermal distortions are thus seen to have a major effect on bearing performance and must be included when designing bearings to operate under high unit loads.

Figure 30 shows the film thickness contour lines, at a minimum film thickness of 0.0004 in. where thermal distortions are neglected. Figure 31 shows the contour lines for the same minimum film thickness, but with the thermal distortions included. Note from these figures that:

a.) The pad deformations are several times the minimum film thickness

b.) The thermal deflections are of the same order as those directly due to the hydrodynamic pressures.

These figures underline again the importance of elasticity in pivoted pad thrust bearing analysis and the need to include the effects of thermal distortions in such analysis.

4. Influence of Geometric Parameters

Figures 32 and 33 show, respectively, the influence of pad thickness and $\frac{L}{R}$ ratio on bearing performance (In Figure 32, the designation "standard pad" refers to the pad shown in Figure A-2).

Note from Figure 32 that at 600 psi (which is on the high side of the range of unit loadings for thrust bearings in marine use) the curves are relatively flat, showing that thickness changes will not much effect bearing performance. When, however, operation under higher loads is required, pad thickness is seen to have a greater effect. Thus, for a bearing which is required to carry 800 psi, Figure 32 shows that a 30% increase in pad thickness would achieve a substantial increase in minimum film thickness and an even more important reduction in maximum temperature

Figure 33 shows that there is an optimum $\frac{L}{R}$ ratio, both from the standpoints of maximum temperature and minimum film thickness. While the optimum $\frac{L}{R}$ ratio varies to some extent with load, it is in the neighborhood of 0.5 within the range of loads studied.

5. Comparison with Rigid Pad

Thus far the discussion has been limited to centrally pivoted pads which deform elastically under load, and because of the thermal gradients generated by the shear losses. The negative effects of large deformations which occur under high loads was pointed out. It must, however, be remembered that, particularly for the case of centrally pivoted pads, some deformation is desirable for adequate load capacity. The reason for this is that, in order to satisfy equilibrium of moments, the resultant of the hydrodynamic pressures must pass through the pivot. Thus, for the case of centrally pivoted pads, the pressure profiles should be nearly symmetrical about the radial centerline. This condition is achieved when the active faces of the pads exhibit a slight convexity. Because of the deflections, pivoted pads will automatically achieve this convexity when run under load.

In the case of flat rigid pads, it is generally desirable to have an off-center pivot, so that the non-symmetrical pressure profiles, associated with flat inclined sliders can be achieved. A centrally pivoted, rigid, flat pad, on the other hand, must rely on the viscosity variations over its length, to allow generation of hydrodynamic pressure which satisfy moment equilibrium.

The tabulation on the next page compares, at one operating point, the unit loads and maximum temperatures for an elastic centrally pivoted pad with those for a rigid pad with optimum pivot and with a central pivot. Note that the unit loads carried by the elastic pad and by the flat, rigid pad with optimum pivot are comparable, whereas that carried by the flat, rigid, centrally pivoted pad is much smaller.

## Comparison of Rigid and Elastic Pads

$R = 15.5$ in.

$L = 7.75$ in.

$\theta_T = 38.25^\circ$

$N = 5.33$ rps

$T_{GR} = 130^\circ F$

$h_{min} = 0.001$ in.

oil = 2190 T

| Type of Pad | Unit Loading (psi) | Max. Film Temp. ($^\circ F$) |
|---|---|---|
| Rigid flat pad with optimum pivot ($r_p\% = 51$; $\theta_p\% = 61$) | 660 | 179 |
| Rigid flat pad, centrally pivoted. ($r_p\% = 51$; $\theta_p\% = 50$) | 370 | 204 |
| Elastic, initially flat pad, centrally pivoted (thickness and pivot location per Fig. A-2) | 642 | 194 |

## VI. Summary and Principal Conclusions

A method of thrust bearing analysis was given which includes the effects of temperature variations and elastic deflections induced by load and thermal gradients. Calculations were made using this method of analysis, for a wide range of speeds, loads and bearing configurations. Using the calculation results, a set of design charts were prepared for standard geometry bearings in the size and speed ranges of present day marine practice. Film temperature was shown to be a major limiting factor of bearing performance both because of reduced oil viscosity and thermal distortion of the pads.

The writers feel that the following are the three principal conclusions of the study:

1. Elastic deflections of the pads are several times the minimum film thickness. Thermal deflections are of the same order as those due directly to the hydrodynamic pressure loading. These deflections seriously affect the performance of the bearing and must be included in the analysis. Analysis which neglects pad elasticity and the effects of thermal gradients gives an erroneous and optimistic picture of thrust bearing operation at high loads. For operation under high loads, improvement in performance can be gained by minimizing deflections and by lowering the groove mixing temperature.

2. The maximum temperature reached in the film is drastically different from both the average film temperature and the average drain temperature. The slope of the maximum temperature vs. unit load curve rises very sharply at high loads. Highly loaded bearings of conventional design have, therefore, little margin of safety for overload conditions.

3. Accurate determination of the minimum film thickness in a bearing can theoretically be made by temperature measurements alone. It is desirable for this purpose to measure both the maximum film temperature and the groove temperature. This method offers greater accuracy than present direct film thickness indicators.

## VII. Recommendations:

The authors feel that future thrust bearing investigations should be aimed at:

1. Modification of the Energy Equation, to include heat conduction.
2. Analysis of thrust bearings under transient conditions in the fluid film.
3. Analysis of thrust bearings under turbulent conditions in the fluid film.
4. Meticulous and well instrumented experimental study of tilting pad thrust bearing performance. It is realized that such experimental work would undoubtedly be both difficult and expensive. It is, however, essential in order to test the validity of analytical work and present understanding of bearing performance.
5. Utilize the analytical and experimental results to optimize the dimensions of bearing designs in present use and to generate new designs capable of much improved load carrying capacity.

# APPENDIX I

## Method of Solution of Elasticity Equation

### 1. Assumed Conditions

Aside from the usual assumptions of elasticity theory, the following have been used in the numerical solution of Eq. 3:

a. Only deflection due to bending is considered; the contributions due to shear deformation and to membrane and crushing stresses are omitted.

b. The support plate, or button, is circular, of uniform thickness, and at uniform temperature.

c. The support point is at the center of the support plate.

d. Load is transmitted between the support plate and the sector pad through line contact around the outer edge of the plate; the two parts are in contact around the entire circumference.

e. No moment is transmitted through the plate-to-pad joint.

f. Sharp discontinuities in the pad thickness are averaged out over finite area subdivisions; and local stress concentrations are ignored.

g. Temperature of the bottom of the pad is assumed to vary linearly with radial and circumferential locations.

h. Temperature of the top of the pad is assumed the same as the lubricant film temperature.

i. No attempt is made to consider actual heat flow distribution; the temperature, in effect, is assumed to act as if it varies linearly through the pad thickness at every point.

### 2. Coordinate Systems

The three sets of coordinates used are shown in Fig. A-1. Axis-of-rotation coordinates ( $r$ , $\theta_c$) are used for subdividing the pad and for calculations based on these subdivisions, including all integrations over the pad surface and boundary. Point-of-support coordinates ($r_c$, $\Phi_c$) are used for description of the deformation modes of both the pad and the support plate. Rectangular coordinates (X, Y) are used for load moment and center of pressure eccentricity calculations. The location of the support point ($r_p$, $\theta_p$), the circle of contact between pad and support plate ($r_c = r_o$), and the boundary coordinates of the pad are also shown.

3. Energy of Bending

The selection of deformation mode functions is critical; it was made in this case with consideration of the symmetry of the support pad and of the unimportance of the absolute level of the system. Consequently, the reference for deflection calculation is taken as the average location of the edge of the support plate; and the shape of the pad is written

$$w = \sum_i A_i f_i (r_c, \phi_c) \tag{A-1}$$

where $A_i$ is a coefficient of length dimension, and $f_i$ is a dimensionless mode shape.

The actual deflection mode shapes for the pad were chosen from among the axially symmetric and wave deflection modes arising in the solution in polar coordinates of the plate bending equation

$$\nabla^4 w = \frac{p}{D} \tag{A-2}$$

for uniform plate thickness, and axially symmetric or wave distributions of load q. These modes were classified as

Symmetric:

$$\left(\frac{r_c}{r_o}\right)^{2+s} - 1 \qquad s = 0, 2, 3, 4, \ldots \tag{A-3}$$

Non-symmetric Type I:

$$\left(\frac{r_c}{r_o}\right)^{m} \begin{cases} \sin n\phi_c \\ \cos n\phi_c \end{cases} \qquad \begin{matrix} n = 2, 3, 4; 5, 6, \ldots \\ m = n \; ; \; 5 \end{matrix} \tag{A-4}$$

Non-symmetric Type II:

$$\left(\frac{r_c}{r_o}\right)^{m+s} \left[\left(\frac{r_c}{r_o}\right)^{2} - 1\right] \begin{cases} \sin n\phi_c \\ \cos n\phi_c \end{cases} \qquad \begin{cases} m = 2, 3 : s = 0, 2, 3, 4, \ldots \\ m = 4, 5 : s = 0, 1, 2, 3, \ldots \end{cases} \tag{A-5}$$

Solutions involving ln r are not included in this list, although they too could be used if desired. The Type I non-symmetric terms are written to be the only ones involving non-zero deflection at the support plate edge, and hence to give the only coupling with that plate.

The boundary condition on the support plate is, therefore, of the form

$$w_o = \sum_i A_i \begin{matrix} \sin n\,\phi_c \\ \cos n\,\phi_c \end{matrix} \qquad \text{(A-6)}$$

corresponding to any Type I terms. For a uniform circular plate under edge load giving such an edge deflection, the bending equation can be solved with this result:

$$w = \sum_i \frac{A_i n(n-1)(1-\nu)}{2(2n+1+\nu)} \left(\frac{r_c}{r_o}\right)^n \left\{ (n+1)\,\frac{(n+2)\,-\nu\,(n-2)}{n\,(n-1)\,(1-\nu)} - \left(\frac{r_c}{r_o}\right)^2 \right\} \begin{matrix} \sin n\,\phi_c \\ \cos n\,\phi_c \end{matrix} \qquad \text{(A-7)}$$

where $\nu$ is Poisson's ratio.

In polar coordinates, the bending energy of a plate with surface "S" can be written as the following surface integral:

$$V = \int_S \frac{D}{2} \left\{ (g+e)^2 - 2\,(1-\nu)\,ge + 2\,(1-\nu)\,k^2 \right\} dS \qquad \text{(A-8)}$$

where

$$D = \frac{Et^3}{12\,(1-\nu)^2} \qquad \text{(A-9)}$$

is the stiffness in terms of Young's Modulus E and plate thickness t; and

$$e = \frac{1}{r}\frac{\partial w}{\partial r} + \frac{1}{r^2}\frac{\partial^2 w}{\partial \theta^2} \qquad \text{(A-10)}$$

$$g = \frac{\partial^2 w}{\partial r^2} \qquad \text{(A-11)}$$

$$k = \frac{\partial}{\partial r}\left(\frac{1}{r}\frac{\partial w}{\partial \theta}\right) \qquad \text{(A-12)}$$

are the deflection derivatives. In the case of the support plate, the deflection (A-7) can be substituted and gives the bending energy

$$V_{SP} = \sum_i A_i^2 \frac{\pi D}{2 r_o^2} \frac{n^2(n^2-1)(1-\nu)(3+\nu)}{(2n+1+\nu)} \tag{A-13}$$

The variation, which is of interest in the Ritz method, is

$$\delta V_{SP} = \sum_i A_i \delta A_i \frac{\pi D}{r_o^2} \frac{n^2(n^2-1)(1-\nu)(3+\nu)}{(2n+1+\nu)} \tag{A-14}$$

In the case of the bearing pad, the nature of the cutouts and the shape of the pad make direct integration for the energy impractical. The result is, therefore, approximated by computing an average or mean value of the integrand for each of the subdivisions of surface used in the lubrication calculation; and these are summed using the weight factors which were developed for the integration of pressure to give load. These weight factors are not quite appropriate for the bending energy, but seem within the accuracy of other approximations. Actually, it is convenient to program the calculation of the variation of the bending energy directly; symbolically,

$$\delta V_P = \sum_{i,j} \bar{I}_{ij} A_i \delta A_j \tag{A-15}$$

The coefficients $\bar{I}_{ij}$ correspond to integrals of the form

$$\bar{I}_{ij} = \int_S D \left\{ (g_i + e_i)(g_j + e_j) - (1-\nu)(g_i e_j + g_j e_i) + 2(1-\nu) k_i k_j \right\} dS \tag{A-16}$$

In this case, both subscript i and subscript j refer to the individual deflection modes and can range over all of the modes which are under consideration for the pad. In general, the cross-coupling terms will not cancel, as they do in the case of the support plate; so that the terms of $\bar{I}_{ij}$ can form a complete matrix of order equal to the number of assumed modes. The $\bar{I}_{ij}$ matrix is obviously symmetric, however, limiting the number of combinations that have to be calculated to that extent.

The variation of the total bending energy is the sum of the pad and support plate values:

$$\delta V = \delta V_P + \delta V_{SP} \tag{A-17}$$

The result of this summation is a matrix $I_{ij}$ of coefficients for the parameters $A_i\ \delta A_j$, which differs from the pad matrix $\underline{I}_{ij}$ only in those main diagonal terms corresponding to type I wave modes coupling with the support plate. The resulting matrix $I_{ij}$ is, therefore, also symmetric. In the present case, this represents the total elastic energy variation; and since it depends only upon the assumed deflection modes and the pad and plate geometry, it can be computed initially before starting any of the iterative stages of the bearing program. Moreover, for the point-supported bearing it turns out that $I_{ij}$ is the complete matrix of coefficients of the linear equations which have to be solved for the deformation parameters $A_i$; consequently, the initial calculations can also include the inversion of $I_{ij}$ to the solution matrix $J_{ij}$, giving a further reduction in the amount of calculation required in the iteration loops.

4. Load Energy Variation

The energy variation corresponding to the lubricant pressure loading is given by the variation of

$$W_p = -\int_S P \sum_j A_j f_j (r_c, \phi_c)\ dS \tag{A-18}$$

where P is the pressure differential across the pad, and is equal to the pressure computed from the solution of the lubrication equations. The support plate is assumed free from pressure differentials. Since the pressure is known only at discrete points, the centers of the mesh areas, numerical integration is again indicated. This is carried out for each deflection mode in the same way as the integration of pressure to obtain total load. The result gives the constants $\overline{K}_j$ of the expression

$$\delta W_p = \sum_j \overline{K}_j\ \delta A_j \tag{A-19}$$

This is the only mechanical loading that needs to be considered.

There is, however, a contribution to the deflection due to the temperature variation through the pad thickness; any possible similar effect in the support plate has been neglected. Rather than attempt a rigorous anlaysis of this effect, the assumptions were made with the objective of conceptually replacing the temperature effect by an equivalent mechanical loading, the energy variation then being relatively simple to write. Thus the listed assumptions effectively describe the temperature field as varying linearly through the pad thickness at every point. Deformation in the plane of the pad could be prevented under these circumstances by developing an internal bending moment, expressed in rectangular coordinates, of

$$M_x = M_y = D(1+\nu)\,\alpha\frac{\Delta T}{t} \qquad \text{(A-20)}$$

where $\alpha$ is the thermal expansion coefficient. These moments are per unit length in the appropriate directions.

The development of such internal moments requires, in effect, a distributed moment loading of

$$m_x = -(1+\nu)\,\alpha\,\frac{\partial}{\partial x}\left(D\frac{\Delta T}{t}\right) \qquad \text{(A-21)}$$

$$m_y = -(1+\nu)\,\alpha\,\frac{\partial}{\partial y}\left(D\frac{\Delta T}{t}\right) \qquad \text{(A-22)}$$

each of these being expressed per unit surface area; and, in addition, concentrated edge moments around the free boundary given by expression (A-20). The total effect of the temperature distribution, and of the foregoing distributed and concentrated moment loads, is to maintain the pad flat and at the same time in moment equilibrium.

The deflection due to temperature can, therefore, be represented by the effect of applying moment loading equal and opposite to that just described.

The potential energy associated with such a load can be written as

$$W_T = \int_S \left(- m_x \frac{\partial w}{\partial x} - m_y \frac{\partial w}{\partial y}\right) dS - \int_\ell M_\ell \frac{\partial w}{\partial n} d\ell \qquad \text{(A-23)}$$

the line integral being taken around the boundary of the pad. Again, as a practical matter, the integrals are approximated by appropriate summations, and the energy variation is calculated directly. Allowance for the description of temperature variation on the bottom of the pad is made by writing the temperature differential as

$$\Delta T = T - \left\{ T_{GR} + q_\theta \cdot \theta + q_r \cdot \frac{\theta}{\theta_{TOT}} \cdot \left[ r - (R - L) \right] \right\} \qquad \text{(A-24)}$$

where $T_{GR}$ is the oil inlet edge temperature; and $q_r$, $q_\theta$ allow for the first power variation along the radial and circumferential directions.

The (x, y) coordinates indicated in (A-20) through (A-23) need not be rigorously identified with a fixed coordinate system, as their function is ultimately only to give means of computing energy density, which is then integrated by the summation method. In the program, they are interpreted as being the local radial and tangential directions at each mesh center or boundary point, since these were the best directions for carrying out the necessary numerical differentiations.

The result of the foregoing temperature calculations is another set of load potential energy terms corresponding to $\delta W_T$; the total

$$\delta W = \delta W_p + \delta W_T \qquad \text{(A-25)}$$

comprises a set of coefficients $K_j$ for the parameters $\delta A_j$.

5. Deflection Equations

By the minimum or stationary energy principle, the equilibrium state is approximated when

$$\delta(V + W) = 0 \qquad \text{(A-26)}$$

or

$$\sum_{i,j} I_{ij} A_i \delta A_j + \sum_j K_j \delta A_j = 0 \qquad \text{(A-27)}$$

Since the variations of the A's are arbitrary, this is equivalent to the set of linear equations represented by the matrix equation

$$\left[I_{ij}\right] \left[A_i\right] + \left[K_j\right] = 0 \qquad \text{(A-28)}$$

The solution is

$$\left[A_i\right] + \left[I_{ij}\right]^{-1} \left[K_j\right] = 0 \qquad \text{(A-29)}$$

or

$$\left[A_i\right] = - \left[J_{ij}\right] \left[K_j\right] \qquad \text{(A-30)}$$

The load energy vector $K_j$ is calculated at each appropriate point in the program, and multiplied by the initially calculated inverse matrix $J_{ij}$ to get the new set of deflection coefficients $A_i$.

6. Functions Used

In the program development, and in the calculations made so far, six deflection modes have been used. They are as follows:

Symmetric:

$$f_1 = \left(\frac{r_c}{r_o}\right)^2 - 1$$

$$f_2 = \left(\frac{r_c}{r_o}\right)^4 - 1 \qquad \text{(A-31)}$$

Non-symmetric Type I:

$$f_3 = \left(\frac{r_c}{r_o}\right)^2 \sin 2\phi_c$$

$$f_4 = \left(\frac{r_c}{r_o}\right)^2 \cos 2\phi_c$$

Non-symmetric Type II:

$$f_5 = \left(\frac{r_c}{r_o}\right)^2 \left[\left(\frac{r_c}{r_o}\right)^2 - 1\right] \sin 2\phi_c$$

$$f_6 = \left(\frac{r_c}{r_o}\right)^2 \left[\left(\frac{r_c}{r_o}\right)^2 - 1\right] \cos 2\phi_c$$

The choice was made somewhat arbitrarily, to include all the types of functions, and to match to as good an approximation as possible what is known and suspected about pad deformation. The validity of the choice has not been tested, but operation of the method appears to be successful.

# APPENDIX II

## INPUT DATA

### 1. Pad Geometry

As described in Appendix I, the programed solution of the Elasticity Equation takes account of the thickness variations in each pad and of the fact that the pads are ring supported on circular disks. In the calculations, the pad is divided into a 13 x 13 field and its thickness profile is represented by the set of thicknesses in each mesh. A typical pad is illustrated in Figure A-2 which shows the information on pad geometry that is introduced as input data in each calculation. This data is shown in Figures A-3 through A-18 for all the geometries analysed in the work reported here.

### 2. Pad Inlet Temperature

The oil temperature in the grooves between pads is, in general, considerably higher than that of the housing inlet pads. This is due to the mixing in each groove of cold inlet oil with hot oil discharged from the preceding pad. The groove temperature is used in the analysis as a boundary condition of the Energy Equation (Eq. 2).

In the calculations described in this report the experimentally obtained plot of groove mixing temperature vs. unit load that was first used in Reference 2, was used again to determine the pad inlet temperature in each calculation. This curve, which is reproduced here is Figure A-19, was used in all the cases calculated, except for casses 110 through 123 (Table XIII). In these cases, which were run for the purpose of studying the effect of varying the groove temperature, curves parallel to that of Figure A-19, but displaced 15°F above and below it were used.

3. Bottom Face Temperatures of the Pad

As shown by the Elasticity Equation (Eq. 3), the thermal distortion of a thrust pad is a function of $\Delta T$, the axial temperature difference between the oil film and the bottom face of the pad (See Eq. A-24). In the calculations, the film temperatures were obtained from the solution of the Energy Equation, while the bottom face temperatures were assumed to be at groove temperature along the inlet edge and to rise at the rate of 40 F per radian, proceeding towards the trailing edge. This gradient was obtained from the data gathered during trials of the U.S.S. Barry. In these trials, the back face temperatures of the 31 in. O.D. bearing pads were measured at several points between the leading and trailing edges.

4. Oil Properties

The lubricant properties that are used in the calculations are: specific heat, mass density and viscosity-temperature relation. In the present calculations, the lubricant properties used were those of 2190 T oil and these are shown in Figure A-20.

## APPENDIX III

## ESTIMATE OF ERRORS

A 13 x 13 mesh was used in the numerical integration of Eqs. 1, 2, and 3. This was the finest grid that could be used in the program. It was also finer than any previously used by the authors or reported in the literature on thrust bearing analysis Comparison was made at one point with a calculation made using an 11 x 11 mesh. The resulting pressure and temperature fields agreed within 1%.

Since an iterative method was used in the calculations, limits were set to determine when the final solution was achieved. These were as follows:

a.) Successive iterations of the pressure field had to repeat within 1%.

b.) Successive iterations of elastic deflections had to repeat within $3 \times 10^{-6}$ in.

c.) The resultant of the pressure field had to coincide with the pivot within $0.2 \times 10^{-3}$ in.

The authors feel that these limits were sufficient to insure that:

a.) Errors in calculated maximum temperature $< 5^{\circ}F$.

b.) Errors in calculated minimum film thickness $< 0.0001$ in.

With regard to the calculated oil flow and horsepower loss, however, much larger errors are introduced in the necessary numerical calculation of the pressure gradients at the edges (see Ref. 2). Based on observation of the point scatter obtained from a large number of calculations, it is felt that, in extreme cases, the calculated oil flow and friction losses may be in error by as much as 10%.

## REFERENCES

1. "Feasibility Study for Propeller Shaft Thrust Bearing Program" B. Sternlicht and E. B. Arwas, T.I.S. Report No. 58GL147.

2. "Propeller Shaft Thrust Bearing Analysis - Phase I" B. Sternlicht and E. B. Arwas, T.I.S. Report No. 59GL81

3. "Influence of Pressure and Temperature on Oil Viscosity in Thrust Bearings", B. Sternlicht, A.S.M.E. Paper No. 57A275.

4. "The Hydrodynamical Theory of Film Lubrication", W.F. Cope, Proc. Royal Society of London, Vol. 197, p. 201, 1949.

5. "Theory of Plates and Shells", S. Timoshenko, McGraw Hill Book Co., 1940, Chapter 3.

6. "Thermal Stress and Deformation", J. N. Goodier, Journal of Applied Mechanics, September 1957.

7. "Application of Digital Computers to Bearing Design", B. Sternlicht and F. J. Maginniss, A.S.M.E., Paper No. 56A73.

8. "Energy and Reynolds Considerations in Thrust Bearing Analysis". B. Sternlicht, I.M.E. Conference on Lubrication and Wear, London, Oct. 1957.

# TABLES

TABLE I

| Case No. | Bearing Size Size O.D. x I.D. (inches) | Pad Angle (Deg.) | Speed R.P.M. | Minimum Film Thickness (inches) | Calculation Results in Table | Comments |
|---|---|---|---|---|---|---|
| 1 through 18 | 25 x 12 1/2 | 51 38.25 and 30.6 | 160 and 320 | 0.0014 0.0007 and 0.0004 | II | Standard Geometry Bearings |
| 19 through 36 | 31 x 15 1/2 | 51 38.25 and 30.6 | 160 and 320 | 0.0014 0.0007 and 0.0004 | III | |
| 37 through 54 | 41 x 20 1/2 | 51 38.25 and 30.6 | 160 and 320 | 0.0015 0.0008 and 0.0005 | IV | |
| 55 through 81 | 50 x 25 | 51 38.25 and 30.6 | 100 170 and 320 | 0.0015 0.0008 and 0.0005 | V | |
| 82 through 87 | 31 x 16 1/2 | 38.25 | 160 and 320 | 0.0014 0.0007 and 0.0005 | VI | Ahead Bearing of DD933. Calculations made for comparison with sea trial data. |
| 88 through 90 | 26 x 17 1/2 | 29 | 160 | 0.0018 0.0010 and 0.0004 | VII | Astern Bearing of DD933. Calculations made for comparison with sea trial data. |
| 91 through 96 | 31 x 16 1/2 | 38.25 | 320 | 0.0014 0.0007 and 0.0004 | VIII | Calculations made to study influence of thermal deformation of the pads |
| 97 through 102 | 26 x 17 1/2 | 29 | 160 | 0.0018 0.0010 and 0.0004 | IX | |
| 103 through 105 | 50 x 25 | 30.6 | 170 | 0.0015 0.0010 and 0.0004 | X | |

TABLE I (Contd.)

| Case No. | Bearing Size Size O. D. xI. D. (inches) | Pad Angle (Deg.) | Speed R. P. M. | Minimum Film Thickness (inches) | Calculation Results in Table | Comments |
|---|---|---|---|---|---|---|
| 106 through 117 | 31 x 15 1/2 | 38.25 | 160 and 320 | 0.0014 0.0007 and 0.0004 | XI and XII | Calculations made to study influence of pad thickness |
| 118 through 123 | 31 x 15 1/2 | 38.25 | 320 | 0.0014 0.0007 and 0.0004 | XIII | Calculations made to study influence of groove temperature |
| 124 through 126 | 31 x 21 | 38.25 | 320 | 0.0014 0.0007 and 0.0004 | XIV | Calculations made to study influence of pad geometry |
| 127 through 129 | 31 x 10 | 38.25 | 320 | 0.0014 0.0007 and 0.0004 | XV | |
| 130 through 132 | 31 x 21 | 38.25 | 320 | 0.0014 0.0007 and 0.0004 | XVI | |
| 133 through 135 | 31 x 15 1/2 | 38.25 | 320 | 0.0014 0.0007 and 0.0004 | XVII | |

## MARINE THRUST BEARING PROGRAM - PHASE II

Table No. II

25" O.D. x 12½" I.D. Thrust Bearing

Effective Bearing Area — 312 sq.in.
Oil — 2190 TEP @ 115°F Inlet Temperature

| Case No. | $\theta_T$ degrees | No. of Pads | N rpm | Thick. per Fig. No. | $m_\theta \times 10^6$ in./in. | $m_r \times 10^6$ in./in. | $h_{min.}$ in. | $T_{gr.}$ F | $T_{avg.}$ F | $T_{max.}$ F | $P_{avg.}$ psi | $P_{max.}$ psi | $W_{tot.}$ (1000 lbs.) | $Q_{tot.}$ gpm | $HP_{tot.}$ |
|---|---|---|---|---|---|---|---|---|---|---|---|---|---|---|---|
| 1 | 51 | 6 | 160 | A-3 | 104 | 9 | 0.0014 | 126 | 137 | 158 | 126 | 268 | 39.4 | 1.69 | 2.97 |
| 2 | 51 | 6 | 160 | A-3 | 189 | 2 | 0.0007 | 138 | 159 | 200 | 482 | 1257 | 146.5 | 1.28 | 3.34 |
| 3 | 51 | 6 | 160 | A-3 | 237 | -2 | 0.0004 | 149 | 180 | 234 | 655 | 2328 | 199.0 | 1.27 | 3.56 |
| 4 | 51 | 6 | 320 | A-3 | 186 | 4 | 0.0014 | 129 | 145 | 178 | 280 | 610 | 85.2 | 3.99 | 9.42 |
| 5 | 51 | 6 | 320 | A-3 | 262 | 6 | 0.0007 | 148 | 176 | 222 | 637 | 1862 | 193.8 | 3.14 | 9.34 |
| 6 | 51 | 6 | 320 | A-3 | 317 | -5 | 0.0004 | 156 | 196 | 269 | 797 | 3156 | 242.2 | 3.30 | 10.9 |
| 7 | 38.25 | 8 | 160 | A-4 | 112 | 4 | 0.0012 | 127 | 139 | 161 | 178 | 368 | 54.1 | 1.74 | 3.25 |
| 8 | 38.25 | 8 | 160 | A-4 | 169 | 3 | 0.0007 | 137 | 158 | 189 | 464 | 1123 | 141.0 | 1.36 | 3.60 |
| 9 | 38.25 | 8 | 160 | A-4 | 211 | 3 | 0.0004 | 150 | 181 | 225 | 676 | 2114 | 205.8 | 1.21 | 3.57 |
| 10 | 38.25 | 8 | 320 | A-4 | 161 | 6 | 0.0014 | 129 | 144 | 171 | 260 | 547 | 79.1 | 4.28 | 9.81 |
| 11 | 38.25 | 8 | 320 | A-4 | 237 | 2 | 0.0007 | 148 | 176 | 214 | 638 | 1669 | 193.8 | 3.22 | 10.1 |
| 12 | 38.25 | 8 | 320 | A-4 | 284 | 3 | 0.0004 | 158 | 198 | 259 | 838 | 2886 | 254.5 | 3.04 | 10.4 |
| 13 | 30.6 | 10 | 160 | A-5 | 111 | 9 | 0.0010 | 128 | 142 | 163 | 227 | 476 | 69.0 | 1.73 | 3.57 |
| 14 | 30.6 | 10 | 160 | A-5 | 136 | 8 | 0.0007 | 134 | 154 | 179 | 405 | 918 | 123.0 | 1.44 | 3.74 |
| 15 | 30.6 | 10 | 160 | A-5 | 160 | 0 | 0.0004 | 149 | 179 | 217 | 656 | 1839 | 199.4 | 1.18 | 3.64 |
| 16 | 30.6 | 10 | 320 | A-5 | 163 | 16 | 0.0012 | 130 | 147 | 170 | 305 | 645 | 92.6 | 4.36 | 10.5 |
| 17 | 30.6 | 10 | 320 | A-5 | 190 | 3 | 0.0007 | 145 | 172 | 203 | 592 | 1436 | 179.9 | 3.30 | 10.4 |
| 18 | 30.6 | 10 | 320 | A-5 | 208 | 3 | 0.0004 | 159 | 199 | 250 | 852 | 2538 | 258.8 | 2.78 | 10.2 |

## MARINE THRUST BEARING PROGRAM - PHASE II

Table No. III

31" O.D. x 15½" I.D. Thrust Bearing

Effective Bearing Area — 480 sq.in.
Oil — 2190 TEP @ 115°F Inlet Temperature

| Case No. | $\theta_T$ degrees | No. of Pads | N rpm | Thick. per Fig. No. | $m_\theta \times 10^6$ in./in. | $m_r \times 10^6$ in./in. | $h_{min.}$ in. | $T_{gr.}$ F | $T_{avg.}$ F | $T_{max.}$ F | $P_{avg.}$ psi | $P_{max.}$ psi | $W_{tot.}$ (1000 lbs.) | $Q_{tot.}$ gpm | $HP_{tot.}$ |
|---|---|---|---|---|---|---|---|---|---|---|---|---|---|---|---|
| 19 | 51 | 6 | 160 | A-6 | 122 | 8 | 0.0014 | 128 | 142 | 169 | 205 | 451 | 98.5 | 2.88 | 6.07 |
| 20 | 51 | 6 | 160 | A-6 | 202 | 2 | 0.0007 | 142 | 167 | 210 | 537 | 1608 | 258.0 | 2.38 | 6.44 |
| 21 | 51 | 6 | 160 | A-6 | 241 | 4 | 0.0004 | 150 | 185 | 250 | 667 | 2734 | 320.0 | 2.46 | 7.20 |
| 22 | 51 | 6 | 320 | A-6 | 214 | 1 | 0.0014 | 135 | 155 | 193 | 402 | 973 | 193.1 | 6.81 | 18.3 |
| 23 | 51 | 6 | 320 | A-6 | 273 | 0 | 0.0007 | 151 | 183 | 238 | 680 | 2260 | 326.3 | 5.91 | 18.4 |
| 24 | 51 | 6 | 320 | A-6 | 317 | -4 | 0.0004 | 157 | 203 | 293 | 800 | 3669 | 384.0 | 6.36 | 22.0 |
| 25 | 38.25 | 8 | 160 | A-7 | 118 | 8 | 0.0014 | 127 | 141 | 164 | 199 | 427 | 95.6 | 3.19 | 6.31 |
| 26 | 38.25 | 8 | 160 | A-7 | 156 | -6 | 0.0007 | 141 | 166 | 200 | 518 | 1348 | 248.5 | 2.32 | 6.83 |
| 27 | 38.25 | 8 | 160 | A-7 | 171 | -18 | 0.0004 | 152 | 188 | 243 | 701 | 2290 | 336.3 | 2.03 | 6.70 |
| 28 | 38.25 | 8 | 320 | A-7 | 178 | -3 | 0.0014 | 133 | 152 | 182 | 359 | 808 | 172.5 | 7.28 | 19.3 |
| 29 | 38.25 | 8 | 320 | A-7 | 203 | -15 | 0.0007 | 151 | 184 | 228 | 687 | 1897 | 329.5 | 5.39 | 18.8 |
| 30 | 38.25 | 8 | 320 | A-7 | 218 | -26 | 0.0004 | 160 | 205 | 284 | 876 | 3073 | 420.5 | 4.91 | 18.9 |
| 31 | 30.6 | 10 | 160 | A-8 | 105 | 11 | 0.0014 | 127 | 139 | 159 | 172 | 365 | 82.7 | 3.55 | 6.60 |
| 32 | 30.6 | 10 | 160 | A-8 | 150 | 1 | 0.0007 | 140 | 164 | 193 | 499 | 1265 | 239.9 | 2.53 | 7.26 |
| 33 | 30.6 | 10 | 160 | A-8 | 169 | -3 | 0.0004 | 153 | 188 | 234 | 711 | 2227 | 341.1 | 2.19 | 7.03 |
| 34 | 30.6 | 10 | 320 | A-8 | 167 | 8 | 0.0014 | 131 | 149 | 174 | 329 | 729 | 158.0 | 8.04 | 20.1 |
| 35 | 30.6 | 10 | 320 | A-8 | 195 | -1 | 0.0007 | 151 | 183 | 219 | 678 | 1832 | 325.7 | 5.77 | 19.60 |
| 36 | 30.6 | 10 | 320 | A-8 | 220 | -7 | 0.0004 | 161 | 206 | 273 | 902 | 3089 | 433.4 | 5.26 | 19.81 |

## MARINE THRUST BEARING PROGRAM - PHASE II

Table No. IV

41" O.D. x 20½" I.D. Thrust Bearing

Effective Bearing Area — 840 sq.in.
Oil — 2190 TEP @ 115°F Inlet Temperature

| Case No. | $\theta_T$ degrees | No. of Pads | N rpm | Thick. per Fig. No. | $m_\theta \times 10^6$ in./in. | $m_r \times 10^6$ in./in. | $h_{min.}$ in. | $T_{gr.}$ F | $T_{avg.}$ F | $T_{max.}$ F | $P_{avg.}$ psi | $P_{max.}$ psi | $W_{tot.}$ (1000 lbs.) | $Q_{tot.}$ gpm | $HP_{tot.}$ |
|---|---|---|---|---|---|---|---|---|---|---|---|---|---|---|---|
| 37 | 51.00 | 6 | 160 | A-9 | 154 | 3 | 0.0015 | 132 | 149 | 184 | 335 | 798 | 282 | 6.09 | 14.73 |
| 38 | 51.00 | 6 | 160 | A-9 | 200 | 2 | 0.0008 | 144 | 171 | 217 | 570 | 1816 | 478 | 5.44 | 15.26 |
| 39 | 51.00 | 6 | 160 | A-9 | 225 | -3 | 0.0005 | 150 | 186 | 255 | 661 | 2740 | 556 | 5.59 | 16.96 |
| 40 | 51.00 | 6 | 320 | A-9 | 226 | -2 | 0.0015 | 140 | 163 | 204 | 497 | 1295 | 417 | 14.59 | 42.19 |
| 41 | 51.00 | 6 | 320 | A-9 | 267 | 2 | 0.0008 | 153 | 187 | 248 | 714 | 2511 | 600 | 13.72 | 44.80 |
| 42 | 51.00 | 6 | 320 | A-9 | 294 | 1 | 0.0005 | 157 | 200 | 298 | 789 | 3614 | 663 | 14.42 | 51.12 |
| 43 | 38.25 | 8 | 160 | A-10 | 137 | 2 | 0.0015 | 130 | 147 | 174 | 309 | 690 | 260 | 6.67 | 15.5 |
| 44 | 38.25 | 8 | 160 | A-10 | 182 | -2 | 0.0008 | 146 | 172 | 210 | 587 | 1668 | 493 | 5.35 | 15.46 |
| 45 | 38.25 | 8 | 160 | A-10 | 208 | -1 | 0.0005 | 153 | 190 | 247 | 710 | 2570 | 597 | 5.22 | 16.30 |
| 46 | 38.25 | 8 | 320 | A-10 | 203 | -2 | 0.0015 | 139 | 162 | 195 | 483 | 1150 | 406 | 15.40 | 45.15 |
| 47 | 38.25 | 8 | 320 | A-10 | 243 | -6 | 0.0008 | 155 | 190 | 240 | 759 | 2343 | 637 | 12.95 | 43.70 |
| 48 | 38.25 | 8 | 320 | A-10 | 274 | -5 | 0.0005 | 160 | 206 | 289 | 870 | 3465 | 731 | 13.05 | 47.57 |
| 49 | 30.60 | 10 | 160 | A-11 | 125 | 9 | 0.0015 | 129 | 144 | 166 | 267 | 587 | 224 | 7.37 | 15.94 |
| 50 | 30.60 | 10 | 160 | A-11 | 154 | -2 | 0.0008 | 144 | 174 | 202 | 562 | 1490 | 472 | 5.54 | 16.37 |
| 51 | 30.60 | 10 | 160 | A-11 | 169 | -2 | 0.0005 | 154 | 190 | 239 | 733 | 2343 | 616 | 4.97 | 16.11 |
| 52 | 30.60 | 10 | 320 | A-11 | 178 | 5 | 0.0015 | 137 | 158 | 185 | 436 | 1009 | 366 | 16.65 | 46.80 |
| 53 | 30.60 | 10 | 320 | A-11 | 197 | -1 | 0.0008 | 155 | 190 | 231 | 749 | 2107 | 629 | 12.84 | 45.00 |
| 54 | 30.60 | 10 | 320 | A-11 | 221 | -8 | 0.0005 | 162 | 208 | 279 | 936 | 3275 | 786 | 12.14 | 46.15 |

## MARINE THRUST BEARING PROGRAM - PHASE II

Table No. V

50" O.D. x 25" I.D. Thrust Bearing

Effective Bearing Area — 1250 sq.in.
Oil — 2190 TEP @ 115°F Inlet Temperature

| Case No. | $\theta_T$ degrees | No. of Pads | N rpm | Thick. per Fig. No. | $m_\theta \times 10^6$ in./in. | $m_r \times 10^6$ in./in. | $h_{min.}$ in. | $T_{gr.}$ F | $T_{avg.}$ F | $T_{max.}$ F | $P_{avg.}$ psi | $P_{max.}$ psi | $W_{tot.}$ (1000 lbs.) | $Q_{tot.}$ gpm | $HP_{tot.}$ |
|---|---|---|---|---|---|---|---|---|---|---|---|---|---|---|---|
| 55 | 51 | 6 | 100 | A-12 | 127 | 4 | 0.0015 | 131 | 148 | 182 | 323 | 770 | 403.0 | 5.66 | 13.2 |
| 56 | 51 | 6 | 100 | A-12 | 163 | 1 | 0.0008 | 141 | 167 | 212 | 517 | 1680 | 646.0 | 5.22 | 14.1 |
| 57 | 51 | 6 | 100 | A-12 | 181 | -3 | 0.0005 | 146 | 179 | 248 | 588 | 2511 | 736.0 | 5.42 | 15.7 |
| 58 | 51 | 6 | 170 | A-12 | 170 | 1 | 0.0015 | 136 | 157 | 197 | 429 | 1105 | 537.0 | 11.10 | 29.7 |
| 59 | 51 | 6 | 170 | A-12 | 204 | -1 | 0.0008 | 146 | 178 | 234 | 600 | 2125 | 750.0 | 10.60 | 31.5 |
| 60 | 51 | 6 | 170 | A-12 | 220 | -7 | 0.0005 | 151 | 190 | 277 | 676 | 3109 | 845.0 | 11.20 | 36.4 |
| 61 | 51 | 6 | 320 | A-12 | 230 | 1 | 0.0015 | 144 | 170 | 214 | 561 | 1583 | 701.0 | 25.18 | 76.42 |
| 62 | 51 | 6 | 320 | A-12 | 261 | -3 | 0.0008 | 154 | 192 | 267 | 733 | 2815 | 916.0 | 24.88 | 85.64 |
| 63 | 51 | 6 | 320 | A-12 | 284 | -7 | 0.0005 | 157 | 204 | 322 | 793 | 3983 | 991.0 | 26.86 | 100.3 |
| 64 | 38.25 | 8 | 100 | A-13 | 113 | 5 | 0.0015 | 130 | 145 | 171 | 290 | 638 | 362.0 | 6.24 | 13.7 |
| 65 | 38.25 | 8 | 100 | A-13 | 152 | -1 | 0.0008 | 143 | 168 | 206 | 541 | 1582 | 676.0 | 5.14 | 14.4 |
| 66 | 38.25 | 8 | 100 | A-13 | 176 | -2 | 0.0005 | 150 | 184 | 240 | 656 | 2441 | 820.0 | 5.09 | 14.7 |
| 67 | 38.25 | 8 | 170 | A-13 | 154 | 1 | 0.0015 | 136 | 155 | 186 | 416 | 1002 | 520.0 | 11.80 | 31.1 |
| 68 | 38.25 | 8 | 170 | A-13 | 191 | -2 | 0.0008 | 150 | 181 | 226 | 656 | 2057 | 820.0 | 10.20 | 31.9 |
| 69 | 38.25 | 8 | 170 | A-13 | 216 | -1 | 0.0005 | 156 | 196 | 270 | 761 | 3067 | 951.0 | 10.30 | 33.8 |
| 70 | 38.25 | 8 | 320 | A-13 | 209 | -3 | 0.0015 | 145 | 171 | 207 | 574 | 1479 | 718.0 | 25.74 | 79.83 |
| 71 | 38.25 | 8 | 320 | A-13 | 248 | -6 | 0.0008 | 158 | 197 | 259 | 815 | 2763 | 1019.0 | 23.30 | 82.48 |
| 72 | 38.25 | 8 | 320 | A-13 | 278 | -4 | 0.0005 | 161 | 212 | 316 | 912 | 4016 | 1140.0 | 24.28 | 91.63 |
| 73 | 30.6 | 10 | 100 | A-14 | 100 | 11 | 0.0015 | 129 | 143 | 163 | 248 | 548 | 309.5 | 6.82 | 14.1 |
| 74 | 30.6 | 10 | 100 | A-14 | 129 | 1 | 0.0008 | 142 | 167 | 198 | 523 | 1412 | 653.5 | 5.29 | 14.7 |
| 75 | 30.6 | 10 | 100 | A-14 | 144 | -2 | 0.0005 | 150 | 186 | 234 | 662 | 2231 | 827.4 | 4.88 | 14.7 |
| 76 | 30.6 | 10 | 170 | A-14 | 136 | 7 | 0.0015 | 133 | 153 | 177 | 373 | 846 | 466.4 | 12.9 | 32.7 |
| 77 | 30.6 | 10 | 170 | A-14 | 161 | 0 | 0.0008 | 150 | 180 | 218 | 647 | 1874 | 808.9 | 10.20 | 31.5 |
| 78 | 30.6 | 10 | 170 | A-14 | 179 | -4 | 0.0005 | 158 | 199 | 262 | 808 | 2861 | 1009.3 | 9.60 | 32.0 |
| 79 | 30.6 | 10 | 320 | A-14 | 178 | 16 | 0.0015 | 142 | 168 | 197 | 535 | 1306 | 668.0 | 27.13 | 84.15 |
| 80 | 30.6 | 10 | 320 | A-14 | 202 | 6 | 0.0008 | 159 | 199 | 249 | 831 | 2532 | 1039.0 | 22.42 | 82.17 |
| 81 | 30.6 | 10 | 320 | A-14 | 224 | -2 | 0.0005 | 163 | 215 | 303 | 985 | 3807 | 1231.0 | 21.91 | 85.01 |

## MARINE THRUST BEARING PROGRAM - PHASE II

Table No. VI

31" O.D. x 16½" I.D. Thrust Bearing

Effective Bearing Area — 459 sq.in.
Oil — 2190 TEP @ 115°F Inlet Temperature

| Case No. | $\theta_T$ degrees | No. of Pads | N rpm | Thick. per Fig. No. | $m_\theta \times 10^6$ in./in. | $m_r \times 10^6$ in./in. | $h_{min.}$ in. | $T_{gr.}$ F | $T_{avg.}$ F | $T_{max.}$ F | $P_{avg.}$ psi | $P_{max.}$ psi | $W_{tot.}$ (1000 lbs.) | $Q_{tot.}$ gpm | $HP_{tot.}$ |
|---|---|---|---|---|---|---|---|---|---|---|---|---|---|---|---|
| 82 | 38.25 | 8 | 160 | A-15 | 183 | 6 | 0.0014 | 114 | 130 | 156 | 296 | 671 | 136.0 | 3.55 | 7.76 |
| 83 | 38.25 | 8 | 160 | A-15 | 252 | 5 | 0.0007 | 128 | 154 | 193 | 604 | 1773 | 277.8 | 2.87 | 8.02 |
| 84 | 38.25 | 8 | 160 | A-15 | 288 | 5 | 0.0004 | 135 | 172 | 233 | 714 | 2671 | 328.0 | 2.80 | 8.25 |
| 85 | 38.25 | 8 | 320 | A-15 | 282 | 0 | 0.0014 | 121 | 142 | 174 | 471 | 1159 | 216.2 | 8.37 | 22.8 |
| 86 | 38.25 | 8 | 320 | A-15 | 329 | 4 | 0.0007 | 136 | 170 | 219 | 735 | 2392 | 337.6 | 6.90 | 21.8 |
| 87 | 38.25 | 8 | 320 | A-15 | 365 | 4 | 0.0004 | 143 | 190 | 273 | 866 | 3749 | 398.0 | 6.87 | 23.6 |

## MARINE THRUST BEARING PROGRAM - PHASE II

Table No. VII

26" O.D. x 17.5" I.D. Thrust Bearing

Effective Bearing Area — 184 sq.in.

Oil — 2190 TEP @ 115°F Inlet Temperature

| Case No. | $\Theta_T$ degrees | No. of Pads | N rpm | Thick. per Fig. No. | $m_\theta \times 10^6$ in./in. | $m_r \times 10^6$ in./in. | $h_{min.}$ in. | $T_{gr.}$ F | $T_{avg.}$ F | $T_{max.}$ F | $P_{avg.}$ psi | $P_{max.}$ psi | $W_{tot.}$ (1000 lbs.) | $Q_{tot.}$ gpm | $HP_{tot.}$ |
|---|---|---|---|---|---|---|---|---|---|---|---|---|---|---|---|
| 88 | 29 | 8 | 160 | A-16 | 44 | 37 | 0.0018 | 110 | 121 | 136 | 32 | 64 | 5.88 | 1.69 | 2.81 |
| 89 | 29 | 8 | 160 | A-16 | 135 | 8 | 0.0010 | 110 | 128 | 160 | 260 | 514 | 47.8 | 1.37 | 3.55 |
| 90 | 29 | 8 | 160 | A-16 | 143 | 4 | 0.0004 | 110 | 135 | 216 | 716 | 1294 | 131.8 | 1.09 | 3.99 |

MARINE THRUST BEARING PROGRAM - PHASE II

Table No. VII

26" O.D. x 17.5" I.D. Thrust Bearing

Effective Bearing Area — 184 sq.in.
Oil — 2190 TEP @ 115°F Inlet Temperature

| Case No. | $\theta_T$ degrees | No. of Pads | N rpm | Thick. per Fig. No. | $m_\theta \times 10^6$ in./in. | $m_r \times 10^6$ in./in. | $h_{min.}$ in. | $T_{gr.}$ F | $T_{avg.}$ F | $T_{max.}$ F | $P_{avg.}$ psi | $P_{max.}$ psi | $W_{tot.}$ (1000 lbs.) | $Q_{tot.}$ gpm | $HP_{tot.}$ |
|---|---|---|---|---|---|---|---|---|---|---|---|---|---|---|---|
| 88 | 29 | 8 | 160 | A-16 | 44 | 37 | 0.0018 | 110 | 121 | 136 | 32 | 64 | 5.88 | 1.69 | 2.81 |
| 89 | 29 | 8 | 160 | A-16 | 135 | 8 | 0.0010 | 110 | 128 | 160 | 260 | 514 | 47.8 | 1.37 | 3.55 |
| 90 | 29 | 8 | 160 | A-16 | 143 | 4 | 0.0004 | 110 | 135 | 216 | 716 | 1294 | 131.8 | 1.09 | 3.99 |

## MARINE THRUST BEARING PROGRAM - PHASE II

Table No. VIII

31" O.D. x 16½" I.D. Thrust Bearing

Effective Bearing Area — 459 sq.in.
Oil — 2190 TEP @ 115°F Inlet Temperature

| Case No. | $\theta_T$ degrees | No. of Pads | N rpm | Thick. per Fig. No. | $m_\theta \times 10^6$ in./in. | $m_r \times 10^6$ in./in. | $h_{min.}$ in. | $T_{gr.}$ F | $T_{avg.}$ F | $T_{max.}$ F | $P_{avg.}$ psi | $P_{max.}$ psi | $W_{tot.}$ (1000 lbs.) | $Q_{tot.}$ gpm | $HP_{tot.}$ |
|---|---|---|---|---|---|---|---|---|---|---|---|---|---|---|---|
| 91 | 38.25 | 8 | 320 | Uniform thickness t = 2.2" | 205 | 3 | 0.0014 | 133 | 151 | 180 | 355 | 820 | 163.0 | 7.54 | 19.0 |
| 92 | 38.25 | 8 | 320 | | 251 | 2 | 0.0007 | 149 | 180 | 225 | 647 | 1955 | 297.0 | 5.94 | 18.4 |
| 93 | 38.25 | 8 | 320 | | 286 | -1 | 0.0004 | 157 | 199 | 280 | 792 | 3191 | 364.2 | 5.81 | 19.4 |
| 94 | 38.25 | 8 | 320 | | 143 | 8 | 0.0014 | 131 | 151 | 183 | 322 | 701 | 147.8 | 6.77 | 19.4 |
| 95 | 38.25 | 5 | 320 | | 162 | 5 | 0.0007 | 156 | 191 | 236 | 768 | 1948 | 353.0 | 4.51 | 18.7 |
| 96 | 38.25 | 8 | 320 | | 174 | 6 | 0.0004 | 165 | 219 | 297 | 1191 | 3579 | 547.0 | 3.78 | 19.7 |

## MARINE THRUST BEARING PROGRAM - PHASE II

Table No. IX

26" O.D. x 17½" I.D. Thrust Bearing

Effective Bearing Area — 184 sq.in.
Oil — 2190 TEP @ 115°F Inlet Temperature

| Case No. | $\theta_T$ degrees | No. of Pads | N rpm | Thick. per Fig. No. | $m_\theta \times 10^6$ in./in. | $m_r \times 10^6$ in./in. | $h_{min.}$ in. | $T_{gr.}$ F | $T_{avg.}$ F | $T_{max.}$ F | $P_{avg.}$ psi | $P_{max.}$ psi | $W_{tot.}$ (1000 lbs.) | $Q_{tot.}$ gpm | $HP_{tot.}$ |
|---|---|---|---|---|---|---|---|---|---|---|---|---|---|---|---|
| 97 | 29 | 8 | 160 | A-16 | 10 | 26 | 0.0018 | 123 | 133 | 145 | 7 | 14 | 1.24 | 1.54 | 2.23 |
| 98 | 29 | 8 | 160 | A-16 | 101 | 16 | 0.0010 | 124 | 139 | 165 | 176 | 350 | 32.4 | 1.24 | 2.88 |
| 99 | 29 | 8 | 160 | A-16 | 106 | 10 | 0.0004 | 135 | 155 | 218 | 525 | 973 | 96.6 | 0.88 | 3.07 |
| 100 | 29 | 8 | 160 | A-16 | | Moment | Balance | Not | Achieved | | | | | | |
| 101 | 29 | 8 | 160 | A-16 | | Moment | Balance | Not | Achieved | | | | | | |
| 102 | 29 | 8 | 160 | A-16 | | Moment | Balance | Not | Achieved | | | | | | |

## MARINE THRUST BEARING PROGRAM - PHASE II

Table No. X

50" O.D. x 25" I.D. Thrust Bearing

Effective Bearing Area — 1250 sq.in.

Oil — 2190 TEP @ 115°F Inlet Temperature

| Case No. | $\theta_T$ degrees | No. of Pads | N rpm | Thick. per Fig. No. | $m_\theta \times 10^6$ in./in. | $m_r \times 10^6$ in./in. | $h_{min.}$ in. | $T_{gr.}$ F | $T_{avg.}$ F | $T_{max.}$ F | $P_{avg.}$ psi | $P_{max.}$ psi | $W_{tot.}$ (1000 lbs.) | $Q_{tot.}$ gpm | $HP_{tot.}$ |
|---|---|---|---|---|---|---|---|---|---|---|---|---|---|---|---|
| 103 | 30.6 | 10 | 170 | A-14 | 49 | 5 | 0.0015 | 129 | 154 | 191 | 240 | 495 | 300.1 | 10.0 | 33.9 |
| 104 | 30.6 | 10 | 170 | A-14 | 51 | -1 | 0.0008 | 147 | 187 | 237 | 604 | 1290 | 755.2 | 6.41 | 30.9 |
| 105 | 30.6 | 10 | 170 | A-14 | 49 | -2 | 0.0004 | 164 | 219 | 285 | 1037 | 2342 | 1296.0 | 4.78 | 30.7 |

## MARINE THRUST BEARING PROGRAM - PHASE II

Table No. XI

31" O.D. x 15½" I.D. Thrust Bearing

Effective Bearing Area — 480 sq.in.

Oil — 2190 TEP @ 115°F Inlet Temperature

| Case No. | $\theta_T$ degrees | No. of Pads | N rpm | Thick. per Fig. No. | $m_\theta \times 10^6$ in./in. | $m_r \times 10^6$ in./in. | $h_{min.}$ in. | $T_{gr.}$ F | $T_{avg.}$ F | $T_{max.}$ F | $P_{avg.}$ psi | $P_{max.}$ psi | $W_{tot.}$ (1000 lbs.) | $Q_{tot.}$ gpm | $HP_{tot.}$ |
|---|---|---|---|---|---|---|---|---|---|---|---|---|---|---|---|
| 106 | 38.25 | 8 | 160 | A-17 | 133 | 6 | 0.0014 | 128 | 141 | 163 | 212 | 461 | 101.5 | 3.29 | 6.29 |
| 107 | 38.25 | 8 | 160 | A-17 | 203 | 1 | 0.0007 | 141 | 165 | 199 | 517 | 1455 | 248.0 | 2.60 | 5.85 |
| 108 | 38.25 | 8 | 160 | A-17 | 236 | 0 | 0.0004 | 150 | 185 | 241 | 654 | 2478 | 314.0 | 2.48 | 7.14 |
| 109 | 38.25 | 8 | 320 | A-17 | 214 | 8 | 0.0014 | 134 | 152 | 180 | 378 | 880 | 181.5 | 7.68 | 19.1 |
| 110 | 38.25 | 8 | 320 | A-17 | 269 | -1 | 0.0007 | 150 | 182 | 226 | 663 | 2050 | 318.5 | 6.21 | 19.0 |
| 111 | 38.25 | 8 | 320 | A-17 | 312 | -2 | 0.0004 | 158 | 202 | 280 | 809 | 3357 | 388.4 | 6.25 | 20.8 |

MARINE THRUST BEARING PROGRAM - PHASE II

Table No. XII

31" O.D. x 15½" I.D. Thrust Bearing

Effective Bearing Area — 480 sq.in.
Oil — 2190 TEP @ 115°F Inlet Temperature

| Case No. | $\theta_T$ degrees | No. of Pads | N rpm | Thick. per Fig. No. | $m_\theta \times 10^6$ in./in. | $m_r \times 10^6$ in./in. | $h_{min.}$ in. | $T_{gr.}$ F | $T_{avg.}$ F | $T_{max.}$ F | $P_{avg.}$ psi | $P_{max.}$ psi | $W_{tot.}$ (1000 lbs.) | $Q_{tot.}$ gpm | $HP_{tot.}$ |
|---|---|---|---|---|---|---|---|---|---|---|---|---|---|---|---|
| 112 | 38.25 | 8 | 160 | A-18 | 99 | 4 | 0.0014 | 127 | 141 | 165 | 184 | 391 | 88.5 | 3.07 | 6.37 |
| 113 | 38.25 | 8 | 160 | A-18 | 159 | 0 | 0.0007 | 144 | 169 | 204 | 555 | 1420 | 266.3 | 2.27 | 6.87 |
| 114 | 38.25 | 8 | 160 | A-18 | 193 | -8 | 0.0004 | 156 | 192 | 246 | 771 | 2563 | 370.0 | 2.07 | 6.81 |
| 115 | 38.25 | 8 | 320 | A-18 | 164 | -1 | 0.0014 | 133 | 152 | 185 | 368 | 797 | 173.5 | 7.07 | 19.1 |
| 116 | 38.25 | 8 | 320 | A-18 | 212 | -7 | 0.0007 | 155 | 188 | 232 | 746 | 2039 | 358.5 | 5.27 | 18.8 |
| 117 | 38.25 | 8 | 320 | A-18 | 259 | -12 | 0.0004 | 162 | 209 | 286 | 950 | 3523 | 456.0 | 5.21 | 20.6 |

MARINE THRUST BEARING PROGRAM - PHASE II

Table No. XIII

31" O.D. x 15½" I.D. Thrust Bearing

Effective Bearing Area — 480 sq.in.
Oil — 2190 TEP @ 115°F Inlet Temperature

| Case No. | $\theta_T$ degrees | No. of Pads | N rpm | Thick. per Fig. No. | $m_\theta \times 10^6$ in./in. | $m_r \times 10^6$ in./in. | $h_{min.}$ in. | $T_{gr.}$ F | $T_{avg.}$ F | $T_{max.}$ F | $P_{avg.}$ psi | $P_{max.}$ psi | $W_{tot.}$ (1000 lbs.) | $Q_{tot.}$ gpm | $HP_{tot.}$ |
|---|---|---|---|---|---|---|---|---|---|---|---|---|---|---|---|
| 118 | 38.25 | 8 | 320 | A-7 | 207 | - 9 | 0.0014 | 122 | 143 | 176 | 441 | 1001 | 212 | 7.78 | 22.02 |
| 119 | 38.25 | 8 | 320 | A-7 | 231 | - 20 | 0.0007 | 141 | 176 | 222 | 771 | 2179 | 370 | 5.82 | 20.92 |
| 120 | 38.25 | 8 | 320 | A-7 | 244 | - 28 | 0.0004 | 147 | 196 | 278 | 970 | 3462 | 465 | 5.35 | 21.46 |
| 121 | 38.25 | 8 | 320 | A-7 | 144 | -6 | 0.0014 | 145 | 161 | 189 | 284 | 633 | 136 | 6.77 | 16.60 |
| 122 | 38.25 | 8 | 320 | A-7 | 184 | -16 | 0.0007 | 164 | 193 | 234 | 636 | 1704 | 306 | 5.08 | 16.91 |
| 123 | 38.25 | 8 | 320 | A-7 | 198 | -24 | 0.0004 | 173 | 214 | 291 | 810 | 2811 | 389 | 4.59 | 17.29 |

MARINE THRUST BEARING PROGRAM - PHASE II

Table No. XIV

31" O.D. x 21.08"I.D. Thrust Bearing

Effective Bearing Area — 344 sq.in.
Oil — 2190 TEP @ 115°F Inlet Temperature

| Case No. | $\theta_T$ degrees | No. of Pads | N rpm | Thick. per Fig. No. | $m\theta \times 10^6$ in./in. | $m_r \times 10^6$ in./in. | $h_{min.}$ in. | $T_{gr.}$ F | $T_{avg.}$ F | $T_{max.}$ F | $P_{avg.}$ psi | $P_{max.}$ psi | $W_{tot.}$ (1000 lbs.) | $Q_{tot.}$ gpm | $HP_{tot.}$ |
|---|---|---|---|---|---|---|---|---|---|---|---|---|---|---|---|
| 124 | 38.25 | 8 | 320 | Uniform thickness t = 2.385 | 212 | 12 | 0.0014 | 129 | 149 | 180 | 278 | 625 | 95.8 | 6.67 | 18.0 |
| 125 | 38.25 | 8 | 320 | | 266 | 10 | 0.0007 | 147 | 179 | 231 | 616 | 1827 | 212.2 | 5.14 | 16.9 |
| 126 | 38.25 | 8 | 320 | | 294 | 5 | 0.0004 | 159 | 201 | 290 | 839 | 3260 | 289.0 | 5.04 | 18.8 |

MARINE THRUST BEARING PROGRAM - PHASE II

Table No. XV

31" O.D. x 9.92" I.D. Thrust Bearing

Effective Bearing Area — 576 sq.in.
Oil — 2190 TEP @ 115°F Inlet Temperature

| Case No. | $\theta_T$ degrees | No. of Pads | N rpm | Thick. per Fig. No. | $m_\theta \times 10^6$ in./in. | $m_r \times 10^6$ in./in. | $h_{min.}$ in. | $T_{gr.}$ F | $T_{avg.}$ F | $T_{max.}$ F | $P_{avg.}$ psi | $P_{max.}$ psi | $W_{tot.}$ (1000 lbs.) | $Q_{tot.}$ gpm | $HP_{tot.}$ |
|---|---|---|---|---|---|---|---|---|---|---|---|---|---|---|---|
| 127 | 38.25 | 8 | 320 | Uniform thickness t = 2.385" | 144 | 46 | 0.0014 | 131 | 149 | 172 | 316 | 744 | 182.3 | 7.81 | 19.4 |
| 128 | 38.25 | 8 | 320 | | 194 | 34 | 0.0007 | 147 | 179 | 217 | 603 | 1885 | 347.5 | 6.44 | 19.4 |
| 129 | 38.25 | 8 | 320 | | 223 | 29 | 0.0004 | 155 | 199 | 271 | 752 | 3141 | 433.0 | 6.12 | 19.1 |

MARINE THRUST BEARING PROGRAM - PHASE II

Table No. XVI

31" O.D. x 21" I.D. Thrust Bearing

Effective Bearing Area — 347 sq.in.
Oil — 2190 TEP @ 115°F Inlet Temperature

| Case No. | $\theta_T$ degrees | No. of Pads | N rpm | Thick. per Fig. No. | $m_\theta \times 10^6$ in./in. | $m_r \times 10^6$ in./in. | $h_{min.}$ in. | $T_{gr.}$ F | $T_{avg.}$ F | $T_{max.}$ F | $P_{avg.}$ psi | $P_{max.}$ psi | $W_{tot.}$ (1000 lbs.) | $Q_{tot.}$ gpm | $HP_{tot.}$ |
|---|---|---|---|---|---|---|---|---|---|---|---|---|---|---|---|
| 130 | 21.86 | 14 | 320 | Uniform thickness t = 2.385" | 178 | -3 | 0.0014 | 128 | 146 | 168 | 250 | 537 | 86.8 | 8.03 | 19.3 |
| 131 | 21.86 | 14 | 320 | | 201 | -4 | 0.0007 | 149 | 179 | 213 | 637 | 1548 | 220.8 | 5.31 | 19.2 |
| 132 | 21.86 | 14 | 320 | | 218 | -8 | 0.0004 | 163 | 208 | 267 | 995 | 2874 | 345.0 | 4.34 | 19.3 |

MARINE THRUST BEARING PROGRAM - PHASE II

Table No. XVII

31" O.D. x 15½" I.D. Thrust Bearing

Effective Bearing Area — 480 sq.in.
Oil — 2190 TEP @ 115°F Inlet Temperature

| Case No. | $\theta_T$ degrees | No. of Pads | N rpm | Thick. per Fig. No. | $m_\theta \times 10^6$ in./in. | $m_r \times 10^6$ in./in. | $h_{min.}$ in. | $T_{gr.}$ F | $T_{avg.}$ F | $T_{max.}$ F | $P_{avg.}$ psi | $P_{max.}$ psi | $W_{tot.}$ (1000 lbs.) | $Q_{tot.}$ gpm | $HP_{tot.}$ |
|---|---|---|---|---|---|---|---|---|---|---|---|---|---|---|---|
| 133 | 38.25 | 8 | 320 | Uniform thickness t = 2.385" | 178 | -3 | 0.0014 | 133 | 151 | 181 | 354 | 800 | 170.2 | 7.38 | 19.3 |
| 134 | 38.25 | 8 | 320 | | 226 | -1 | 0.0007 | 150 | 182 | 226 | 663 | 1932 | 318.3 | 5.77 | 18.8 |
| 135 | 38.25 | 8 | 320 | | 257 | -3 | 0.0004 | 158 | 203 | 283 | 824 | 3182 | 395.4 | 5.55 | 19.6 |

FIGURES

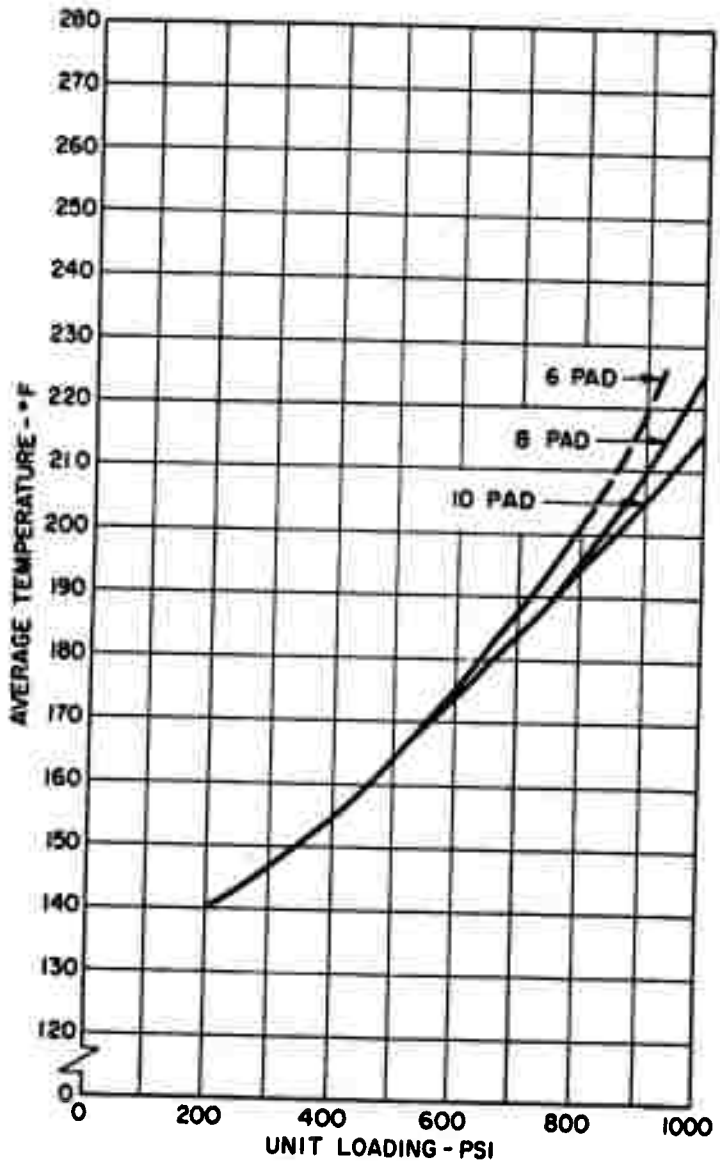


AVERAGE TEMPERATURE CHART

6, 8 and 10 PAD BEARINGS

$\frac{L}{D} = \frac{1}{2}$

OIL - 2190T

HOUSING INLET TEMPERATURE - 115°F

FIGURE 1

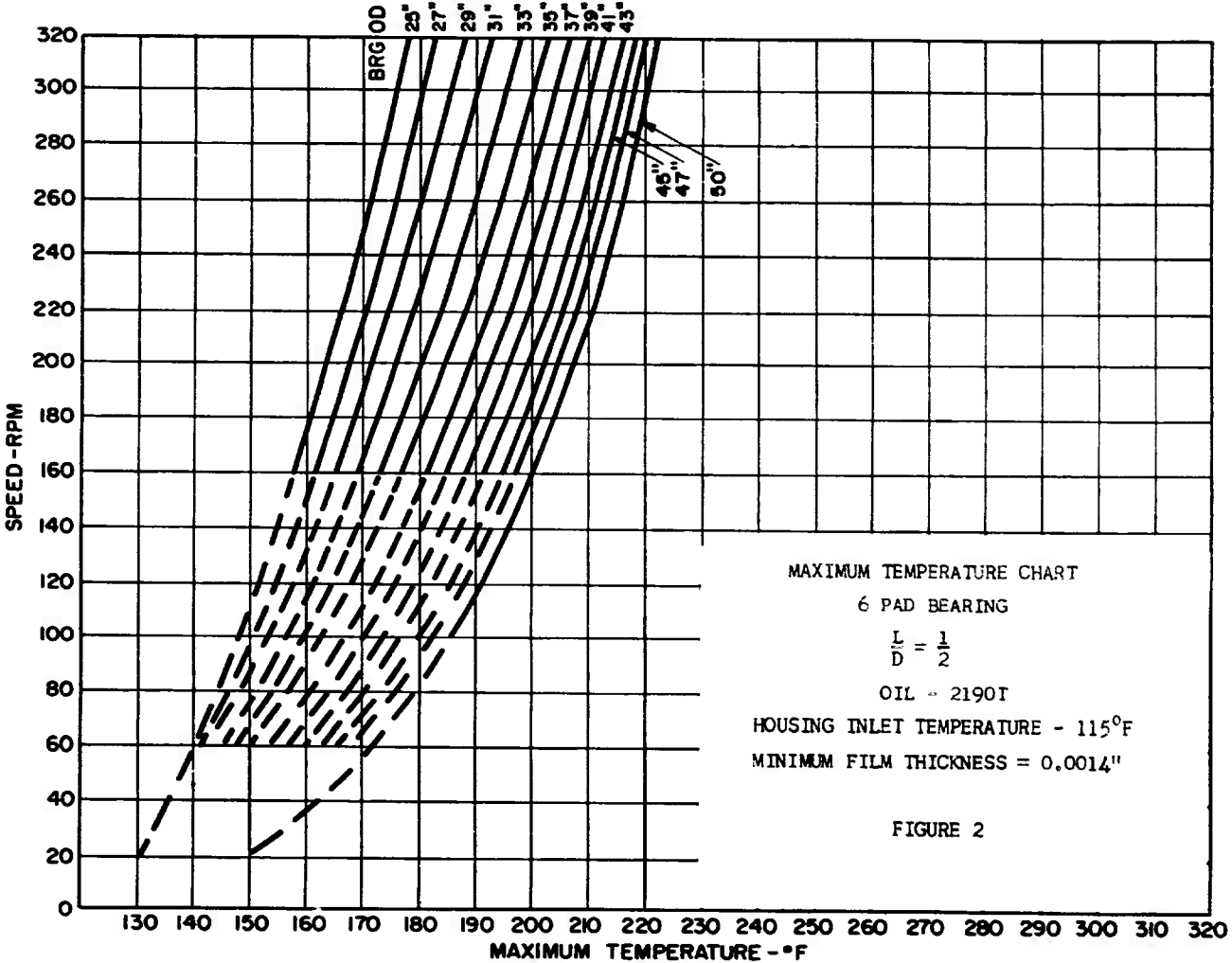
BRG OD
25"
27"
29"
31"
33"
35"
37"
39"
41"
43"
45"
47"
50"
SPEED-RPM
0
20
40
60
80
100
120
140
160
180
200
220
240
260
280
300
320
130 140 150 160 170 180 190 200 210 220 230 240 250 260 270 280 290 300 310 320
MAXIMUM TEMPERATURE - °F
MAXIMUM TEMPERATURE CHART
6 PAD BEARING
L/D = 1/2
OIL - 2190T
HOUSING INLET TEMPERATURE - 115°F
MINIMUM FILM THICKNESS = 0.0014"

FIGURE 2

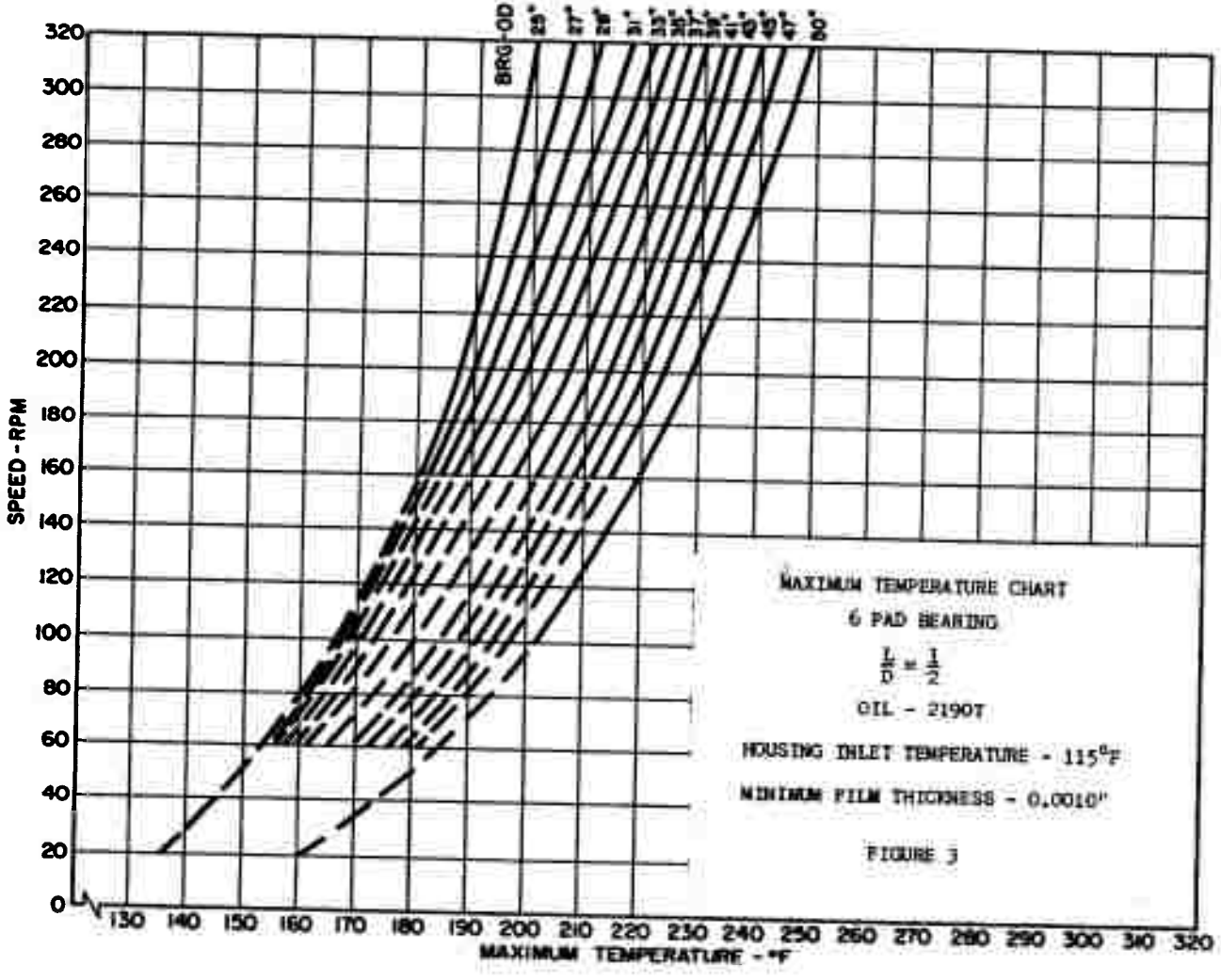
BRG-OD
SPEED - RPM
320
300
280
260
240
220
200
180
160
140
120
100
80
60
40
20
0
130 140 150 160 170 180 190 200 210 220 230 240 250 260 270 280 290 300 310 320
MAXIMUM TEMPERATURE - °F
MAXIMUM TEMPERATURE CHART
6 PAD BEARING
L/D = 1/2
OIL - 2190T
HOUSING INLET TEMPERATURE - 115°F
MINIMUM FILM THICKNESS - 0.0010"
FIGURE 3

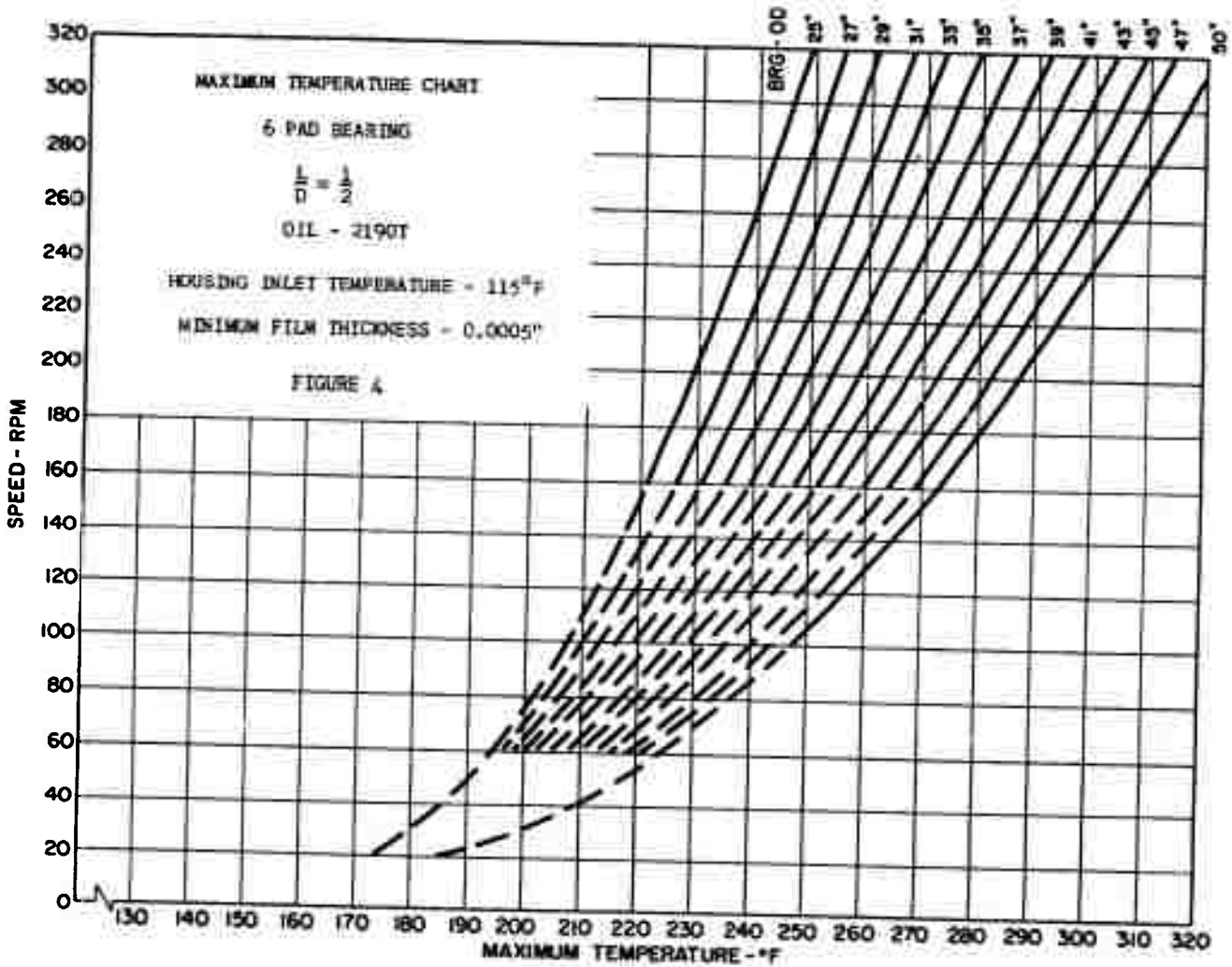
MAXIMUM TEMPERATURE CHART
6 PAD BEARING
L/D = 1/2
OIL - 2190T
HOUSING INLET TEMPERATURE - 115°F
MINIMUM FILM THICKNESS - 0.0005"
FIGURE 4
BRG - OD
25"
27"
29"
31"
33"
35"
37"
39"
41"
43"
45"
47"
50"
SPEED - RPM
0
20
40
60
80
100
120
140
160
180
200
220
240
260
280
300
320
130
140
150
160
170
180
190
200
210
220
230
240
250
260
270
280
290
300
310
320
MAXIMUM TEMPERATURE - °F

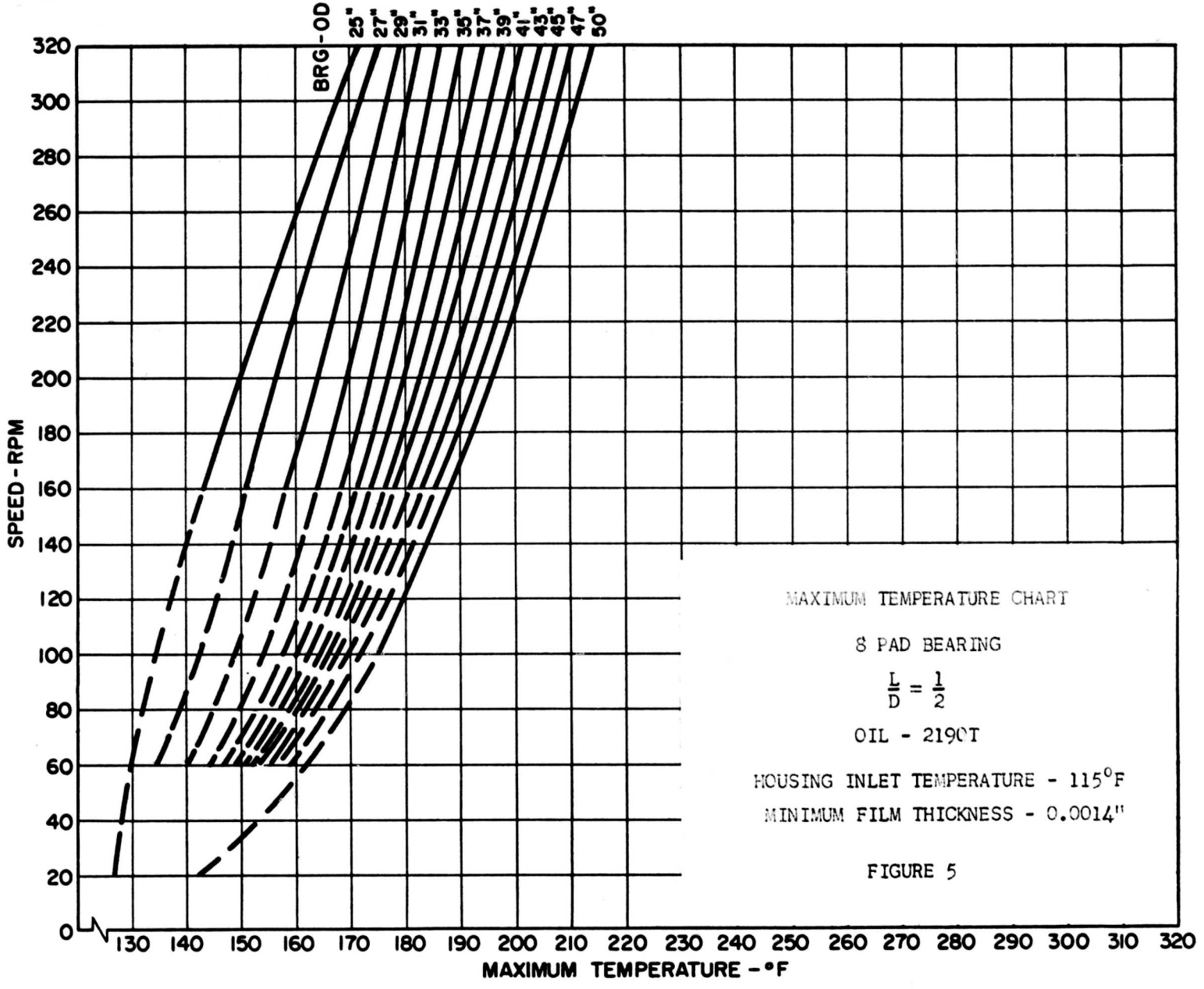
BRG-OD
25"
27"
29"
31"
33"
35"
37"
39"
41"
43"
45"
47"
50"
SPEED-RPM
0
20
40
60
80
100
120
140
160
180
200
220
240
260
280
300
320
130 140 150 160 170 180 190 200 210 220 230 240 250 260 270 280 290 300 310 320
MAXIMUM TEMPERATURE - °F
MAXIMUM TEMPERATURE CHART
8 PAD BEARING
L/D = 1/2
OIL - 2190T
HOUSING INLET TEMPERATURE - 115°F
MINIMUM FILM THICKNESS - 0.0014"

FIGURE 5

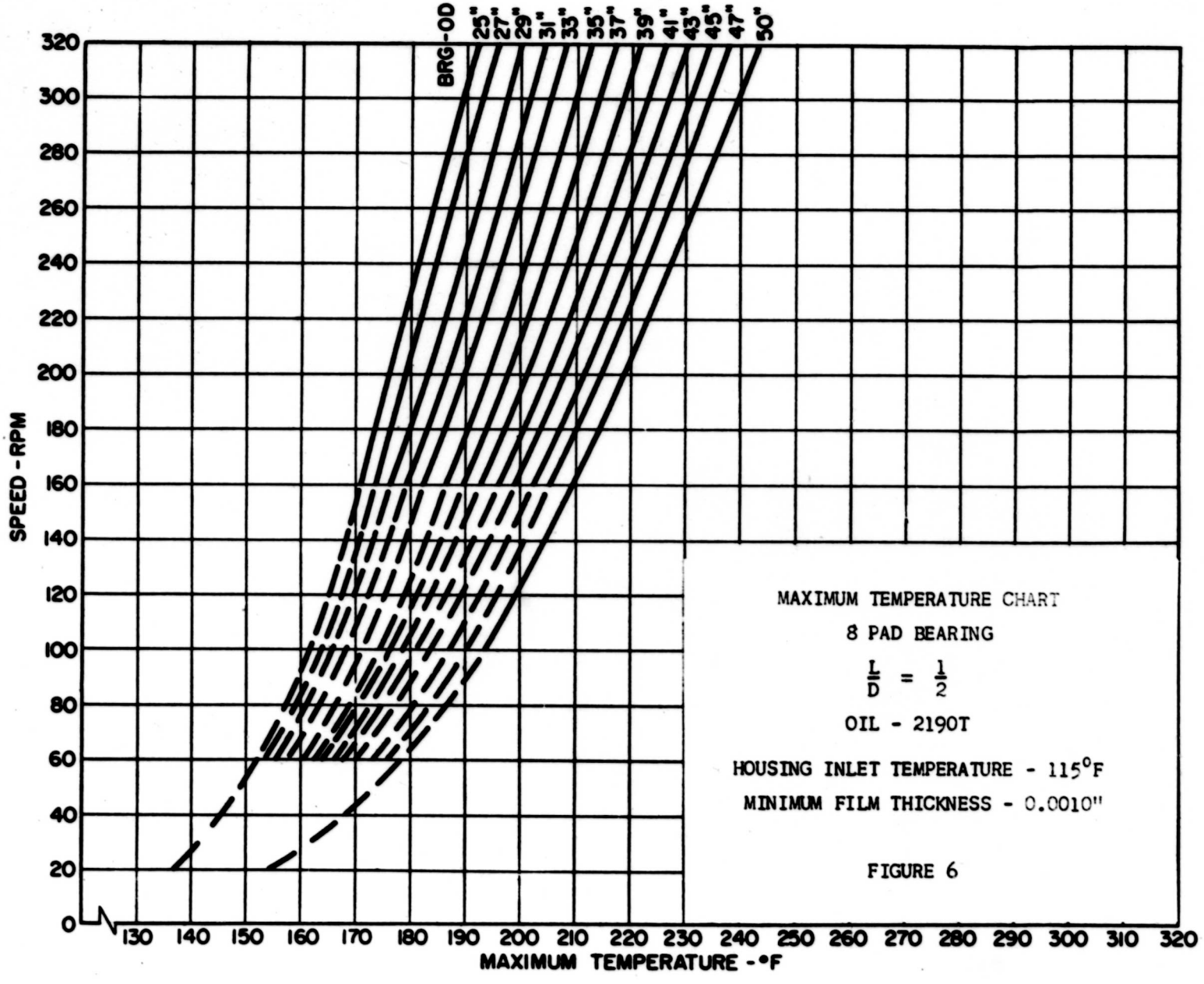
BRG-OD
25"
27"
29"
31"
33"
35"
37"
39"
41"
43"
45"
47"
50"
SPEED - RPM
0
20
40
60
80
100
120
140
160
180
200
220
240
260
280
300
320
130
140
150
160
170
180
190
200
210
220
230
240
250
260
270
280
290
300
310
320
MAXIMUM TEMPERATURE - °F
MAXIMUM TEMPERATURE CHART
8 PAD BEARING
L/D = 1/2
OIL - 2190T
HOUSING INLET TEMPERATURE - 115°F
MINIMUM FILM THICKNESS - 0.0010"

FIGURE 6

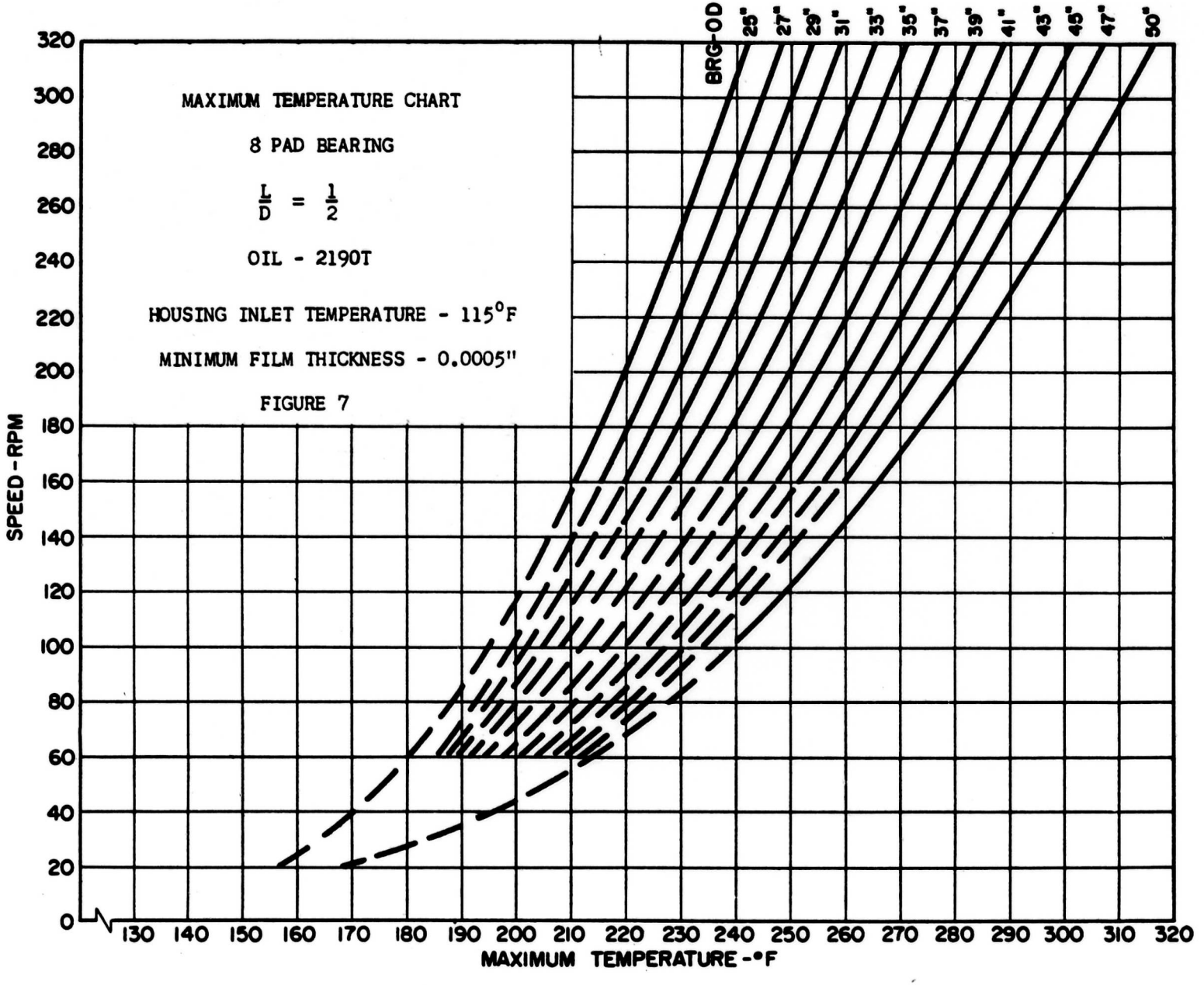
MAXIMUM TEMPERATURE CHART
8 PAD BEARING
L/D = 1/2
OIL - 2190T
HOUSING INLET TEMPERATURE - 115°F
MINIMUM FILM THICKNESS - 0.0005"
FIGURE 7
BRG-OD
25"
27"
29"
31"
33"
35"
37"
39"
41"
43"
45"
47"
50"
SPEED-RPM
0
20
40
60
80
100
120
140
160
180
200
220
240
260
280
300
320
130 140 150 160 170 180 190 200 210 220 230 240 250 260 270 280 290 300 310 320
MAXIMUM TEMPERATURE-°F

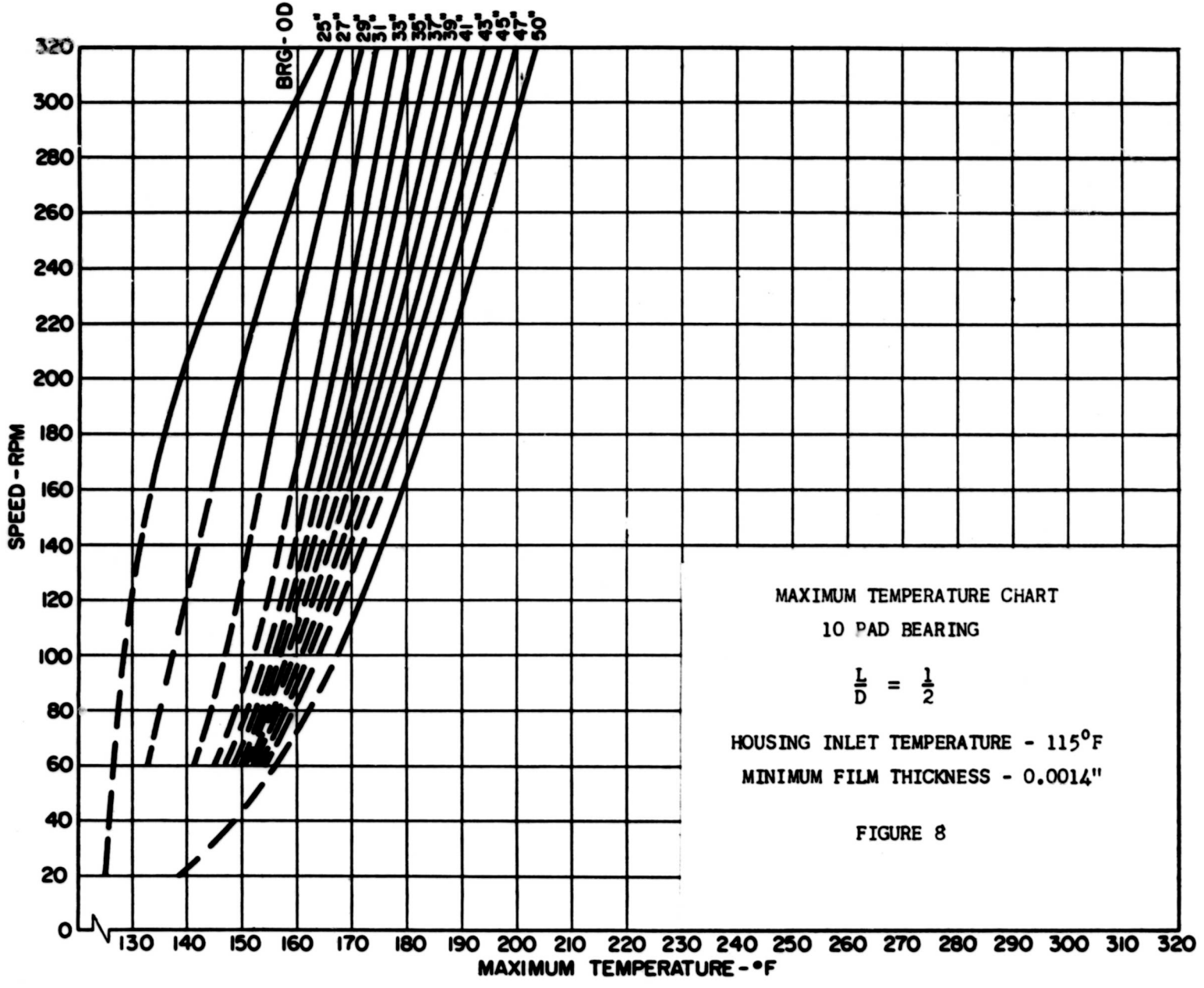


MAXIMUM TEMPERATURE CHART

10 PAD BEARING

$\frac{L}{D} = \frac{1}{2}$

HOUSING INLET TEMPERATURE - 115°F

MINIMUM FILM THICKNESS - 0.0014"

FIGURE 8

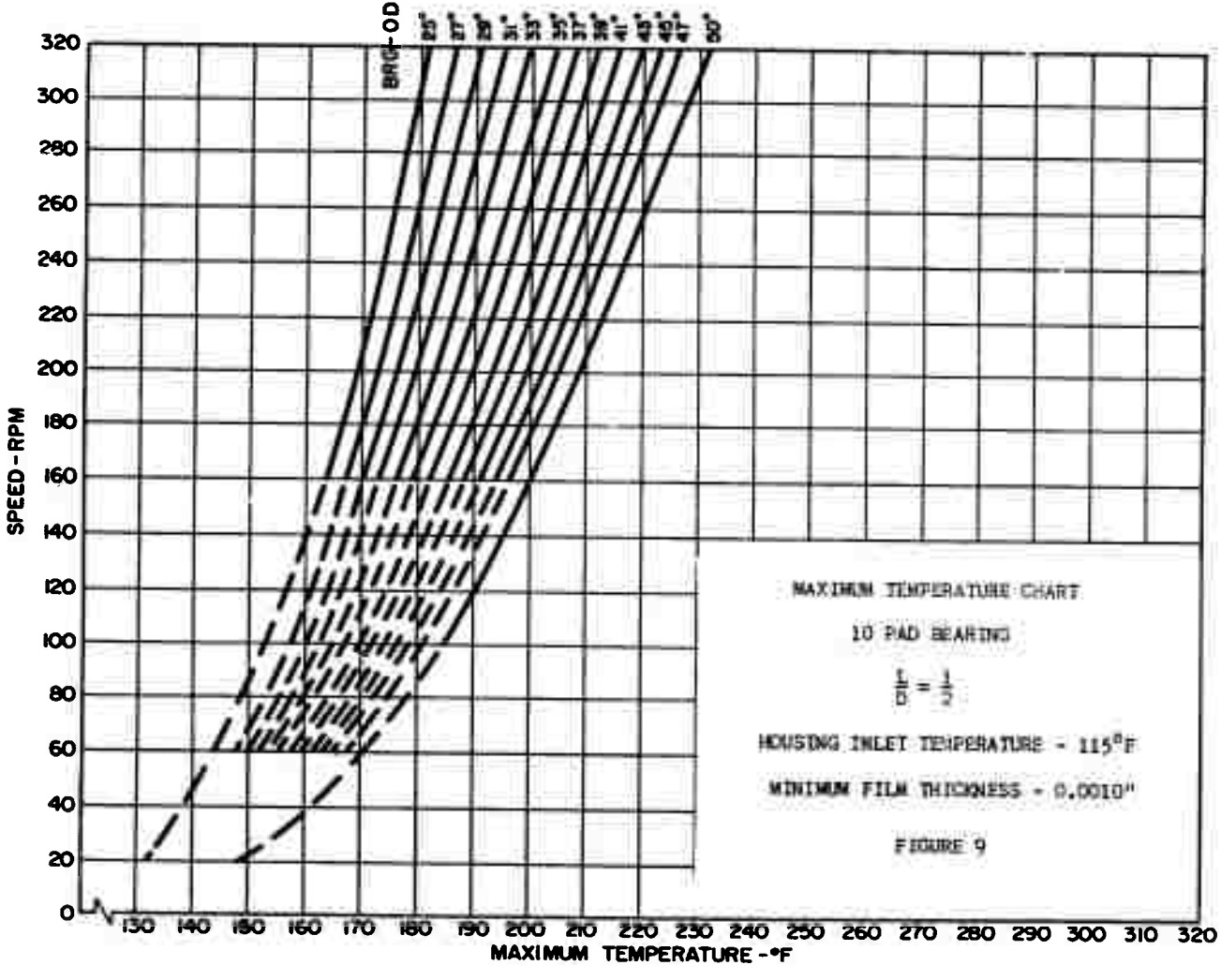
BRG-OD
SPEED-RPM
MAXIMUM TEMPERATURE -°F
0
20
40
60
80
100
120
140
160
180
200
220
240
260
280
300
320
130
140
150
160
170
180
190
200
210
220
230
240
250
260
270
280
290
300
310
320
MAXIMUM TEMPERATURE CHART
10 PAD BEARING
$\frac{L}{D} = \frac{1}{2}$
HOUSING INLET TEMPERATURE - 115°F
MINIMUM FILM THICKNESS - 0.0010"

FIGURE 9

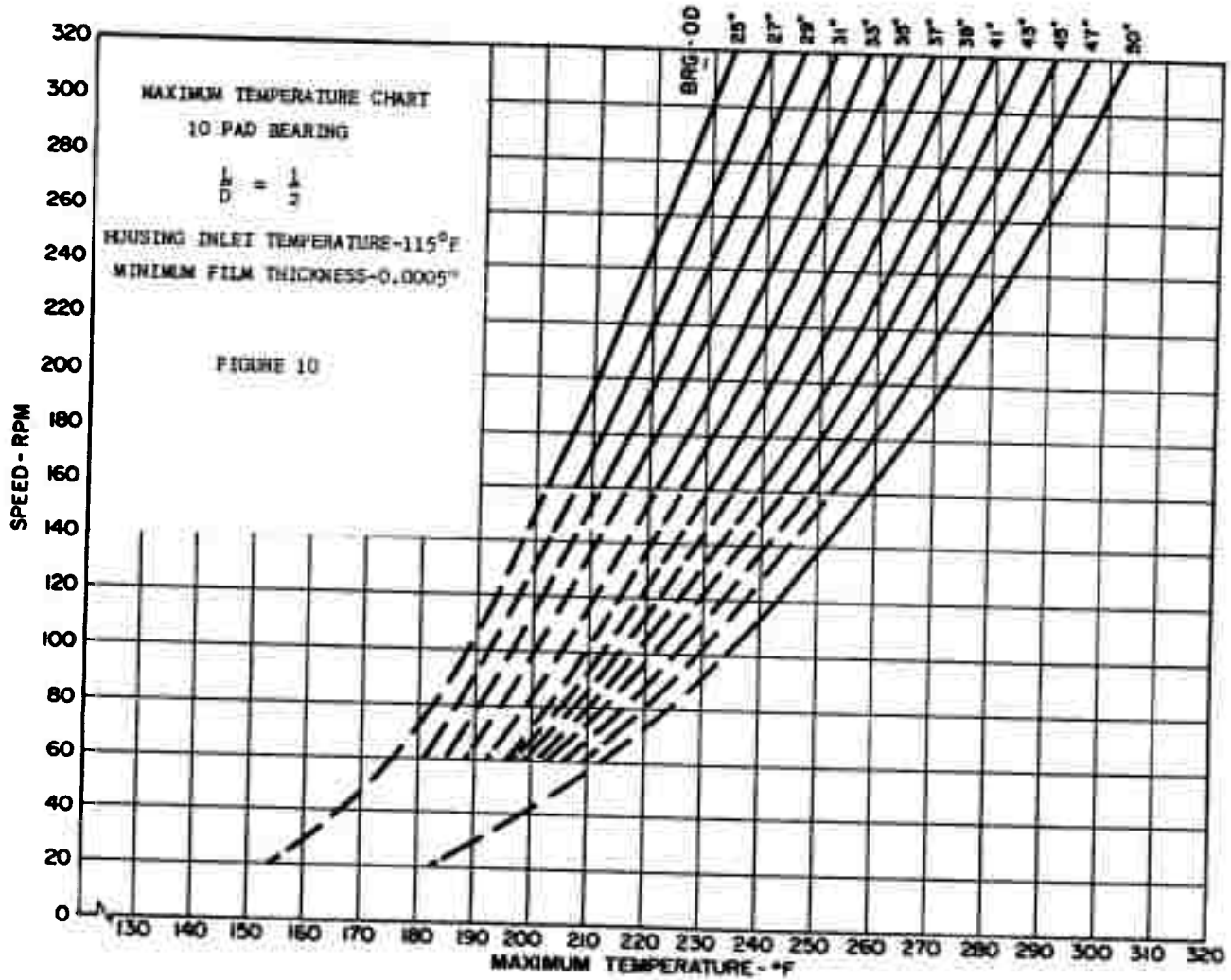
MAXIMUM TEMPERATURE CHART
10 PAD BEARING
L/D = 1/2
HOUSING INLET TEMPERATURE-115°F
MINIMUM FILM THICKNESS-0.0005"
FIGURE 10
BRG. OD
SPEED - RPM
MAXIMUM TEMPERATURE - °F
0
20
40
60
80
100
120
140
160
180
200
220
240
260
280
300
320
130
140
150
160
170
180
190
200
210
220
230
240
250
260
270
280
290
300
310
320

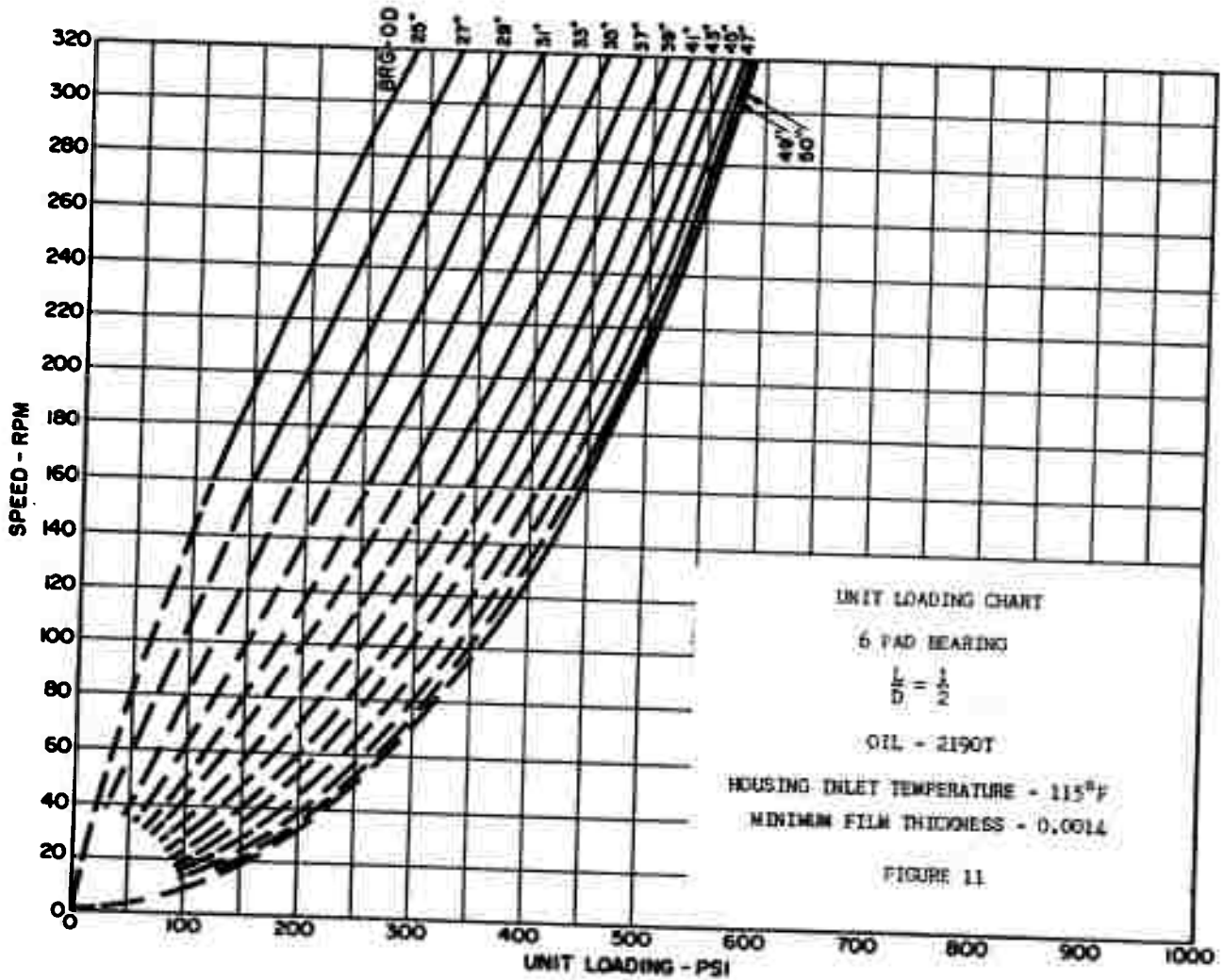
BRG-OD
SPEED - RPM
UNIT LOADING - PSI
0
20
40
60
80
100
120
140
160
180
200
220
240
260
280
300
320
100
200
300
400
500
600
700
800
900
1000
UNIT LOADING CHART
6 PAD BEARING
L/D = 1/2
OIL - 2190T
HOUSING INLET TEMPERATURE - 115°F
MINIMUM FILM THICKNESS - 0.0014

FIGURE 11

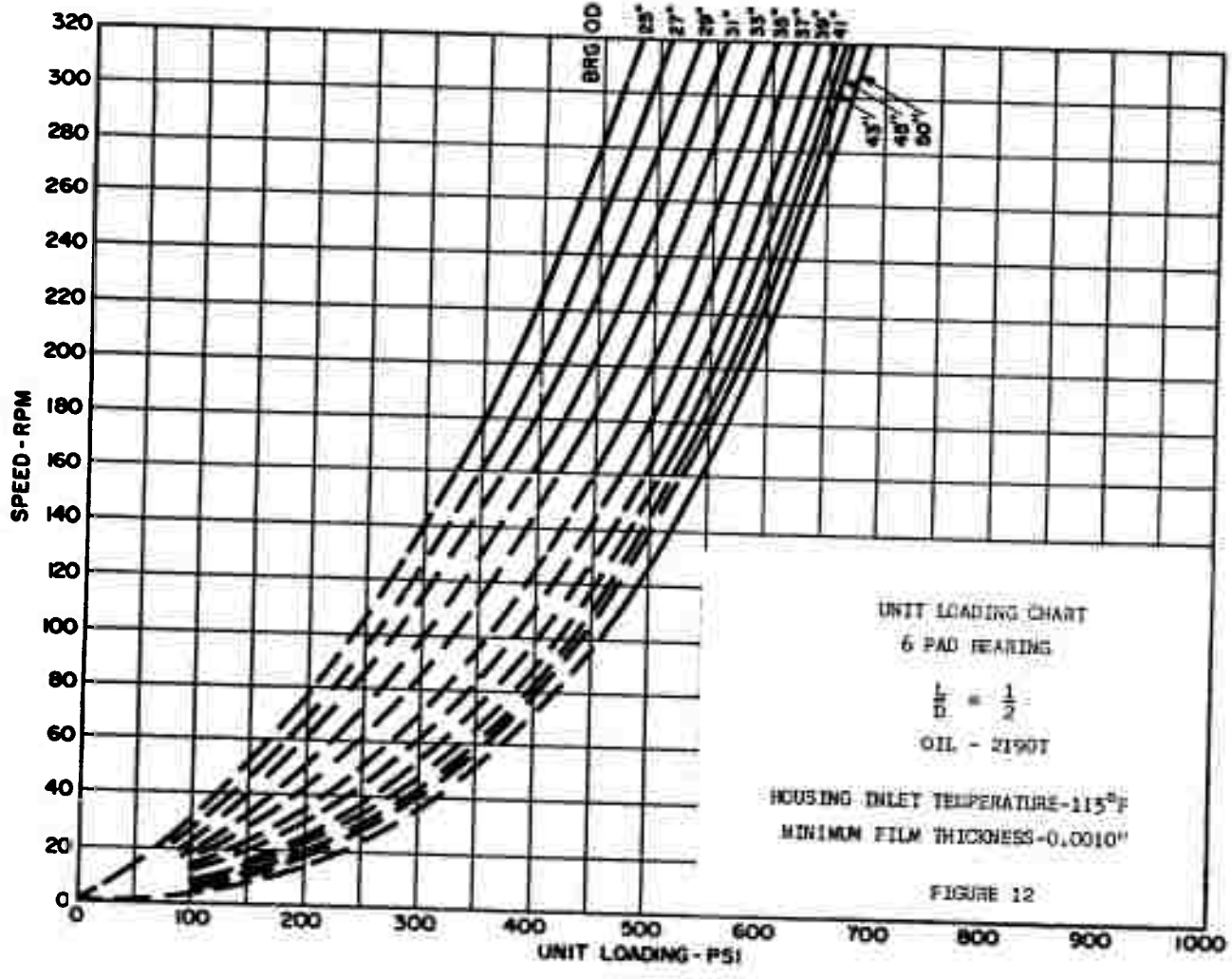
BRG OD
SPEED - RPM
UNIT LOADING - PSI
0
20
40
60
80
100
120
140
160
180
200
220
240
260
280
300
320
0
100
200
300
400
500
600
700
800
900
1000
UNIT LOADING CHART
6 PAD BEARING
L/D = 1/2
OIL - 2190T
HOUSING INLET TEMPERATURE-115°F
MINIMUM FILM THICKNESS-0.0010"

FIGURE 12

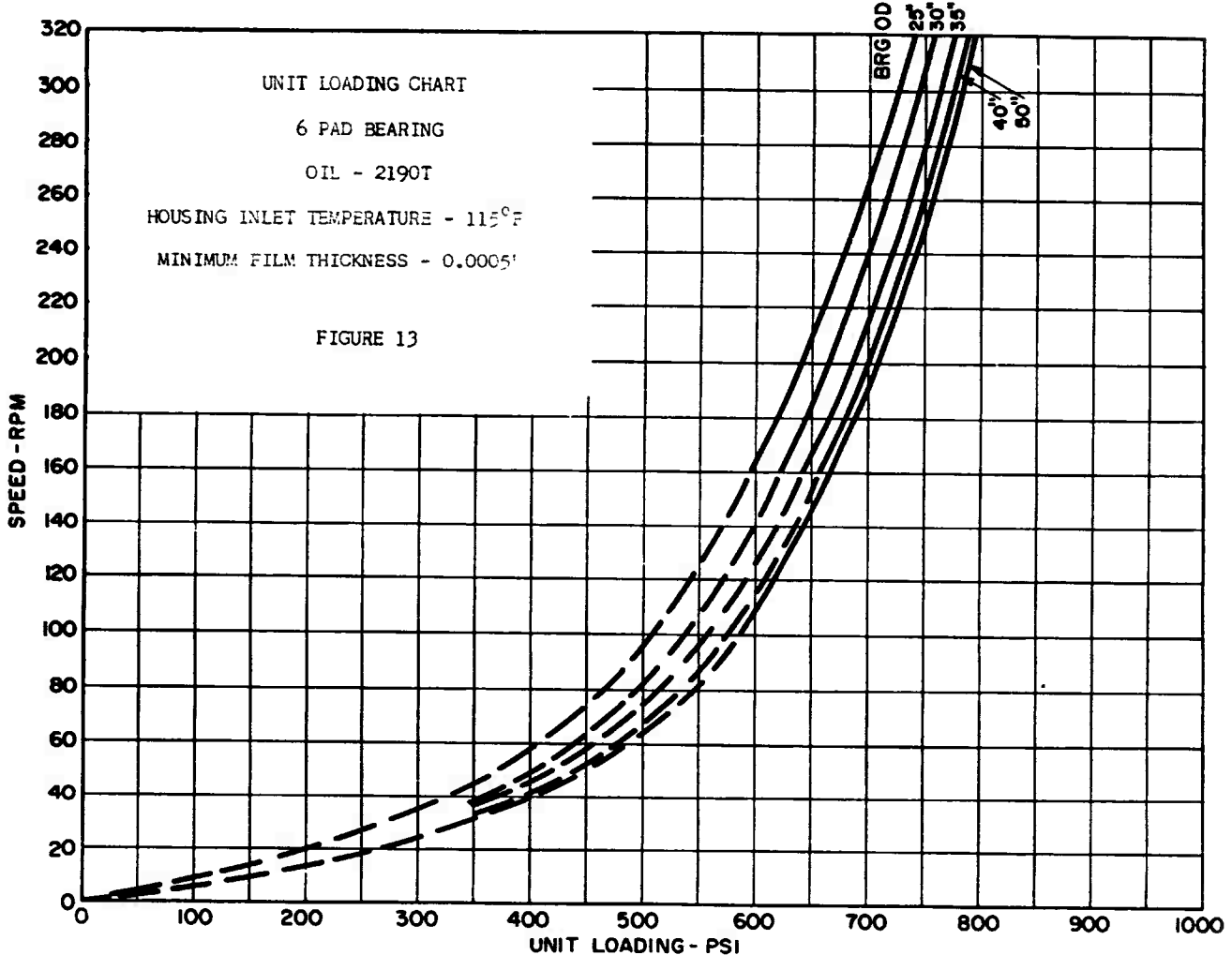
UNIT LOADING CHART
6 PAD BEARING
OIL - 2190T
HOUSING INLET TEMPERATURE - 115°F
MINIMUM FILM THICKNESS - 0.0005'
FIGURE 13
BRG OD
25"
30"
35"
40"
50"
SPEED - RPM
UNIT LOADING - PSI
0
20
40
60
80
100
120
140
160
180
200
220
240
260
280
300
320
0
100
200
300
400
500
600
700
800
900
1000

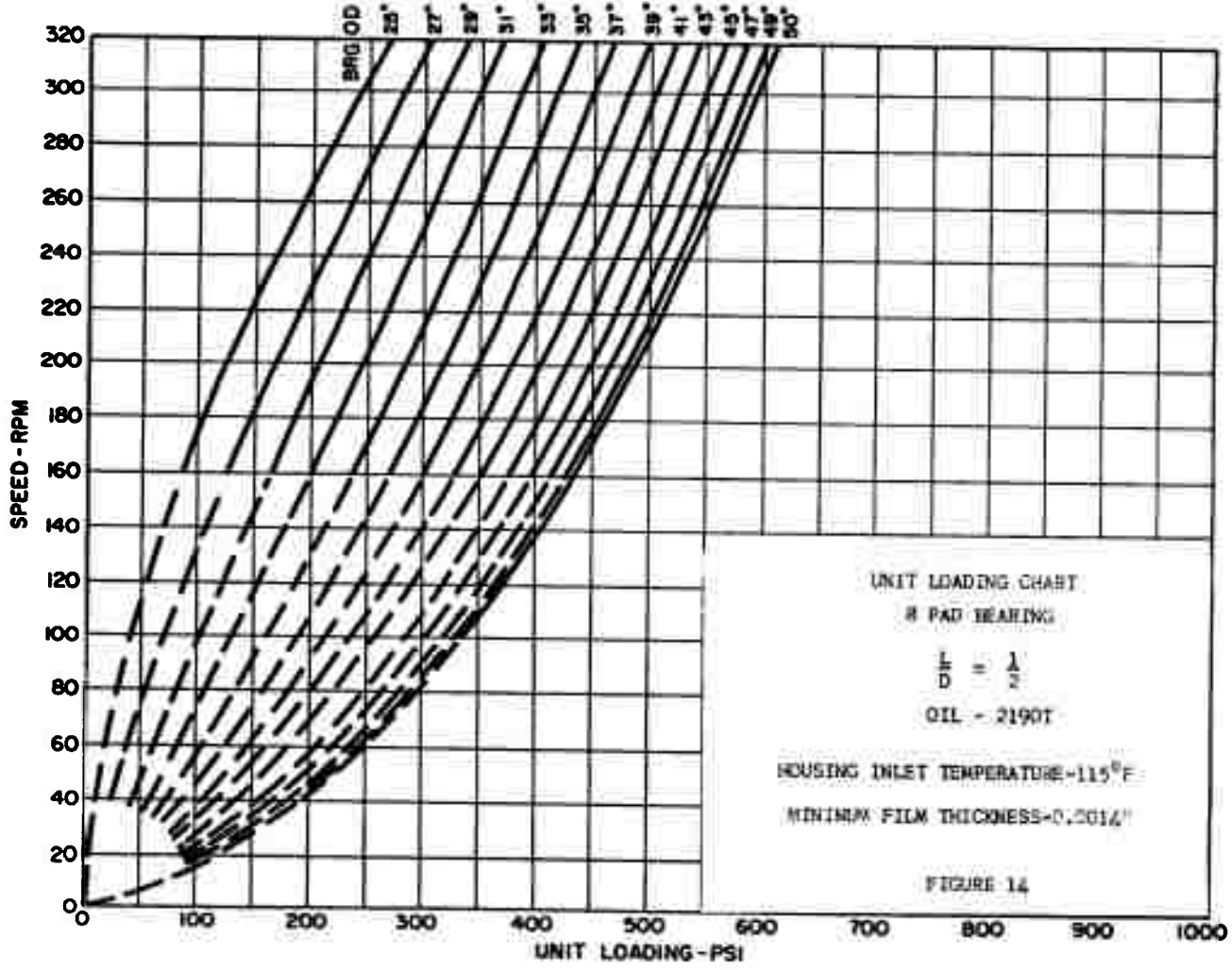
SPEED - RPM
UNIT LOADING - PSI
0
20
40
60
80
100
120
140
160
180
200
220
240
260
280
300
320
100
200
300
400
500
600
700
800
900
1000
UNIT LOADING CHART
8 PAD BEARING
L/D = 1/2
OIL - 2190T
HOUSING INLET TEMPERATURE-115°F
MINIMUM FILM THICKNESS-0.0014"

FIGURE 14

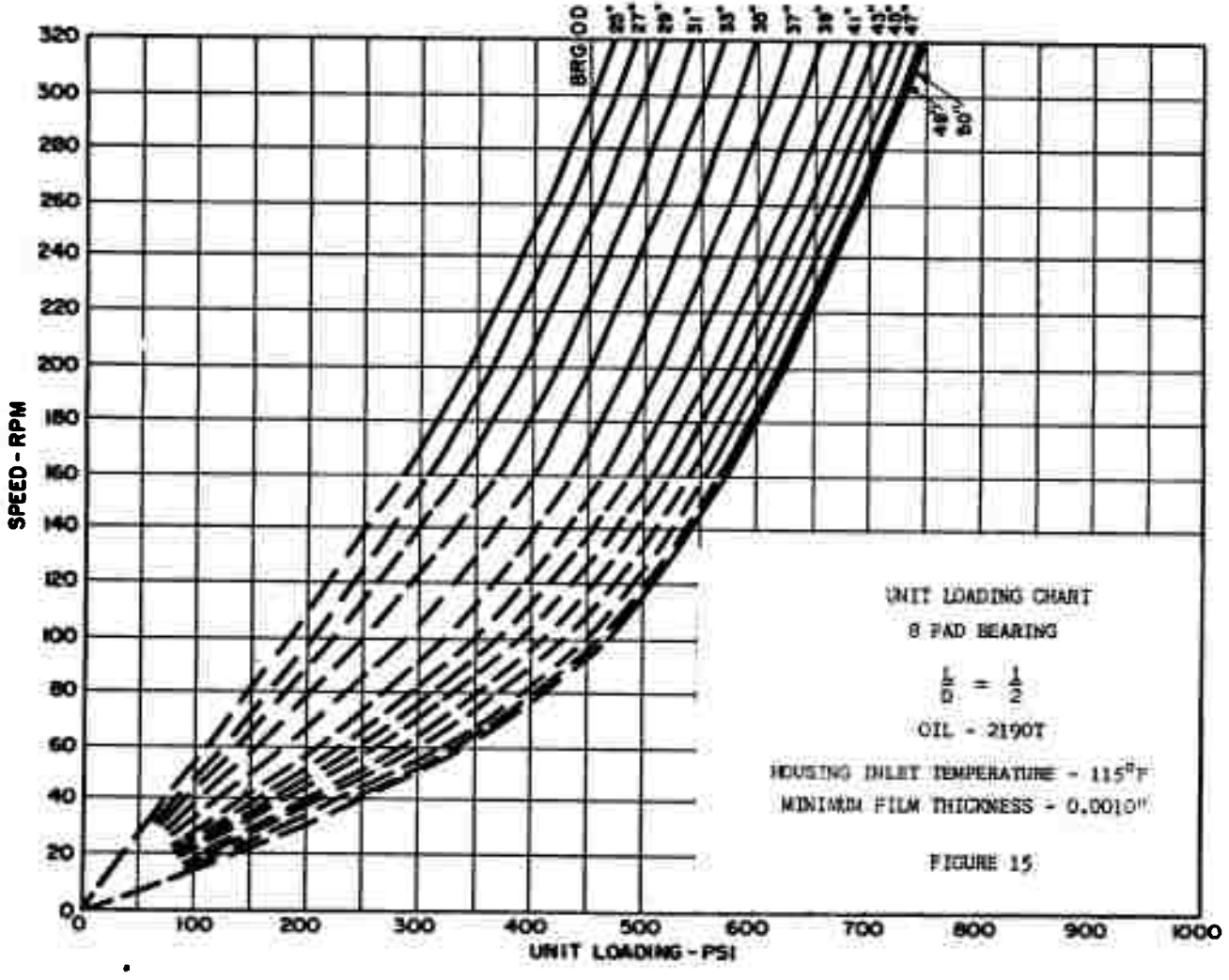
SPEED - RPM
UNIT LOADING - PSI
BRG OD
48"
80"
UNIT LOADING CHART
8 PAD BEARING
L/D = 1/2
OIL - 2190T
HOUSING INLET TEMPERATURE - 115°F
MINIMUM FILM THICKNESS - 0.0010"
FIGURE 15

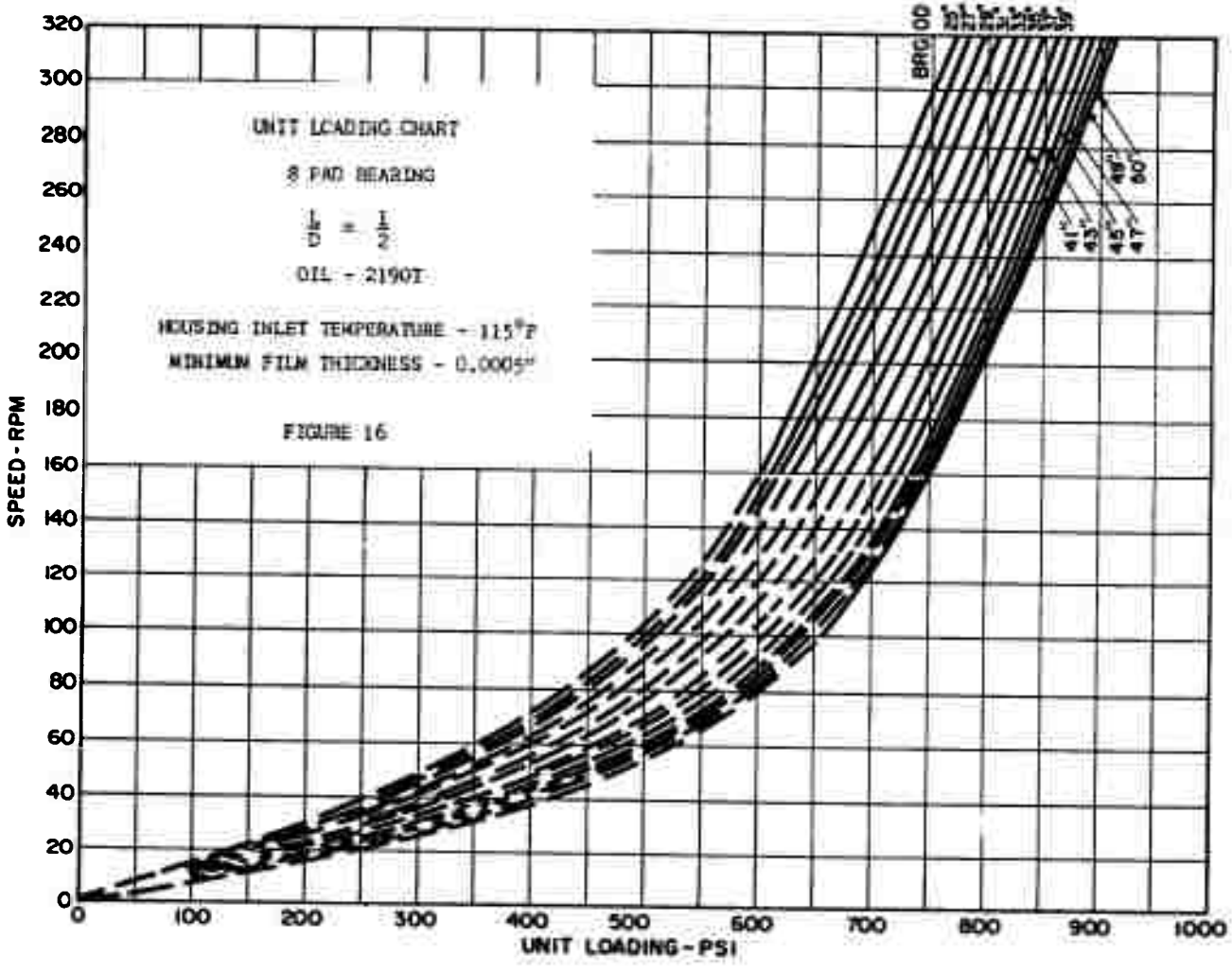
UNIT LOADING CHART
8 PAD BEARING
$\frac{L}{D} = \frac{1}{2}$
OIL - 2190T
HOUSING INLET TEMPERATURE - 115°F
MINIMUM FILM THICKNESS - 0.0005"
FIGURE 16
BRG OD
41"
43"
45"
47"
49"
50"
SPEED - RPM
0
20
40
60
80
100
120
140
160
180
200
220
240
260
280
300
320
0
100
200
300
400
500
600
700
800
900
1000
UNIT LOADING - PSI

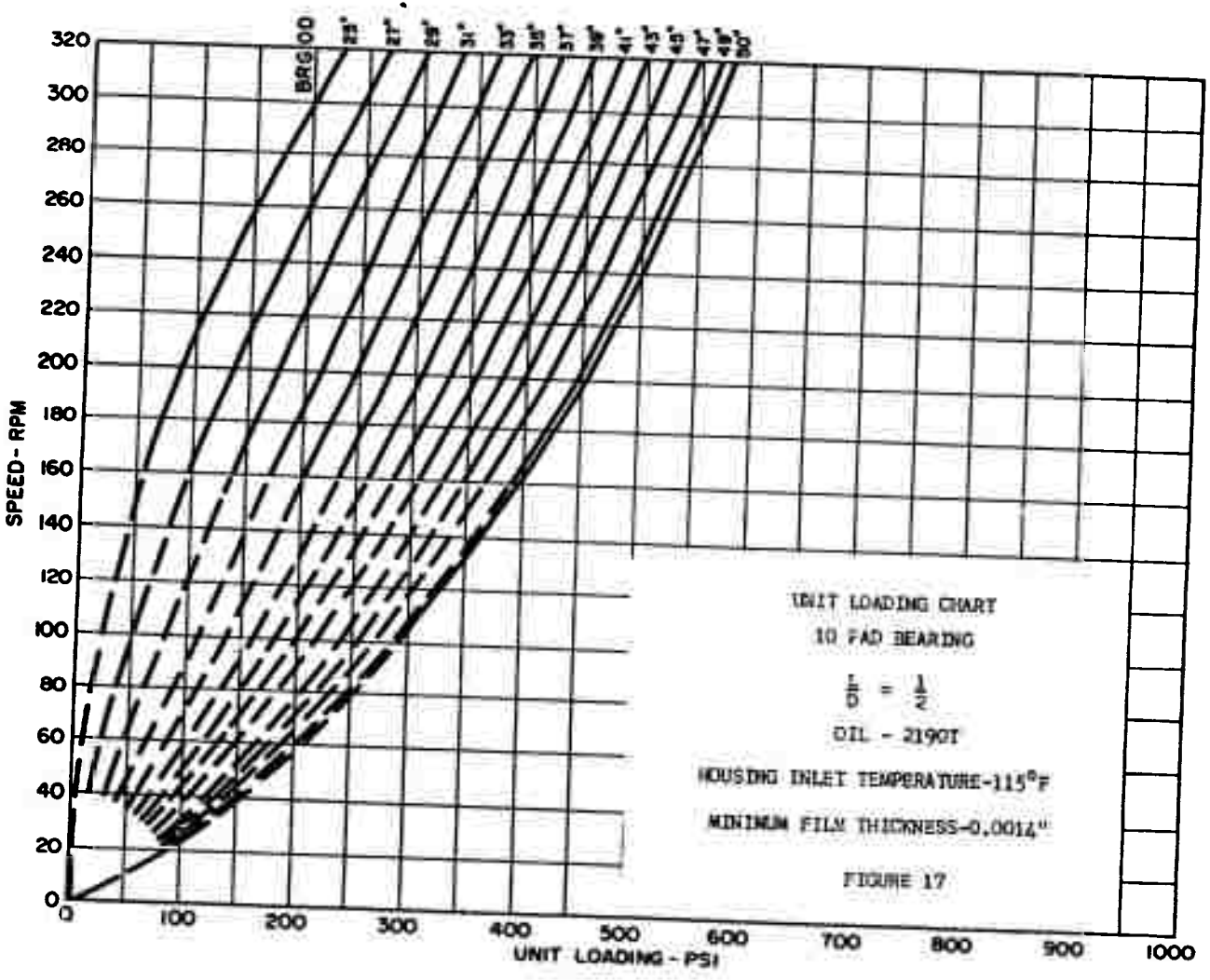
BRG OD
SPEED - RPM
UNIT LOADING - PSI
0
20
40
60
80
100
120
140
160
180
200
220
240
260
280
300
320
0
100
200
300
400
500
600
700
800
900
1000
UNIT LOADING CHART
10 PAD BEARING
L/D = 1/2
OIL - 2190T
HOUSING INLET TEMPERATURE-115°F
MINIMUM FILM THICKNESS-0.0014"

FIGURE 17

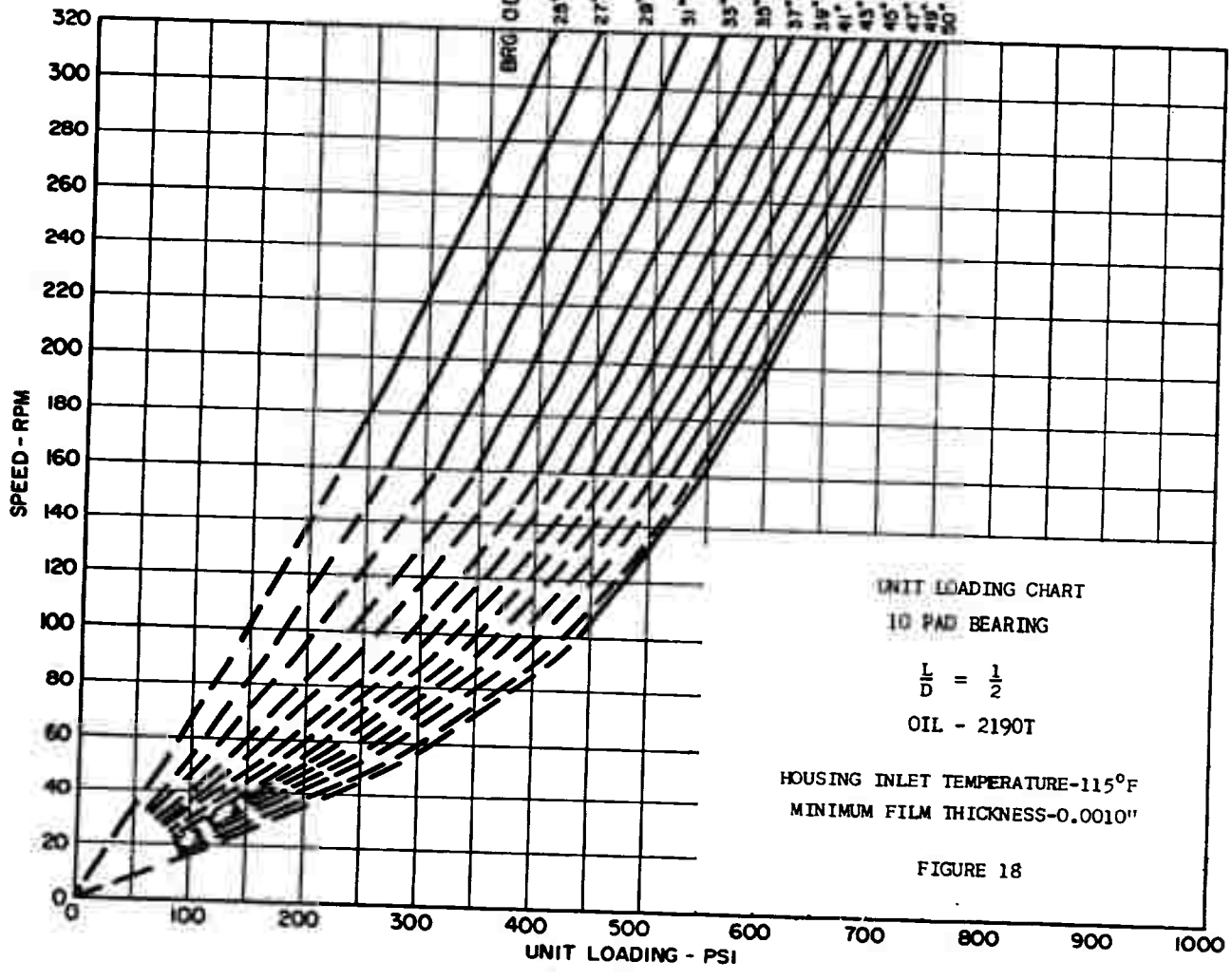
BRG O.D.
25"
27"
29"
31"
33"
35"
37"
39"
41"
43"
45"
47"
49"
50"
SPEED - RPM
320
300
280
260
240
220
200
180
160
140
120
100
80
60
40
20
0
0
100
200
300
400
500
600
700
800
900
1000
UNIT LOADING - PSI
UNIT LOADING CHART
10 PAD BEARING
L/D = 1/2
OIL - 2190T
HOUSING INLET TEMPERATURE-115°F
MINIMUM FILM THICKNESS-0.0010"

FIGURE 18

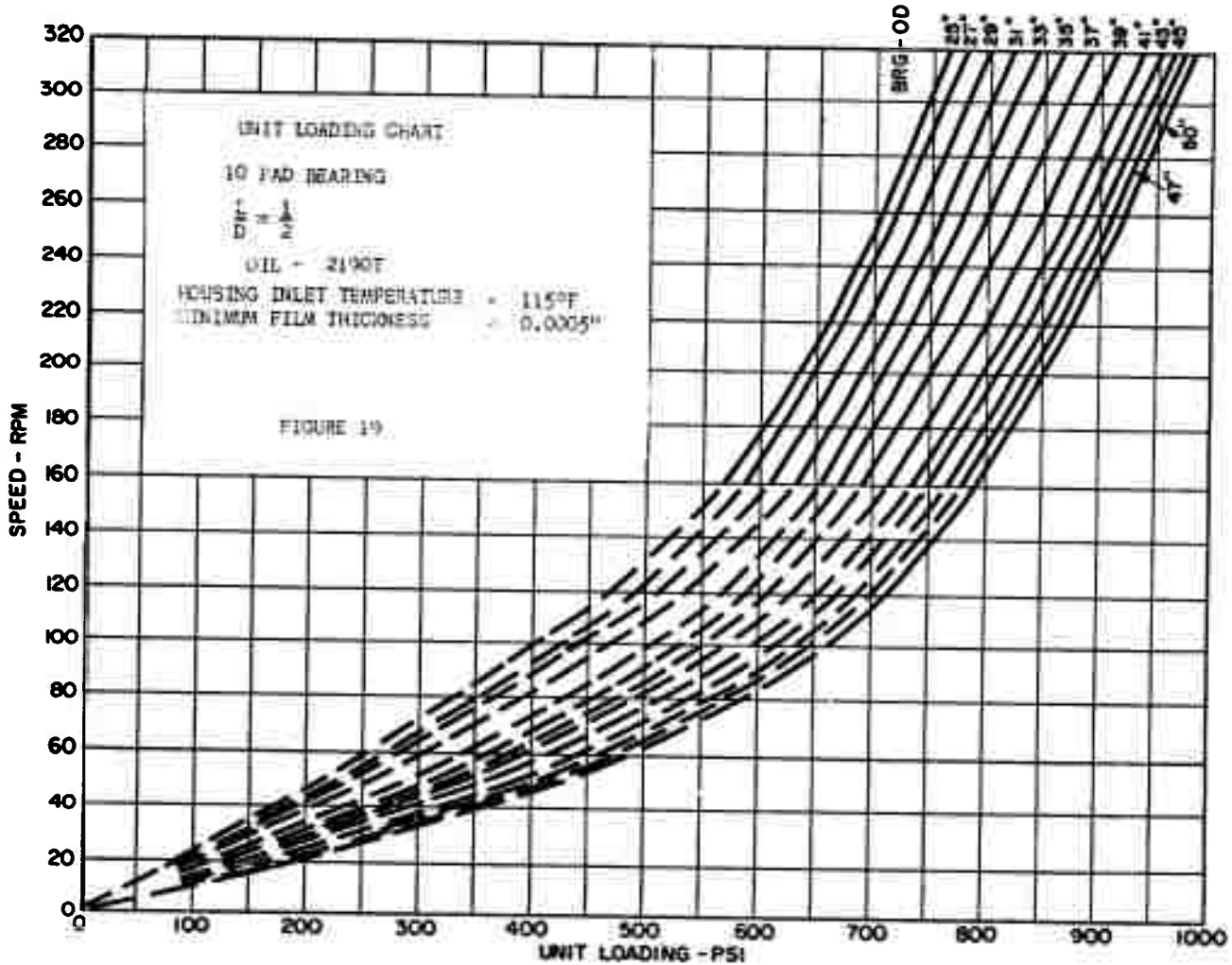
UNIT LOADING CHART
10 PAD BEARING
L/D = 1/2
OIL - 21 POT
HOUSING INLET TEMPERATURE - 115°F
MINIMUM FILM THICKNESS - 0.0005"
FIGURE 19
BRG - OD
SPEED - RPM
UNIT LOADING - PSI
0
20
40
60
80
100
120
140
160
180
200
220
240
260
280
300
320
100
200
300
400
500
600
700
800
900
1000

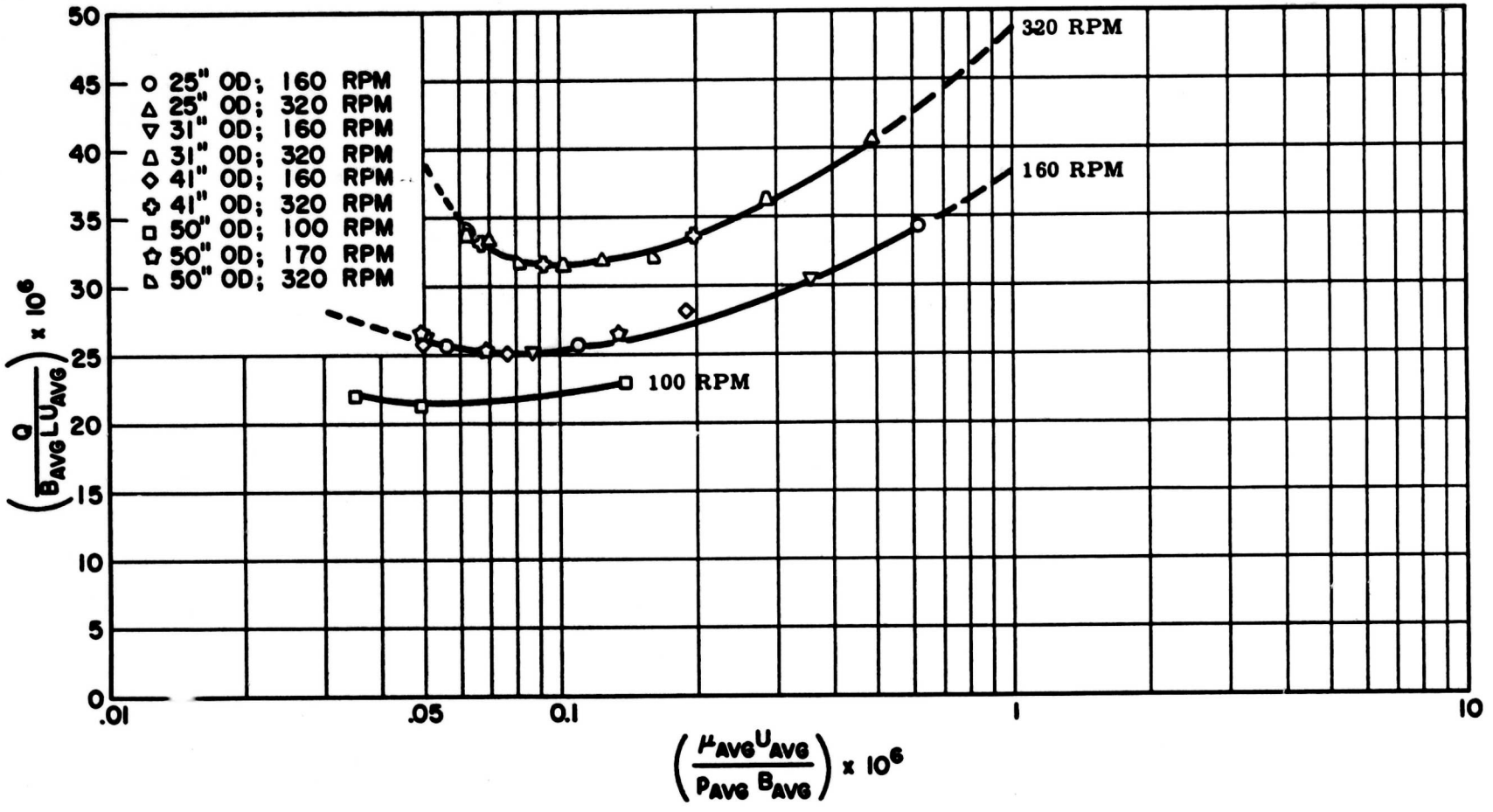


CHART OF OIL FLOW PER PAD

6 PAD BEARING

OIL - 2190T

AVERAGE TEMPERATURE PER FIG. 1

FIGURE 20

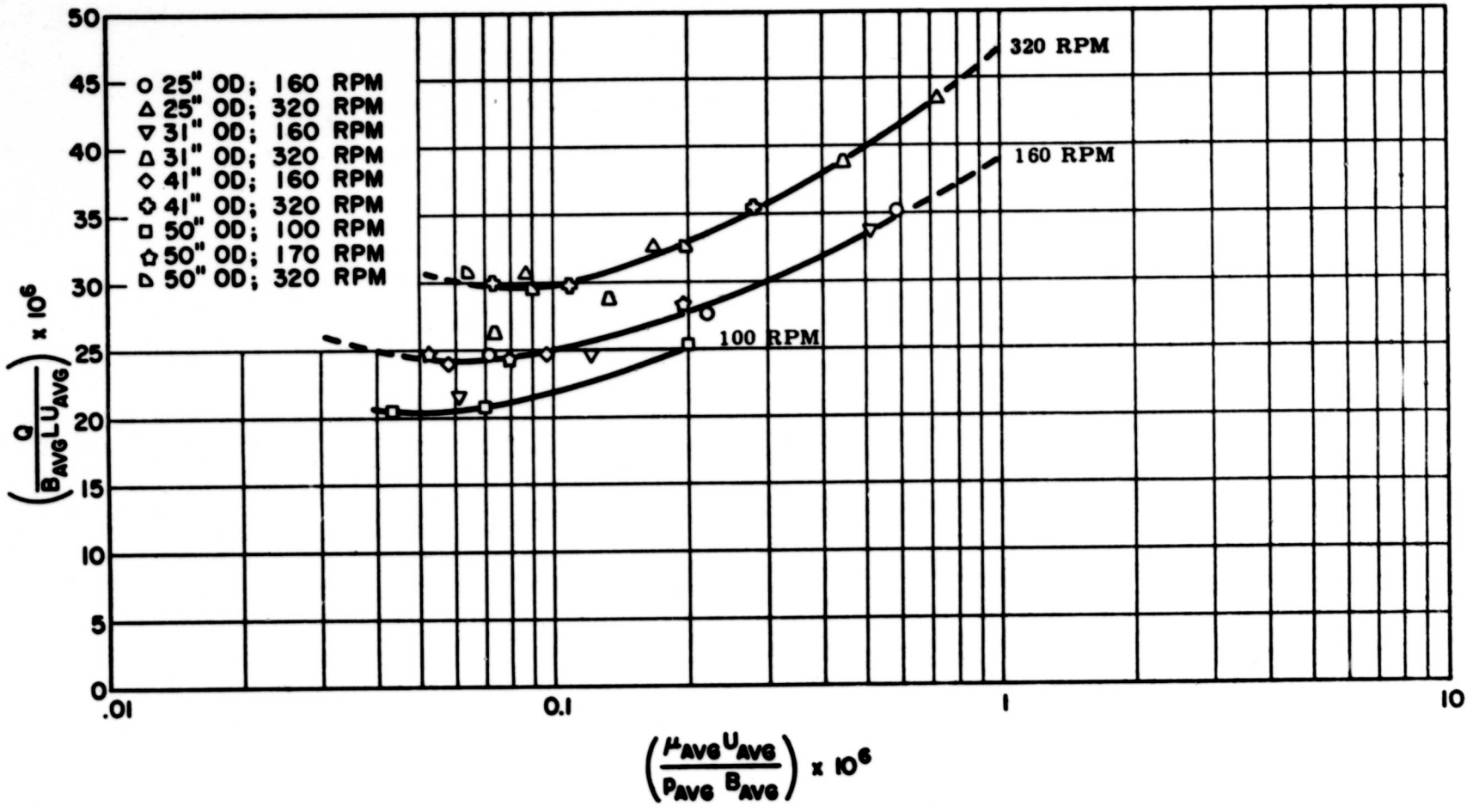


CHART OF OIL FLOW PER PAD

8 PAD BEARING OIL 2190T

AVERAGE TEMPERATURE PER FIG. 1

FIGURE 21

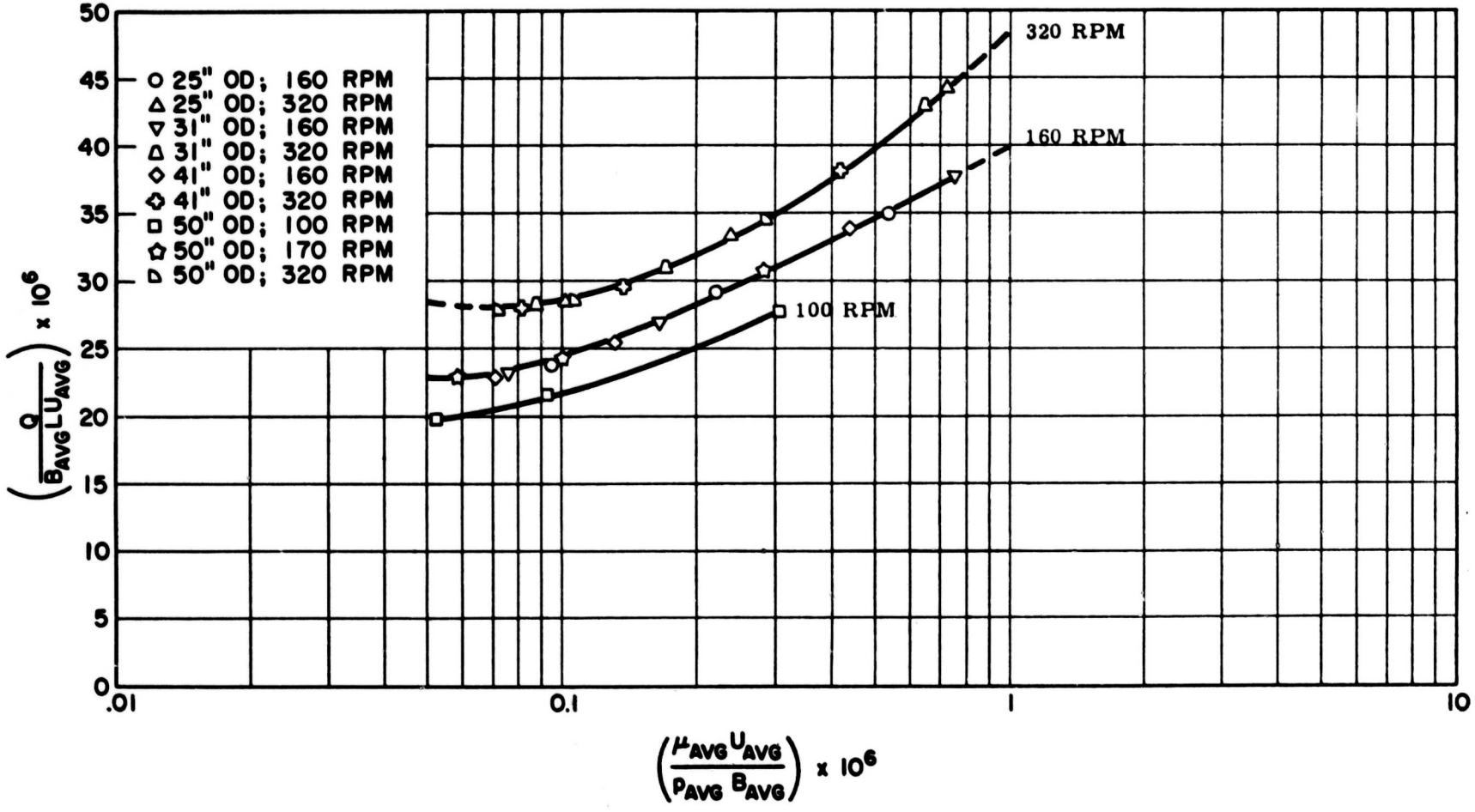


CHART OF OIL FLOW PER PAD

10 PAD BEARING

OIL - 2190T

AVERAGE TEMPERATURE PER FIG. 1

FIGURE 22

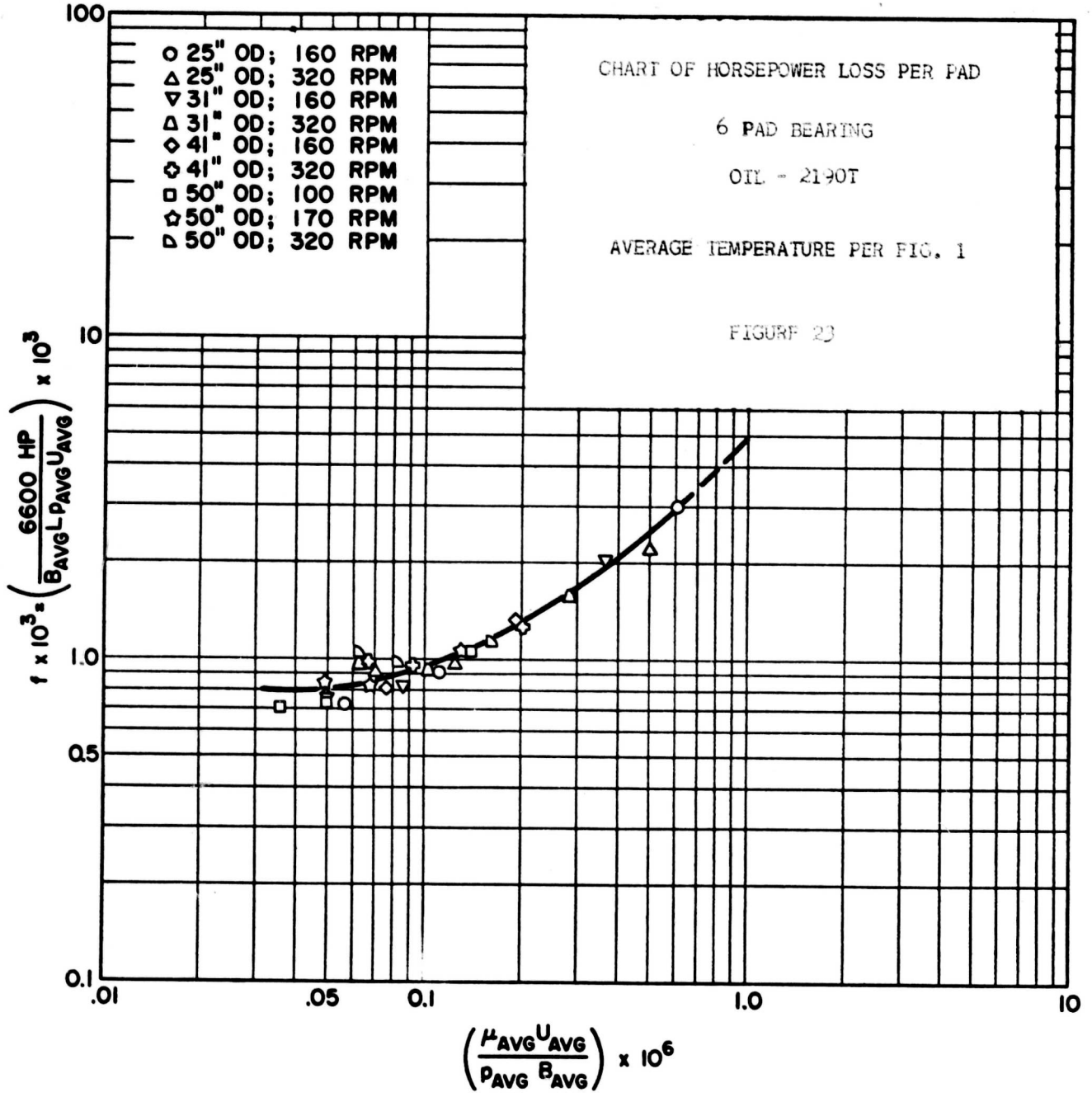
CHART OF HORSEPOWER LOSS PER PAD
6 PAD BEARING
OIL - 2190T
AVERAGE TEMPERATURE PER FIG. 1
FIGURE 23
○ 25" OD; 160 RPM
△ 25" OD; 320 RPM
▽ 31" OD; 160 RPM
△ 31" OD; 320 RPM
◇ 41" OD; 160 RPM
☆ 41" OD; 320 RPM
□ 50" OD; 100 RPM
☆ 50" OD; 170 RPM
▷ 50" OD; 320 RPM
100
10
1.0
0.5
0.1
.01
.05
0.1
1.0
10
$f \times 10^3 = \left(\frac{6600\ HP}{B_{AVG} L P_{AVG} U_{AVG}}\right) \times 10^3$
$\left(\frac{\mu_{AVG} U_{AVG}}{P_{AVG} B_{AVG}}\right) \times 10^6$

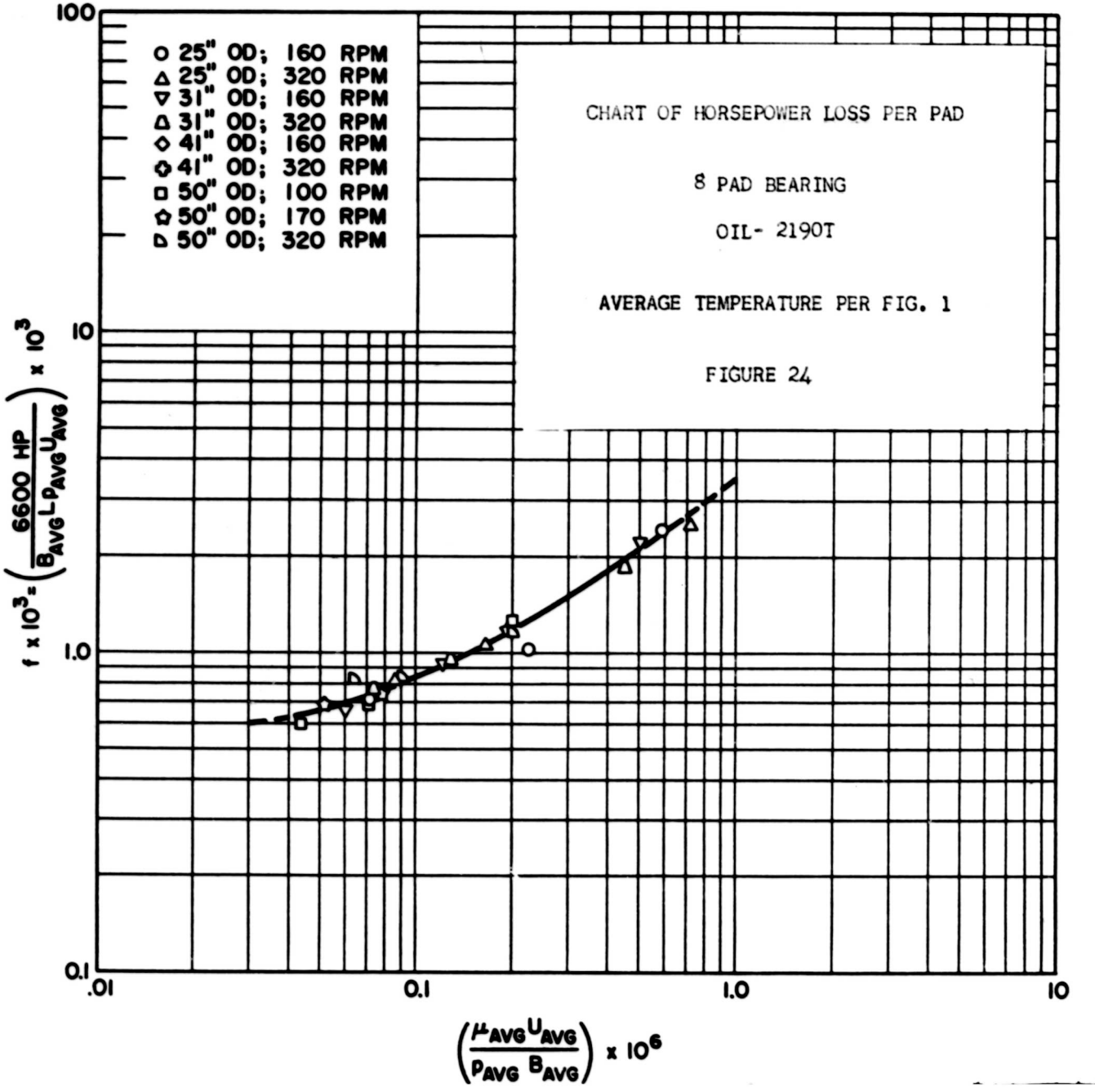
○ 25" OD; 160 RPM
△ 25" OD; 320 RPM
▽ 31" OD; 160 RPM
△ 31" OD; 320 RPM
◇ 41" OD; 160 RPM
✧ 41" OD; 320 RPM
□ 50" OD; 100 RPM
☆ 50" OD; 170 RPM
▷ 50" OD; 320 RPM
CHART OF HORSEPOWER LOSS PER PAD
8 PAD BEARING
OIL- 2190T
AVERAGE TEMPERATURE PER FIG. 1
FIGURE 24
100
10
1.0
0.1
.01
0.1
1.0
10
$f \times 10^3 = \left(\frac{6600\ HP}{B_{AVG} L P_{AVG} U_{AVG}}\right) \times 10^3$
$\left(\frac{\mu_{AVG} U_{AVG}}{P_{AVG} B_{AVG}}\right) \times 10^6$

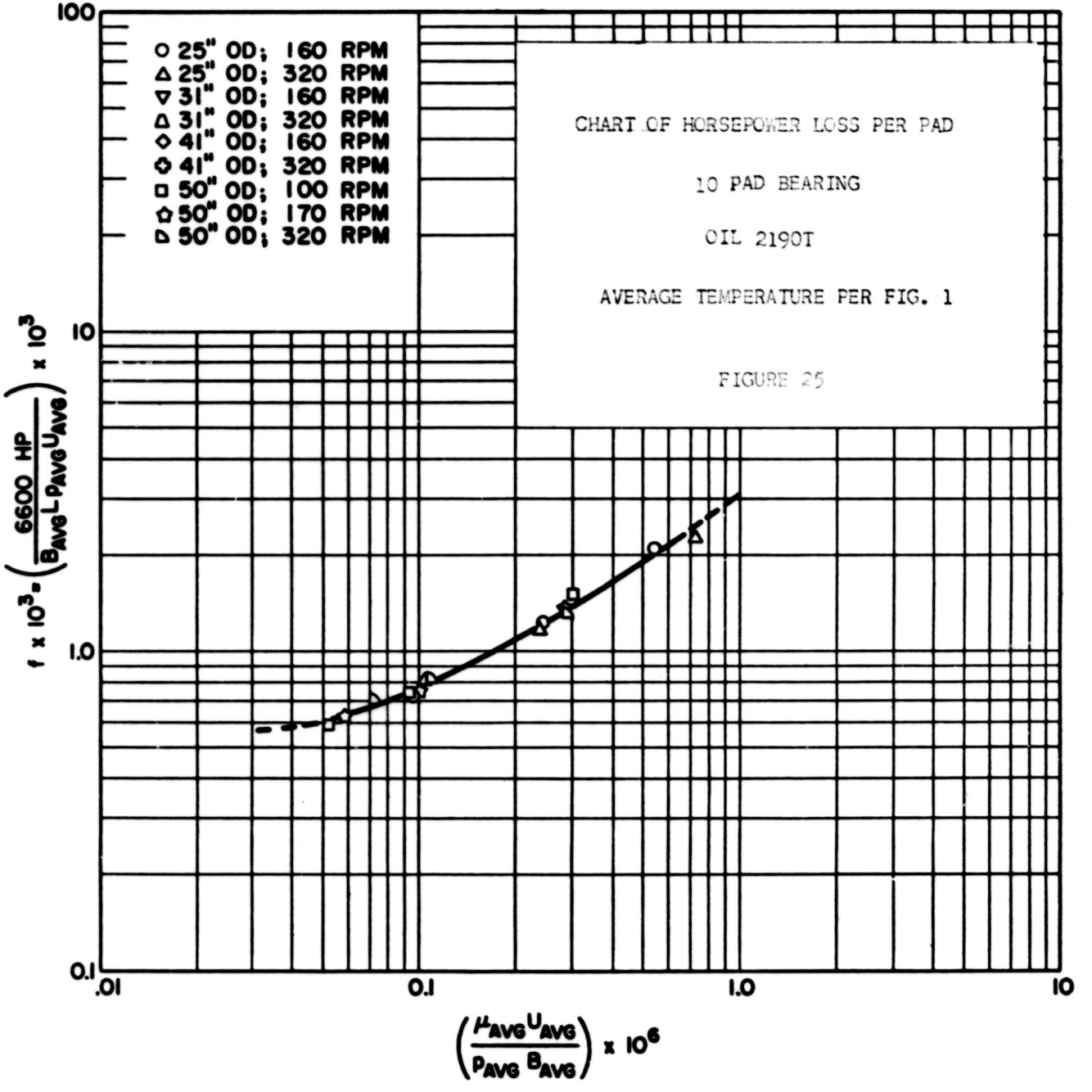
○ 25" OD; 160 RPM
△ 25" OD; 320 RPM
▽ 31" OD; 160 RPM
△ 31" OD; 320 RPM
◇ 41" OD; 160 RPM
◇ 41" OD; 320 RPM
□ 50" OD; 100 RPM
☆ 50" OD; 170 RPM
△ 50" OD; 320 RPM
CHART OF HORSEPOWER LOSS PER PAD
10 PAD BEARING
OIL 2190T
AVERAGE TEMPERATURE PER FIG. 1
FIGURE 25
100
10
1.0
0.1
.01
0.1
1.0
10
$f \times 10^3 = \left(\frac{6600\ HP}{B_{AVG} L P_{AVG} U_{AVG}}\right) \times 10^3$
$\left(\frac{\mu_{AVG} U_{AVG}}{P_{AVG} B_{AVG}}\right) \times 10^6$

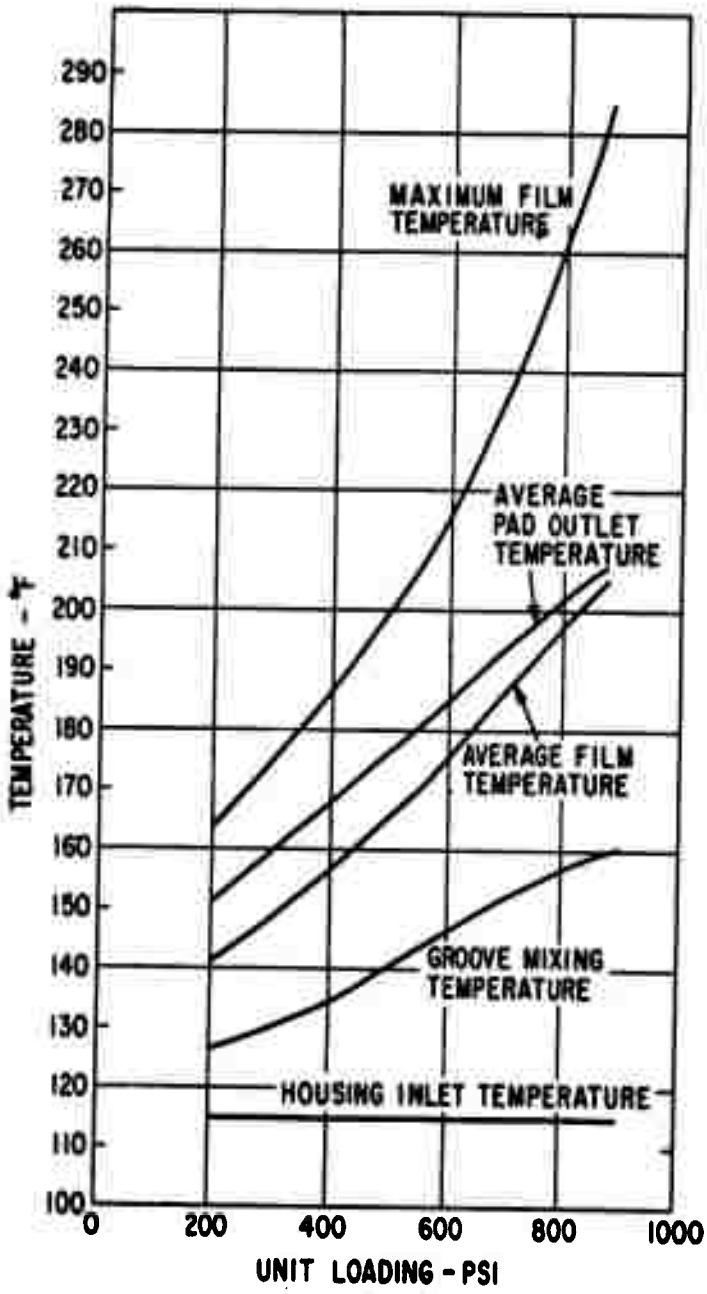


OIL TEMPERATURE VS. UNIT LOADING

(Pad Geometry Per Fig. A-2; Oil 2190T)

FIGURE 26

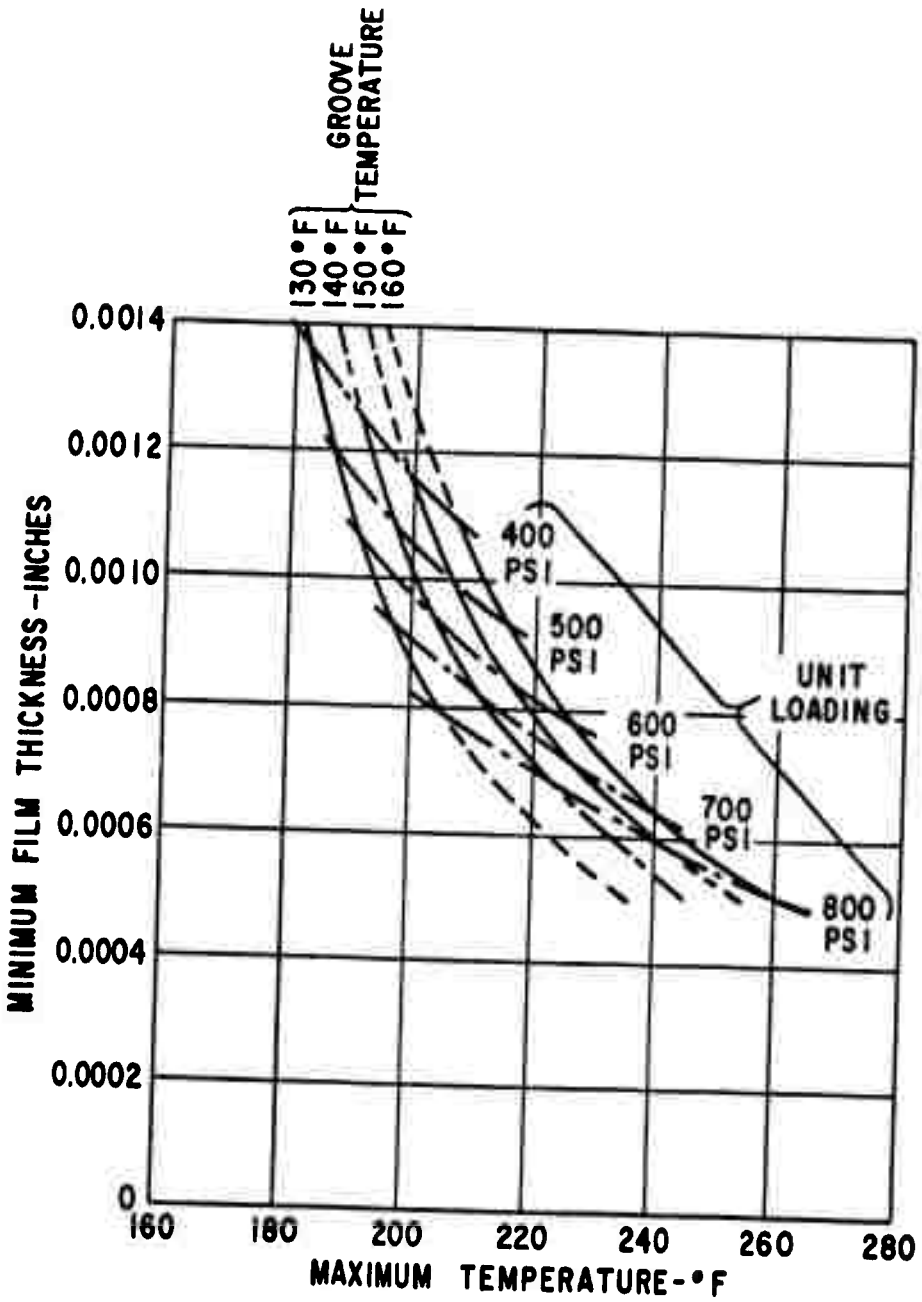


INFLUENCE OF GROOVE MIXING TEMPERATURE

(Pad Dimensions Per Fig.A-2; Oil-2190T; Speed-320 RPM)

FIGURE 27

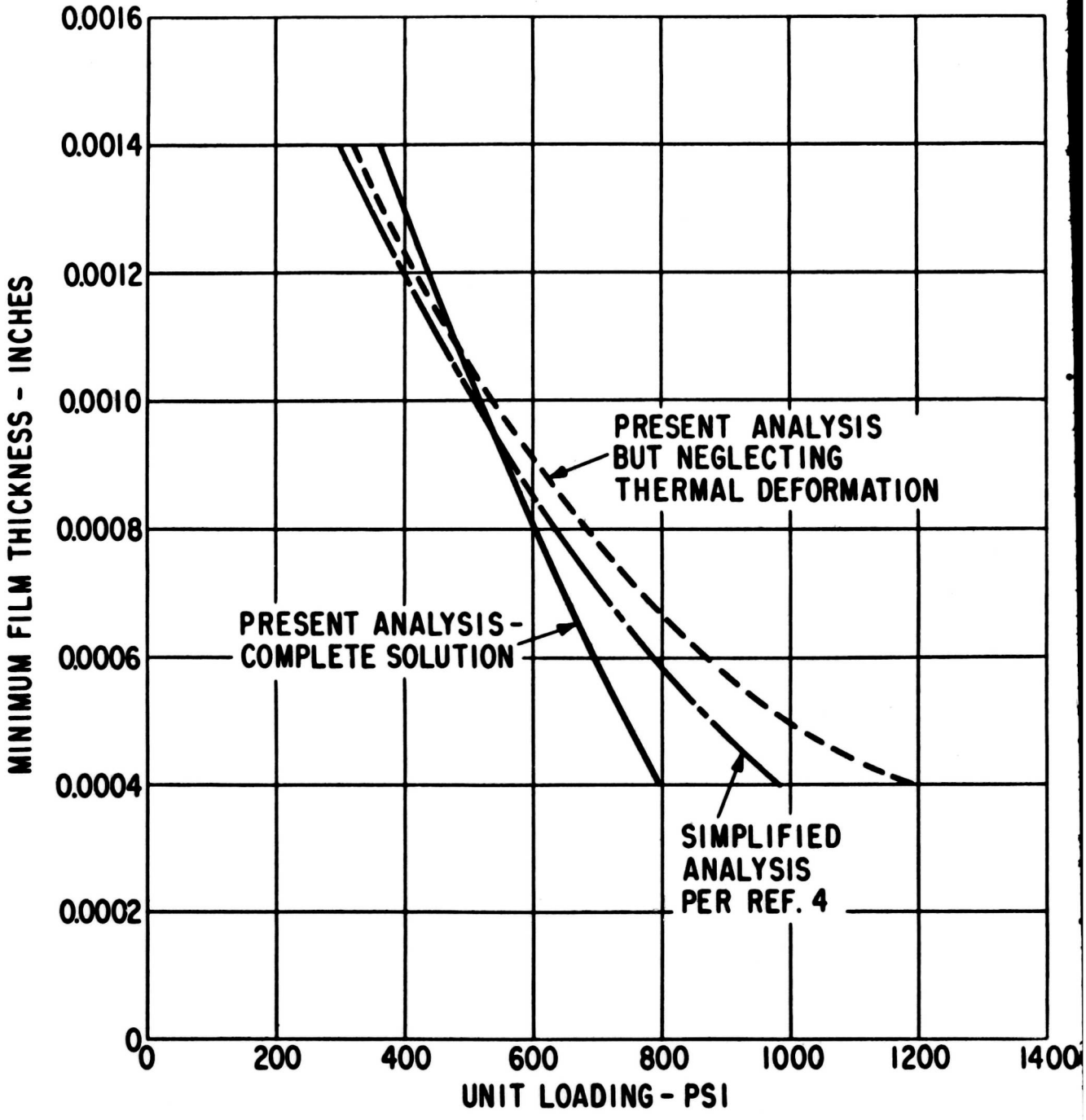


COMPARISON OF ANALYTICAL RESULTS -
MINIMUM FILM THICKNESS VS. UNIT LOADING

(31"O.D.x16½"I.D.Bearing; 2190T-Oil; 320 RPM )

FIGURE 28

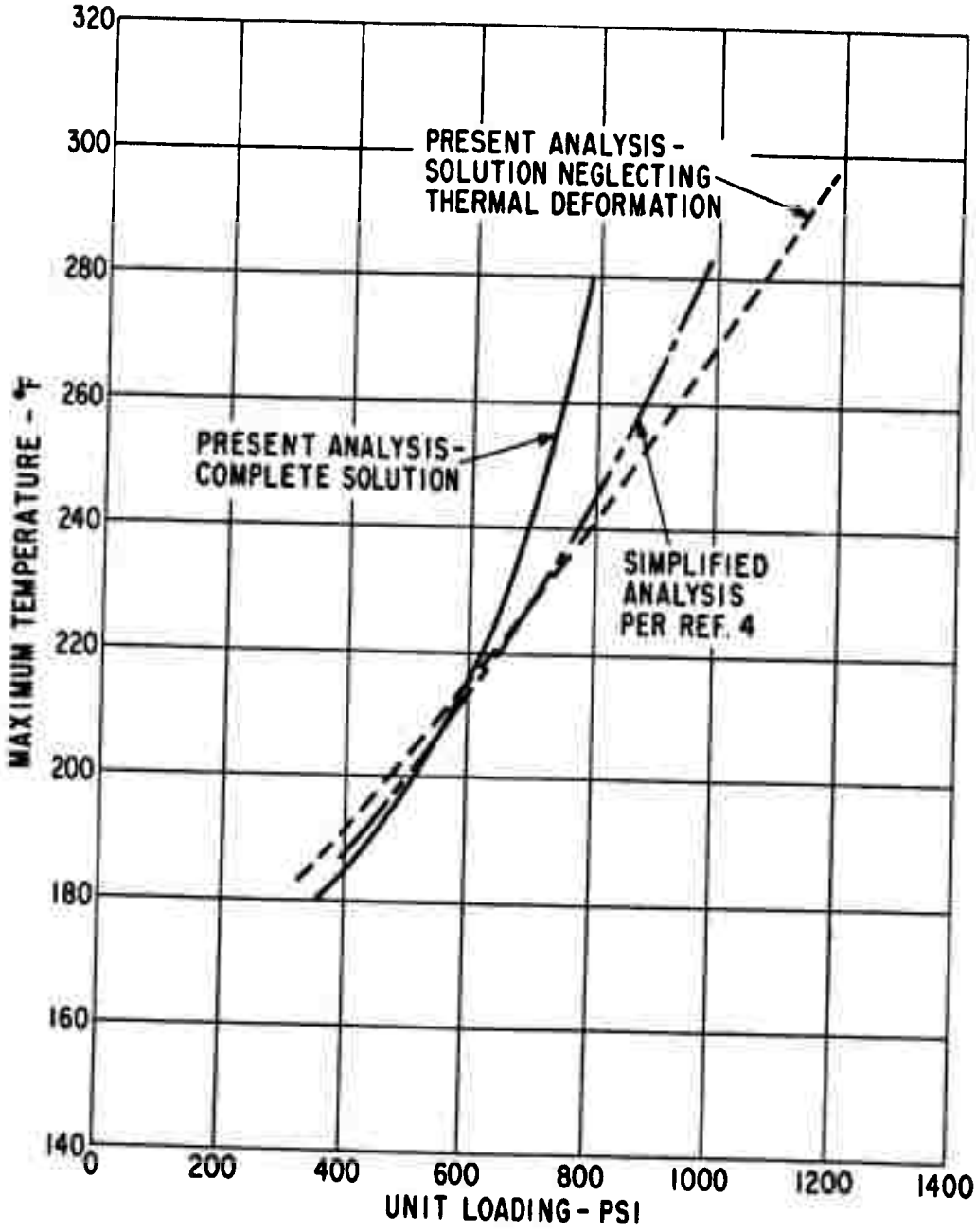


COMPARISON OF ANALYTICAL RESULTS -
MAXIMUM TEMPERATURE VS. UNIT LOADING

(31"O.D.x16-1/2"I.D.Bearing; 2190T-011; 320 R.P.M.)

FIGURE 29

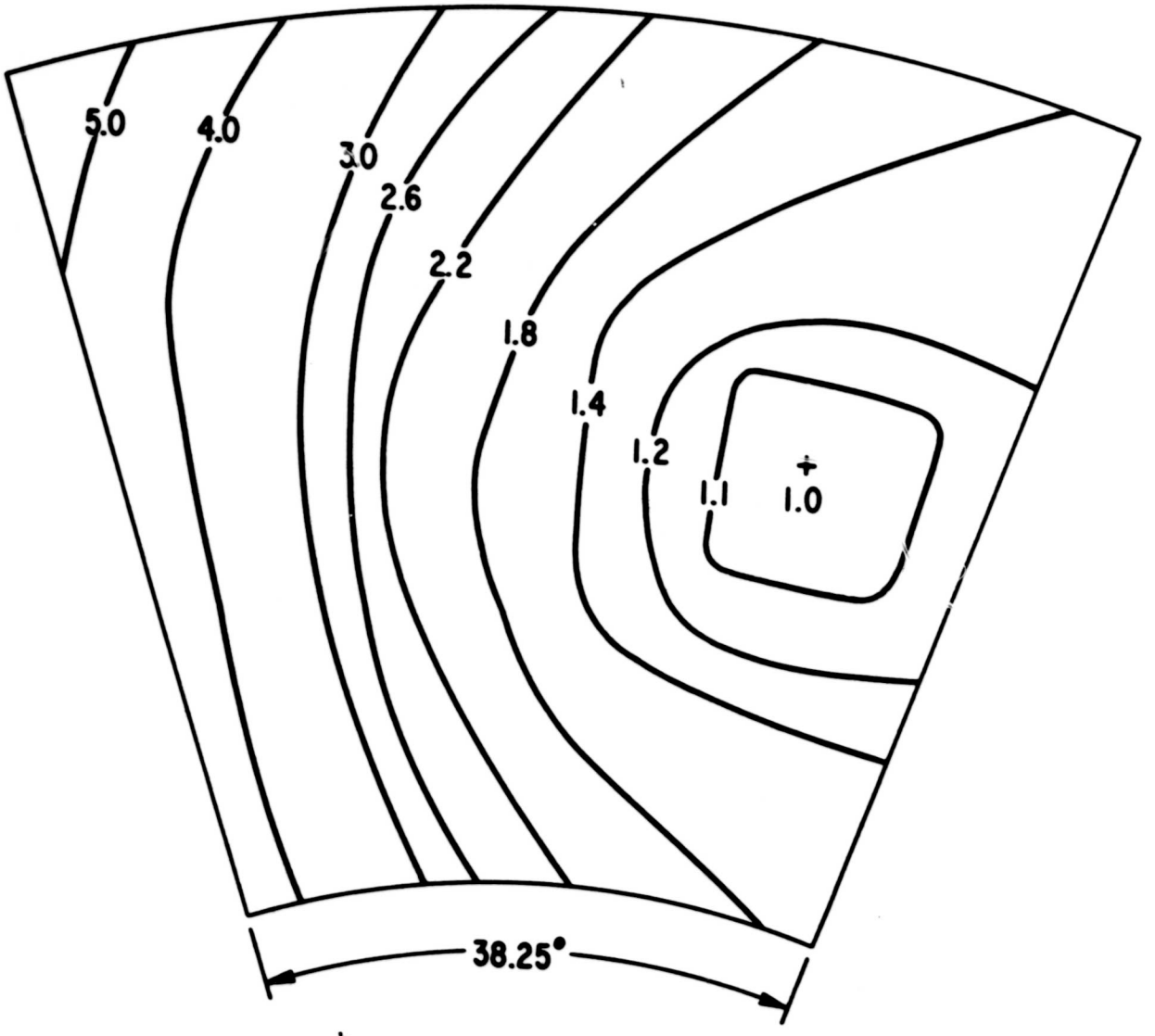


CONTOUR LINES OF $\frac{h}{h_{min.}}$, FOR $h_{min.}$ =0.0004" - THERMAL DEFLECTIONS NEGLECTED

(31"O.D.x16-1/2"I.D.Bearing; 2190T-Oil; 320 R.P.M.)

FIGURE 30

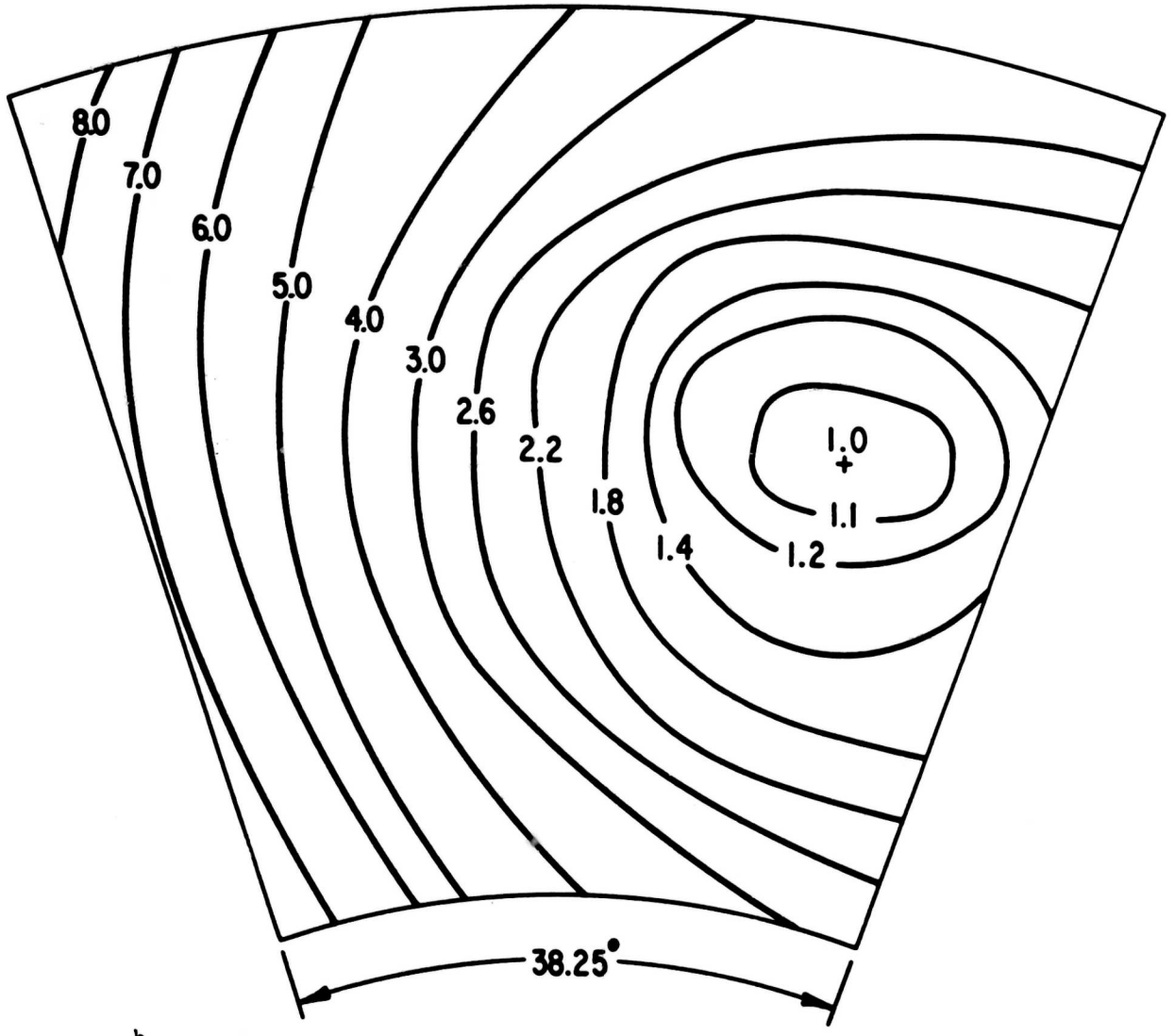


CONTOUR LINES OF $\left(\frac{h}{h_{min}}\right)$ FOR $h_{min}$ = 0.0004 " - THERMAL DEFLECTIONS INCLUDED

(31" O.D. x 16 1/2" I.D. Bearing; 2190T - Oil; 320 R.P.M.)

FIGURE 31

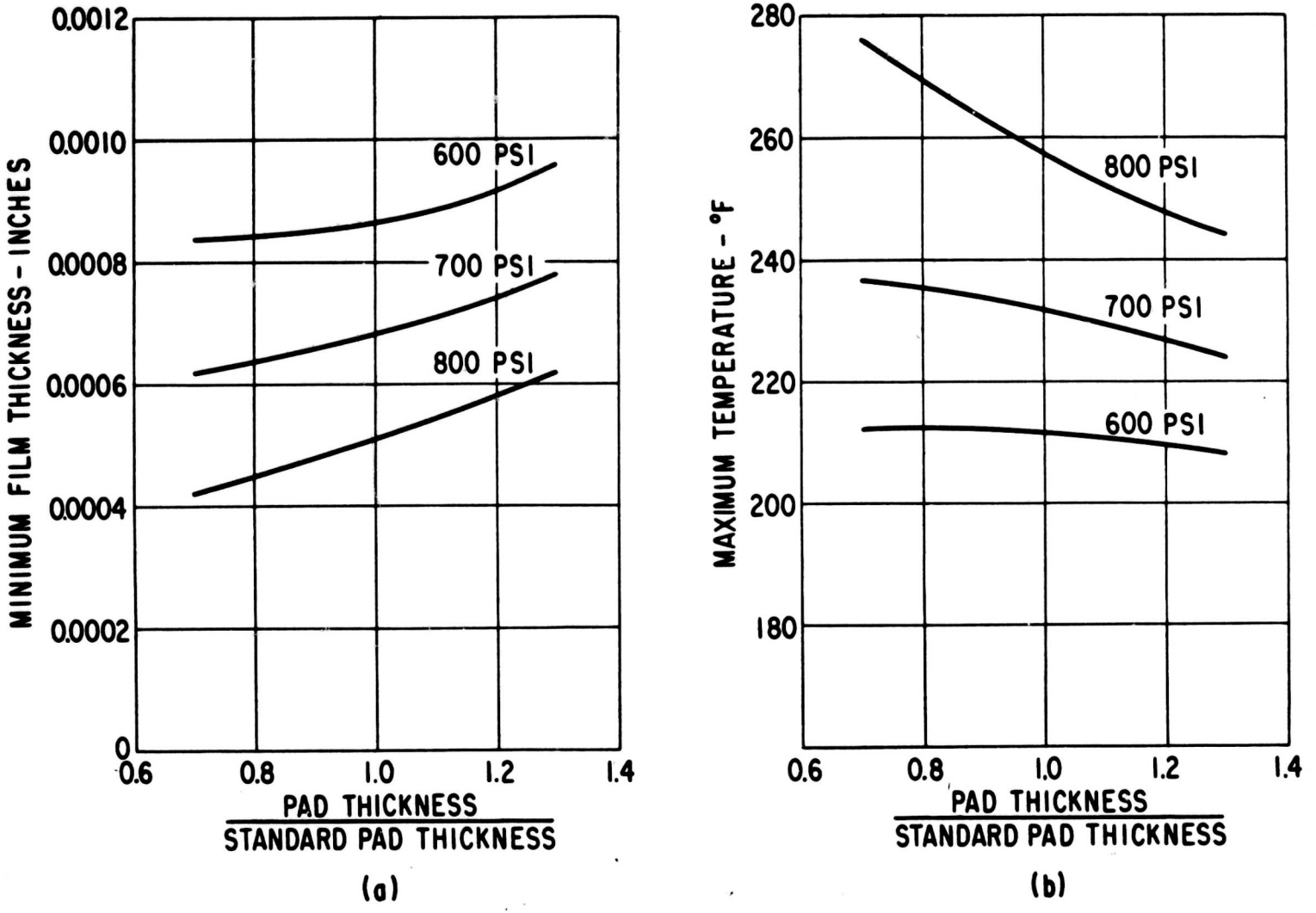


INFLUENCE OF PAD THICKNESS

(31" O.D. x 15 1/2" I.D. Bearing; 2190T - Oil; 320 R.P.M.)

FIGURE 32

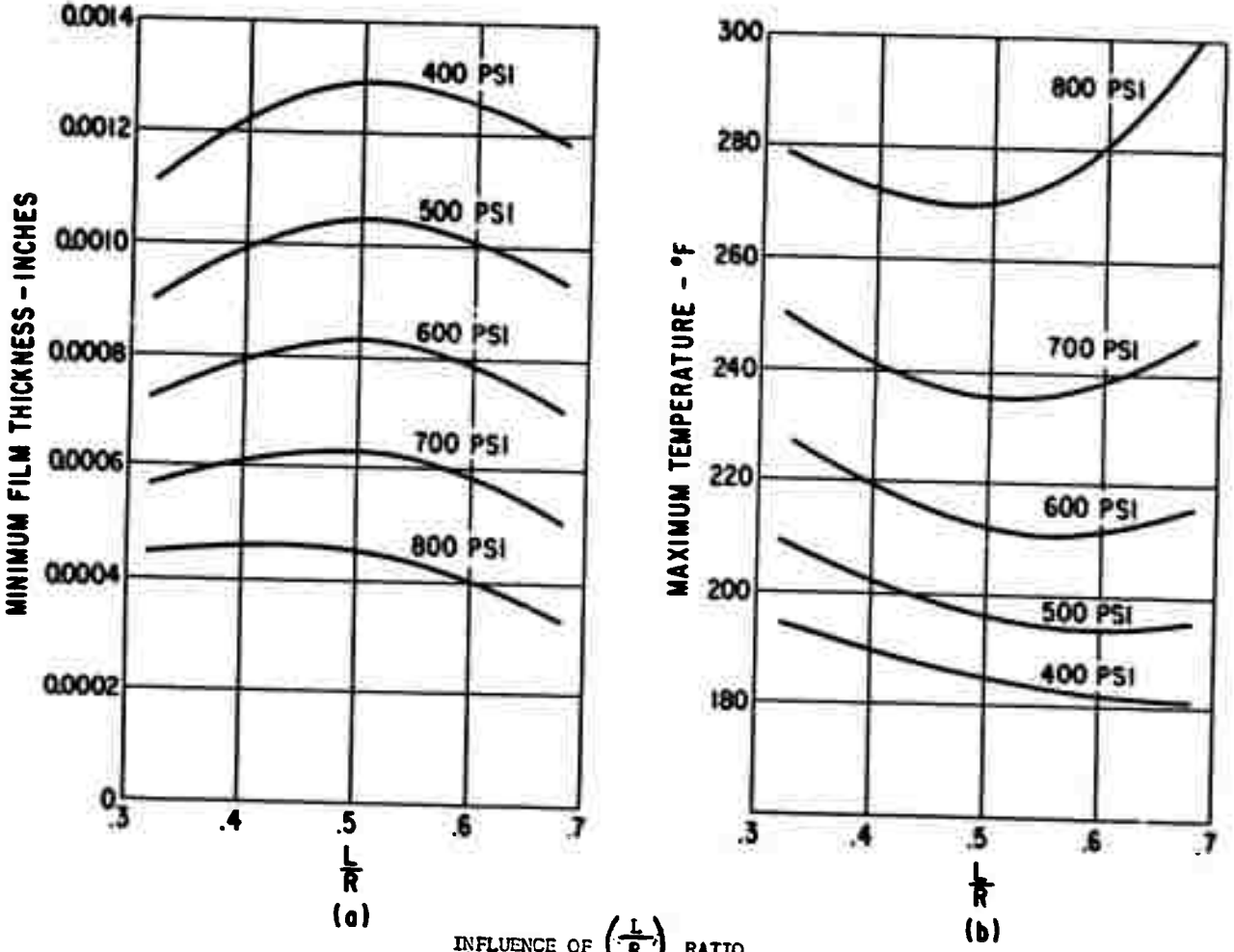


INFLUENCE OF $\left(\frac{L}{R}\right)$ RATIO

(31" O.D. Bearing; 2190T - Oil; 320 R.P.M.)

FIGURE 33

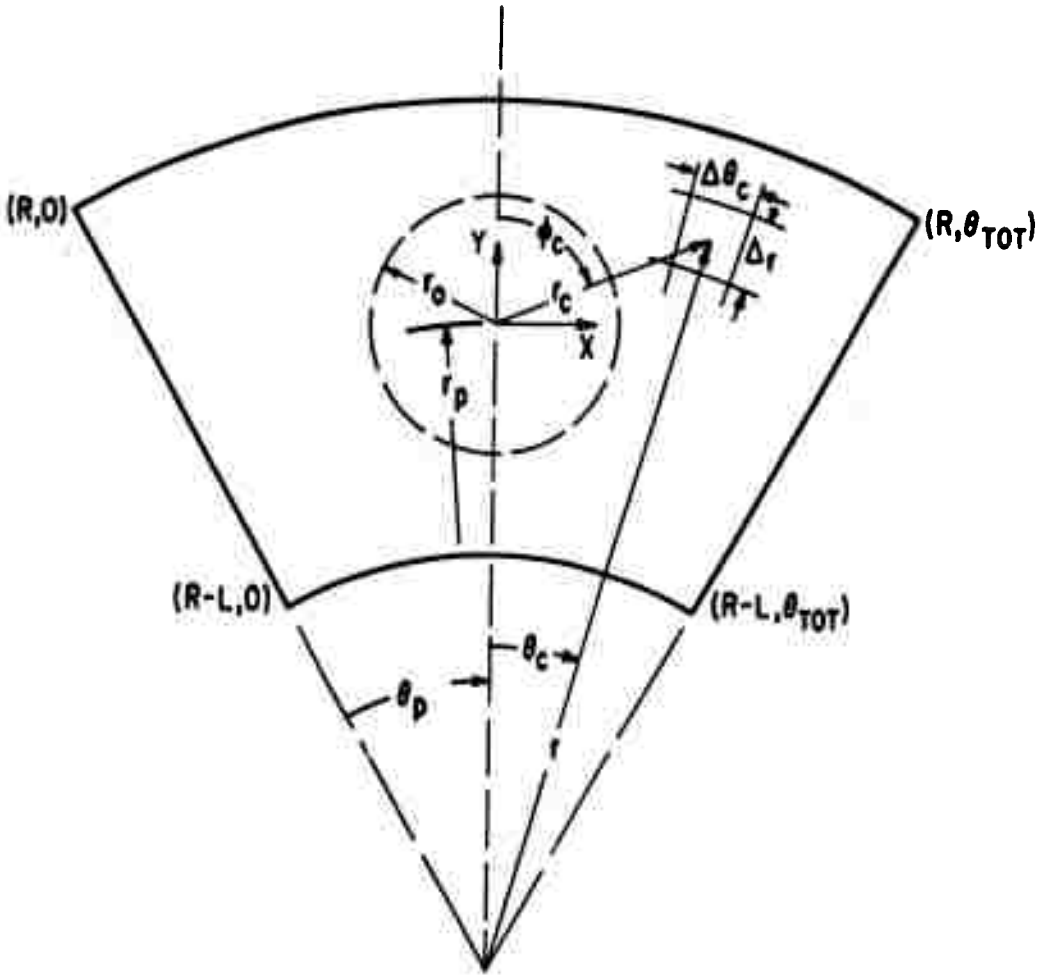


COORDINATE SYSTEM

FIGURE A-1

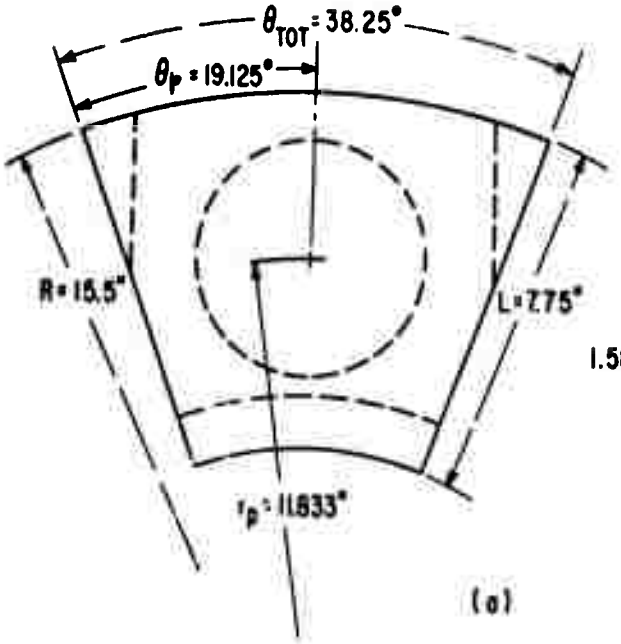


(a)

r = R

| | | | | | | | | | | | | |
|---|---|---|---|---|---|---|---|---|---|---|---|---|
| 1.625 | 2.242 | 2.860 | 2.860 | 2.860 | 2.860 | 2.860 | 2.860 | 2.860 | 2.860 | 2.860 | 2.242 | 1.625 |
| 1.625 | 2.551 | 2.860 | 2.860 | 2.860 | 2.860 | 2.860 | 2.860 | 2.860 | 2.860 | 2.860 | 2.551 | 1.625 |
| 1.625 | 2.860 | 2.860 | 2.860 | 2.285 | 1.997 | 1.710 | 1.997 | 2.285 | 2.860 | 2.860 | 2.860 | 1.625 |
| 1.934 | 2.860 | 2.860 | 2.285 | 1.679 | 1.616 | 1.585 | 1.616 | 1.679 | 2.285 | 2.860 | 2.860 | 1.934 |
| 2.242 | 2.860 | 2.572 | 1.679 | 1.585 | 1.585 | 1.585 | 1.585 | 1.585 | 1.679 | 2.572 | 2.860 | 2.242 |
| 2.551 | 2.860 | 2.285 | 1.647 | 1.585 | 1.585 | 1.585 | 1.585 | 1.585 | 1.647 | 2.285 | 2.860 | 2.551 |
| 2.860 | 2.860 | 1.997 | 1.616 | 1.585 | 1.585 | 1.585 | 1.585 | 1.585 | 1.616 | 1.997 | 2.860 | 2.860 |
| 2.860 | 2.860 | 2.285 | 1.647 | 1.585 | 1.585 | 1.585 | 1.585 | 1.585 | 1.647 | 2.285 | 2.860 | 2.860 |
| 2.860 | 2.860 | 2.572 | 1.710 | 1.616 | 1.585 | 1.585 | 1.585 | 1.616 | 1.710 | 2.572 | 2.860 | 2.860 |
| 2.860 | 2.860 | 2.860 | 2.572 | 1.710 | 1.679 | 1.679 | 1.679 | 1.710 | 2.572 | 2.860 | 2.860 | 2.860 |
| 2.860 | 2.860 | 2.860 | 2.860 | 2.860 | 2.572 | 2.572 | 2.572 | 2.860 | 2.860 | 2.860 | 2.860 | 2.860 |
| 1.625 | 1.625 | 1.625 | 1.625 | 1.625 | 1.625 | 1.625 | 1.625 | 1.625 | 1.625 | 1.625 | 1.625 | 1.625 |
| 1.625 | 1.625 | 1.625 | 1.625 | 1.625 | 1.625 | 1.625 | 1.625 | 1.625 | 1.625 | 1.625 | 1.625 | 1.625 |

r = R-L

θ = 0

(b)

θ = $\theta_{TOT}$

PAD GEOMETRY AND DIMENSIONS OF 31"O.D.x15-1/2"I.D., 8 PAD BEARING

FIGURE A-2

## PAD THICKNESS PROFILE

r = R

| | | | | | | | | | | | | |
|---|---|---|---|---|---|---|---|---|---|---|---|---|
| 1.310 | 1.808 | 2.306 | 2.306 | 2.306 | 2.306 | 2.306 | 2.306 | 2.306 | 2.306 | 2.306 | 1.808 | 1.310 |
| 1.310 | 2.057 | 2.306 | 2.306 | 2.306 | 2.306 | 2.306 | 2.306 | 2.306 | 2.306 | 2.306 | 2.057 | 1.310 |
| 1.310 | 2.306 | 2.306 | 2.306 | 2.306 | 1.843 | 1.610 | 1.843 | 2.306 | 2.306 | 2.306 | 2.306 | 1.310 |
| 1.560 | 2.306 | 2.306 | 2.306 | 1.843 | 1.354 | 1.303 | 1.354 | 1.843 | 2.306 | 2.306 | 2.306 | 1.560 |
| 1.808 | 2.306 | 2.306 | 2.074 | 1.354 | 1.278 | 1.278 | 1.278 | 7.354 | 2.074 | 2.306 | 2.306 | 1.808 |
| 2.057 | 2.306 | 2.306 | 1.843 | 1.303 | 1.278 | 1.278 | 1.278 | 1.303 | 1.843 | 2.306 | 2.306 | 2.057 |
| 2.306 | 2.306 | 2.306 | 1.843 | 1.303 | 1.278 | 1.278 | 1.278 | 1.303 | 1.843 | 2.306 | 2.306 | 2.306 |
| 2.306 | 2.306 | 2.306 | 1.843 | 1.303 | 1.278 | 1.278 | 1.278 | 1.303 | 1.843 | 2.306 | 2.306 | 2.306 |
| 2.306 | 2.306 | 2.306 | 2.074 | 1.328 | 1.278 | 1.278 | 1.278 | 1.328 | 2.074 | 2.306 | 2.306 | 2.306 |
| 2.306 | 2.306 | 2.306 | 2.306 | 1.610 | 1.610 | 1.328 | 1.610 | 1.610 | 2.306 | 2.306 | 2.306 | 2.306 |
| 2.306 | 2.306 | 2.306 | 2.306 | 2.306 | 1.644 | 1.610 | 1.641 | 2.306 | 2.306 | 2.306 | 2.306 | 2.306 |
| 1.310 | 1.310 | 1.310 | 1.310 | 1.310 | 1.310 | 1.310 | 1.310 | 1.310 | 1.310 | 1.310 | 1.310 | 1.310 |
| 1.310 | 1.310 | 1.310 | 1.310 | 1.310 | 1.310 | 1.310 | 1.310 | 1.310 | 1.310 | 1.310 | 1.310 | 1.310 |

r = R-L

θ = 0

R = 12.5"

L = 6.25"

$\theta_T$ = 51°

$r_p$ = 9.404"

$\theta_p$ = 25.5°

$R_B$ = 1.512"

$t_B$ = 0.976"

Pad dimensions - 25 in. O.D. x 12 1/2 in. I.D. 8 pad bearing

Figure A-3

PAD THICKNESS PROFILE

r = R

| | | | | | | | | | | | | |
|---|---|---|---|---|---|---|---|---|---|---|---|---|
| 1.310 | 1.808 | 2.306 | 2.306 | 2.306 | 2.306 | 2.306 | 2.306 | 2.306 | 2.306 | 2.306 | 1.808 | 1.310 |
| 1.310 | 2.057 | 2.306 | 2.306 | 2.306 | 2.306 | 2.306 | 2.306 | 2.306 | 2.306 | 2.306 | 2.057 | 1.310 |
| 1.310 | 2.306 | 2.306 | 2.306 | 1.843 | 1.610 | 1.379 | 1.610 | 1.843 | 2.306 | 2.306 | 2.306 | 1.310 |
| 1.560 | 2.306 | 2.306 | 1.843 | 1.354 | 1.303 | 1.278 | 1.303 | 1.354 | 1.843 | 2.306 | 2.306 | 1.560 |
| 1.808 | 2.306 | 2.074 | 1.354 | 1.278 | 1.278 | 1.278 | 1.278 | 1.278 | 1.354 | 2.074 | 2.306 | 1.808 |
| 2.057 | 2.306 | 1.843 | 1.328 | 1.278 | 1.278 | 1.278 | 1.278 | 1.278 | 1.328 | 1.843 | 2.306 | 2.057 |
| 1.844 | 2.306 | 1.610 | 1.303 | 1.278 | 1.278 | 1.278 | 1.278 | 1.278 | 1.303 | 1.610 | 2.306 | 1.844 |
| 1.844 | 2.306 | 1.843 | 1.328 | 1.278 | 1.278 | 1.278 | 1.278 | 1.278 | 1.328 | 1.843 | 1.206 | 1.844 |
| 1.844 | 2.306 | 2.074 | 1.379 | 1.303 | 1.278 | 1.278 | 1.278 | 1.303 | 1.379 | 2.074 | 2.306 | 1.844 |
| 1.844 | 2.306 | 2.306 | 2.074 | 1.379 | 1.354 | 1.354 | 1.354 | 1.379 | 2.074 | 2.306 | 2.306 | 1.844 |
| 1.844 | 2.306 | 2.306 | 2.306 | 2.306 | 2.074 | 2.074 | 2.074 | 2.306 | 2.306 | 2.306 | 2.306 | 1.844 |
| 1.310 | 1.310 | 1.310 | 1.310 | 1.310 | 1.310 | 1.310 | 1.310 | 1.310 | 1.310 | 1.310 | 1.310 | 1.310 |
| 1.310 | 1.310 | 1.310 | 1.310 | 1.310 | 1.310 | 1.310 | 1.310 | 1.310 | 1.310 | 1.310 | 1.310 | 1.310 |

r = R-L

θ =

R = 12.5"

L = 6.25"

$\theta_T$ = 38.25°

$r_p$ = 9.543"

$\theta_p$ = 19.125°

$R_B$ = 1.512"

$t_B$ = 0.976"

Pad Dimensions- 25 in. O.D. x 12 1/2 in. I.D. - 8 pad bearing

Figure A-4

PAD THICKNESS PROFILE

| r = R | | | | | | | | | | | | | |
|---|---|---|---|---|---|---|---|---|---|---|---|---|---|
| | 1.310 | 1.808 | 2.306 | 2.306 | 2.306 | 2.306 | 2.306 | 2.306 | 2.306 | 2.306 | 2.306 | 1.808 | 1.310 |
| | 1.310 | 2.057 | 2.306 | 2.306 | 2.306 | 2.306 | 2.074 | 2.306 | 2.306 | 2.306 | 2.306 | 2.057 | 1.310 |
| | 1.310 | 2.306 | 2.306 | 1.610 | 1.610 | 1.379 | 1.354 | 1.379 | 1.610 | 1.610 | 2.306 | 2.306 | 1.310 |
| | 1.560 | 2.306 | 2.074 | 1.379 | 1.328 | 1.278 | 1.278 | 1.278 | 1.328 | 1.379 | 2.074 | 2.306 | 1.560 |
| | 1.808 | 2.306 | 1.379 | 1.303 | 1.278 | 1.278 | 1.278 | 1.278 | 1.278 | 1.303 | 1.379 | 2.306 | 1.808 |
| | 2.057 | 1.843 | 1.354 | 1.278 | 1.278 | 1.278 | 1.278 | 1.278 | 1.278 | 1.278 | 1.359 | 1.843 | 2.057 |
| | 2.306 | 1.943 | 1.354 | 1.278 | 1.278 | 1.278 | 1.278 | 1.278 | 1.278 | 1.278 | 1.359 | 1.843 | 2.306 |
| | 2.306 | 1.943 | 1.379 | 1.278 | 1.278 | 1.278 | 1.278 | 1.278 | 1.278 | 1.278 | 1.379 | 1.943 | 2.306 |
| | 2.306 | 2.306 | 1.997 | 1.354 | 1.303 | 1.278 | 1.278 | 1.278 | 1.303 | 1.354 | 1.997 | 2.306 | 2.306 |
| | 2.306 | 2.306 | 2.306 | 1.843 | 1.379 | 1.379 | 1.354 | 1.379 | 1.379 | 1.843 | 2.306 | 2.306 | 2.306 |
| | 2.306 | 2.306 | 2.306 | 2.306 | 2.306 | 2.306 | 2.074 | 2.306 | 2.306 | 2.306 | 2.306 | 2.306 | 2.306 |
| | 1.310 | 1.310 | 1.310 | 1.310 | 1.310 | 1.310 | 1.310 | 1.310 | 1.310 | 1.310 | 1.310 | 1.310 | 1.310 |
| r = R-L | 1.310 | 1.310 | 1.310 | 1.310 | 1.310 | 1.310 | 1.310 | 1.310 | 1.310 | 1.310 | 1.310 | 1.310 | 1.310 |

$\theta = \theta_T$

$R = 12.5"$

$L = 6.25"$

$\theta_T = 30.6^\circ$

$r_p = 9.607"$

$\theta_p = 15.3^\circ$

$R_B = 1.512"$

$t_B = 0.976"$

Pad dimensions - 25 in. O.D. x 12 1/2 in. I.D. 10 pad bearing

Figure A-5

PAD THICKNESS PROFILE

| r = R | | | | | | | | | | | | | |
|---|---|---|---|---|---|---|---|---|---|---|---|---|---|
| | 1.625 | 2.242 | 2.860 | 2.860 | 2.860 | 2.860 | 2.860 | 2.860 | 2.860 | 2.860 | 2.860 | 2.242 | 1.625 |
| | 1.625 | 2.551 | 2.860 | 2.860 | 2.860 | 2.860 | 2.860 | 2.860 | 2.860 | 2.860 | 2.860 | 2.551 | 1.625 |
| | 1.625 | 2.860 | 2.860 | 2.860 | 2.860 | 2.285 | 1.997 | 2.285 | 2.860 | 2.860 | 2.860 | 2.860 | 1.625 |
| | 1.934 | 2.860 | 2.860 | 2.860 | 2.285 | 1.679 | 1.616 | 1.679 | 2.285 | 2.860 | 2.860 | 2.860 | 1.934 |
| | 2.242 | 2.860 | 2.860 | 2.572 | 1.679 | 1.585 | 1.585 | 1.585 | 1.679 | 2.572 | 2.860 | 2.860 | 2.342 |
| | 2.551 | 2.860 | 2.860 | 2.285 | 1.616 | 1.585 | 1.585 | 1.585 | 1.616 | 2.285 | 2.860 | 2.860 | 2.551 |
| | 2.860 | 2.860 | 2.860 | 2.285 | 1.616 | 1.585 | 1.585 | 1.585 | 1.616 | 2.285 | 2.860 | 2.860 | 2.860 |
| | 2.860 | 2.860 | 2.860 | 2.285 | 1.616 | 1.585 | 1.585 | 1.585 | 1.616 | 2.285 | 2.860 | 2.860 | 2.860 |
| | 2.860 | 2.860 | 2.860 | 2.572 | 1.647 | 1.585 | 1.585 | 1.585 | 1.647 | 2.572 | 2.860 | 2.860 | 2.860 |
| | 2.860 | 2.860 | 2.860 | 2.860 | 1.997 | 1.679 | 1.647 | 1.679 | 1.997 | 2.860 | 2.860 | 2.860 | 2.860 |
| | 2.860 | 2.860 | 2.860 | 2.860 | 2.860 | 2.035 | 1.997 | 2.035 | 2.860 | 2.860 | 2.860 | 2.860 | 2.860 |
| | 1.625 | 1.625 | 1.625 | 1.625 | 1.625 | 1.625 | 1.625 | 1.625 | 1.625 | 1.625 | 1.625 | 1.625 | 1.625 |
| r = R-L | 1.625 | 1.625 | 1.625 | 1.625 | 1.625 | 1.625 | 1.625 | 1.625 | 1.625 | 1.625 | 1.625 | 1.625 | 1.625 |

θ =

$R = 15.500"$

$L = 7.750^{o}$

$\theta_T = 51^{o}$

$r_p = 11.661"$

$\theta_p = 25.5^{o}$

$R_B = 1.875"$

$t_B = 1.21"$

Pad dimensions - 31 O.D. x 15 1/2 in I.D. - 6 pad bearing

Figure A-6

PAD THICKNESS PROFILE

| r = R | | | | | | | | | | | | | |
|---|---|---|---|---|---|---|---|---|---|---|---|---|---|
| | 1.625 | 2.242 | 2.860 | 2.860 | 2.860 | 2.860 | 2.860 | 2.860 | 2.860 | 2.860 | 2.860 | 2.242 | 1.625 |
| | 1.625 | 2.551 | 2.860 | 2.860 | 2.860 | 2.860 | 2.860 | 2.860 | 2.860 | 2.860 | 2.860 | 2.551 | 1.625 |
| | 1.625 | 2.860 | 2.860 | 2.860 | 2.285 | 1.997 | 1.710 | 1.997 | 2.285 | 2.860 | 2.860 | 2.860 | 1.625 |
| | 1.934 | 2.860 | 2.860 | 2.285 | 1.679 | 1.616 | 1.585 | 1.616 | 1.679 | 2.285 | 2.860 | 2.860 | 1.934 |
| | 2.242 | 2.860 | 2.572 | 1.679 | 1.585 | 1.585 | 1.585 | 1.585 | 1.585 | 1.679 | 2.572 | 2.860 | 2.242 |
| | 2.551 | 2.860 | 2.285 | 1.647 | 1.585 | 1.585 | 1.585 | 1.585 | 1.585 | 1.647 | 2.285 | 2.860 | 2.551 |
| | 2.860 | 2.860 | 1.997 | 1.616 | 1.585 | 1.585 | 1.585 | 1.585 | 1.585 | 1.616 | 1.997 | 2.860 | 2.860 |
| | 2.860 | 2.860 | 2.285 | 1.647 | 1.585 | 1.585 | 1.585 | 1.585 | 1.585 | 1.647 | 2.285 | 2.860 | 2.860 |
| | 2.860 | 2.860 | 2.572 | 1.710 | 1.616 | 1.585 | 1.585 | 1.585 | 1.616 | 1.710 | 2.572 | 2.860 | 2.860 |
| | 2.860 | 2.860 | 2.860 | 2.572 | 1.710 | 1.679 | 1.679 | 1.679 | 1.710 | 2.572 | 2.860 | 2.860 | 2.860 |
| | 2.860 | 2.860 | 2.860 | 2.860 | 2.860 | 2.572 | 2.572 | 2.572 | 2.860 | 2.860 | 2.860 | 2.860 | 2.860 |
| | 1.625 | 1.625 | 1.625 | 1.625 | 1.625 | 1.625 | 1.625 | 1.625 | 1.625 | 1.625 | 1.625 | 1.625 | 1.625 |
| r = R-L | 1.625 | 1.625 | 1.625 | 1.625 | 1.625 | 1.625 | 1.625 | 1.625 | 1.625 | 1.625 | 1.625 | 1.625 | 1.625 |

$\theta = \theta_T$

$R = 15.500"$

$L = 7.750"$

$\theta_T = 38.25^\circ$

$r_p = 11.833"$

$\theta_p = 13.125^\circ$

$R_B = 1.875"$

$t_B = 1.210"$

Pad dimensions - 31 in. O.D. x 15 1/2 in. I.D. 8 pad bearing

Figure A-7

PAD THICKNESS PROFILE

r = R

| | | | | | | | | | | | | | |
|---|---|---|---|---|---|---|---|---|---|---|---|---|---|
| 1.625 | 2.242 | 2.860 | 2.860 | 2.860 | 2.860 | 2.860 | 2.860 | 2.860 | 2.860 | 2.860 | 2.242 | 1.625 |
| 1.625 | 2.551 | 2.860 | 2.860 | 2.860 | 2.860 | 2.572 | 2.860 | 2.860 | 2.860 | 2.860 | 2.551 | 1.625 |
| 1.625 | 2.860 | 2.860 | 1.997 | 1.997 | 1.710 | 1.679 | 1.710 | 1.997 | 1.997 | 2.860 | 2.860 | 1.625 |
| 1.934 | 2.860 | 2.572 | 1.710 | 1.647 | 1.585 | 1.585 | 1.585 | 1.647 | 1.710 | 2.572 | 2.860 | 1.934 |
| 2.242 | 2.860 | 1.710 | 1.616 | 1.585 | 1.585 | 1.585 | 1.585 | 1.585 | 1.616 | 1.710 | 2.860 | 2.242 |
| 2.551 | 2.285 | 1.679 | 1.585 | 1.585 | 1.585 | 1.585 | 1.585 | 1.585 | 1.585 | 1.679 | 2.285 | 2.551 |
| 2.860 | 2.285 | 1.679 | 1.585 | 1.585 | 1.585 | 1.585 | 1.585 | 1.585 | 1.585 | 1.679 | 2.285 | 2.860 |
| 2.860 | 2.285 | 1.710 | 1.585 | 1.585 | 1.585 | 1.585 | 1.585 | 1.585 | 1.585 | 1.710 | 2.285 | 2.860 |
| 2.860 | 2.860 | 1.997 | 1.679 | 1.616 | 1.585 | 1.585 | 1.585 | 1.616 | 1.679 | 1.997 | 2.860 | 2.860 |
| 2.860 | 2.860 | 2.860 | 2.285 | 1.710 | 1.710 | 1.679 | 1.710 | 1.710 | 2.285 | 2.860 | 2.860 | 2.860 |
| 2.860 | 2.860 | 2.860 | 2.860 | 2.860 | 2.860 | 2.572 | 2.860 | 2.860 | 2.860 | 2.860 | 2.860 | 2.860 |
| 1.625 | 1.625 | 1.625 | 1.625 | 1.625 | 1.625 | 1.625 | 1.625 | 1.625 | 1.625 | 1.625 | 1.625 | 1.625 |
| 1.625 | 1.625 | 1.625 | 1.625 | 1.625 | 1.625 | 1.625 | 1.625 | 1.625 | 1.625 | 1.625 | 1.625 | 1.625 |

r = R-L

θ = θ

$R$ = 15.500"

$L$ = 7.750"

$\theta_T$ = 30.6°

$r_p$ = 11.913"

$\theta_p$ = 15.3°

$R_B$ = 1.875"

$t_B$ = 1.21"

Pad dimensions - 31 in. O.D. x 15 1/2 in. I.D. 10 pad bearing

Figure A-8

PAD THICKNESS PROFILE

| r = R | | | | | | | | | | | | | |
|---|---|---|---|---|---|---|---|---|---|---|---|---|---|
| | 2.149 | 2.965 | 3.782 | 3.783 | 3.783 | 3.783 | 3.783 | .3783 | 3.783 | 3.783 | 3.783 | 2.965 | 2.149 |
| | 2.149 | 3.373 | 3.783 | 3.783 | 3.783 | 3.783 | 3.783 | 3.783 | 3.783 | 3.783 | 3.783 | 3.373 | 2.149 |
| | 2.149 | 3.783 | 3.783 | 3.783 | 3.783 | 3.022 | 2.641 | 3.022 | 3.783 | 3.783 | 3.783 | 3.783 | 2.149 |
| | 2.558 | 3.783 | 3.783 | 3.783 | 3.022 | 2.220 | 2.137 | 2.220 | 3.022 | 3.783 | 3.783 | 3.783 | 2.658 |
| | 2.965 | 3.783 | 3.783 | 3.401 | 2.220 | 2.096 | 2.096 | 2.096 | 2.220 | 3.401 | 3.783 | 3.783 | 2.965 |
| | 3.373 | 3.783 | 3.783 | 3.022 | 2.137 | 2.096 | 2.096 | 2.096 | 2.137 | 3.022 | 3.783 | 3.783 | 3.373 |
| | 3.783 | 3.783 | 3.783 | 3.022 | 2.137 | 2.096 | 2.096 | 2.096 | 2.137 | 3.022 | 3.783 | 3.783 | 3.783 |
| | 3.783 | 3.783 | 3.783 | 3.022 | 2.137 | 2.096 | 2.096 | 2.096 | 2.137 | 3.022 | 3.783 | 3.783 | 3.783 |
| | 3.783 | 3.783 | 3.783 | 3.401 | 2.178 | 2.096 | 2.096 | 2.096 | 2.178 | 3.401 | 3.783 | 3.783 | 3.783 |
| | 3.783 | 3.783 | 3.783 | 3.783 | 2.041 | 2.220 | 2.178 | 2.220 | 2.641 | 3.783 | 3.783 | 3.783 | 3.783 |
| | 3.783 | 3.783 | 3.783 | 3.783 | 3.783 | 3.022 | 2.641 | 3.022 | 3.783 | 3.783 | 3.783 | 3.783 | 3.783 |
| | 2.149 | 2.149 | 2.149 | 2.149 | 2.149 | 2.149 | 2.149 | 2.149 | 2.149 | 2.149 | 2.149 | 2.149 | 2.149 |
| r = R-L | 2.149 | 2.149 | 2.149 | 2.149 | 2.149 | 2.149 | 2.149 | 2.149 | 2.149 | 2.149 | 2.149 | 2.149 | 2.149 |

θ =

$R = 20.5"$

$L = 10.25"$

$\theta_T = 51^\circ$

$r_p = 15.423"$

$\theta_p = 25.5^\circ$

$R_B = 2.48"$

$t_B = 1.601"$

Pad dimensions - 41 in. O.D. x 20 1/2 in. I.D. 6 pad bearing

Figure A-9

PAD THICKNESS PROFILE

r = R

| | | | | | | | | | | | | |
|---|---|---|---|---|---|---|---|---|---|---|---|---|
| 2.149 | 2.965 | 3.783 | 3.783 | 3.783 | 3.783 | 3.783 | 3.783 | 3.783 | 3.783 | 3.783 | 2.965 | 2.149 |
| 2.149 | 3.373 | 3.783 | 3.783 | 3.783 | 3.783 | 3.783 | 3.783 | 3.783 | 3.783 | 3.783 | 3.373 | 2.149 |
| 2.149 | 3.783 | 3.783 | 3.783 | 3.022 | 2.641 | 2.262 | 2.641 | 3.022 | 3.783 | 3.783 | 3.783 | 2.149 |
| 2.558 | 3.783 | 3.783 | 3.022 | 2.220 | 2.137 | 2.096 | 2.137 | 2.220 | 3.022 | 3.783 | 3.783 | 2.558 |
| 2.965 | 3.783 | 3.401 | 2.220 | 2.096 | 2.096 | 2.096 | 2.096 | 2.096 | 2.220 | 3.401 | 3.783 | 2.965 |
| 3.373 | 3.783 | 3.022 | 2.178 | 2.096 | 2.096 | 2.096 | 2.096 | 2.096 | 2.178 | 3.022 | 3.783 | 3.373 |
| 3.783 | 3.783 | 2.641 | 2.137 | 2.096 | 2.096 | 2.096 | 2.096 | 2.096 | 2.137 | 2.641 | 3.783 | 3.783 |
| 3.783 | 3.783 | 3.022 | 2.178 | 2.096 | 2.096 | 2.096 | 2.096 | 2.096 | 2.178 | 3.022 | 3.783 | 3.783 |
| 3.783 | 3.783 | 3.401 | 2.262 | 2.137 | 2.096 | 2.096 | 2.096 | 2.137 | 2.262 | 3.401 | 3.783 | 3.783 |
| 3.783 | 3.783 | 3.783 | 3.401 | 2.262 | 2.220 | 2.220 | 2.220 | 2.262 | 3.401 | 3.783 | 3.783 | 3.783 |
| 3.783 | 3.783 | 3.783 | 3.783 | 3.783 | 3.401 | 3.401 | 3.401 | 3.783 | 3.783 | 3.783 | 3.783 | 3.783 |
| 2.149 | 2.149 | 2.149 | 2.149 | 2.149 | 2.149 | 2.149 | 2.149 | 2.149 | 2.149 | 2.149 | 2.149 | 2.149 |
| 2.149 | 2.149 | 2.149 | 2.149 | 2.149 | 2.149 | 2.149 | 2.149 | 2.149 | 2.149 | 2.149 | 2.149 | 2.149 |

r = R-L

θ = 0

R = 20.5"

L = 10.25"

$\theta_T$ = 38.25°

$r_p$ = 15.65"

$\theta_p$ = 19.125°

$R_B$ = 2.48"

$t_B$ = 1.601"

Pad dimensions - 41 in. O.D. x 20 1/2 in. I.D. 8 pad bearing

Figure A-10

PAD THICKNESS PROFILE

| r = R | | | | | | | | | | | | | |
|---|---|---|---|---|---|---|---|---|---|---|---|---|---|
| | 2.149 | 2.965 | 3.783 | 3.783 | 3.783 | 3.783 | 3.783 | 3.783 | 3.783 | 3.783 | 3.783 | 2.965 | 2.149 |
| | 2.149 | 3.374 | 3.783 | 3.783 | 3.783 | 3.783 | 3.401 | 3.783 | 3.783 | 3.783 | 3.783 | 3.374 | 2.149 |
| | 2.149 | 3.783 | 3.783 | 2.041 | 2.641 | 2.262 | 2.220 | 2.262 | 2.641 | 2.641 | 3.783 | 3.783 | 2.149 |
| | 2.558 | 3.783 | 3.401 | 2.262 | 2.178 | 2.096 | 2.096 | 2.096 | 2.178 | 2.262 | 3.401 | 3.783 | 2.558 |
| | 2.965 | 3.783 | 2.262 | 2.137 | 2.096 | 2.096 | 2.096 | 2.096 | 2.096 | 2.137 | 2.262 | 3.783 | 2.965 |
| | 3.373 | 3.022 | 2.220 | 2.096 | 2.096 | 2.096 | 2.096 | 2.096 | 2.096 | 2.096 | 2.220 | 3.022 | 3.373 |
| | 3.783 | 3.022 | 2.220 | 2.096 | 2.096 | 2.096 | 2.096 | 2.096 | 2.096 | 2.096 | 2.220 | 3.022 | 3.783 |
| | 3.783 | 3.022 | 2.226 | 2.096 | 2.096 | 2.096 | 2.096 | 2.096 | 2.096 | 2.096 | 2.262 | 3.022 | 3.783 |
| | 3.783 | 3.783 | 2.641 | 2.220 | 2.137 | 2.096 | 2.096 | 2.096 | 2.137 | 2.220 | 2.641 | 3.783 | 3.783 |
| | 3.783 | 3.783 | 3.783 | 3.022 | 2.262 | 2.262 | 2.220 | 2.262 | 2.262 | 3.022 | 3.783 | 3.783 | 3.783 |
| | 3.783 | 3.783 | 3.783 | 3.783 | 3.783 | 3.783 | 3.401 | 3.783 | 3.783 | 3.783 | 3.783 | 3.783 | 3.783 |
| | 2.149 | 2.149 | 2.149 | 2.149 | 2.149 | 2.149 | 2.149 | 2.149 | 2.149 | 2.149 | 2.149 | 2.149 | 2.149 |
| r = R-L | 2.149 | 2.149 | 2.149 | 2.149 | 2.149 | 2.149 | 2.149 | 2.149 | 2.149 | 2.149 | 2.149 | 2.149 | 2.149 |

$\theta = \theta_1$

$R$ = 20.5"

$L$ = 10.25"

$\theta_T$ = 30.6°

$r_p$ = 15.756"

$\theta_p$ = 15.3°

$R_B$ = 2.48"

$t_B$ = 1.601"

Pad dimensions - 41 In. O.D. x 20 1/2 in. I.D. 10 pad bearing

Figure A-11

PAD THICKNESS PROFILE

r = R

| | | | | | | | | | | | | | |
|---|---|---|---|---|---|---|---|---|---|---|---|---|---|
| 2.621 | 3.616 | 4.613 | 4.613 | 4.613 | 4.613 | 4.613 | 4.613 | 4.613 | 4.613 | 4.613 | 3.616 | 2.621 |
| 2.621 | 4.114 | 4.613 | 4.613 | 4.613 | 4.613 | 4.613 | 4.613 | 4.613 | 4.613 | 4.613 | 4.114 | 2.621 |
| 2.621 | 4.613 | 4.613 | 4.613 | 4.613 | 3.685 | 3.221 | 3.685 | 4.613 | 4.613 | 4.613 | 4.613 | 2.621 |
| 3.119 | 4.613 | 4.613 | 4.613 | 3.685 | 2.708 | 2.606 | 2.708 | 3.685 | 4.613 | 4.613 | 4.613 | 3.119 |
| 3.616 | 4.613 | 4.613 | 4.148 | 2.708 | 2.556 | 2.556 | 2.556 | 2.708 | 4.148 | 4.613 | 4.613 | 3.616 |
| 4.114 | 4.613 | 4.613 | 3.685 | 2.606 | 2.556 | 2.556 | 2.556 | 2.606 | 3.685 | 4.613 | 4.613 | 4.114 |
| 4.613 | 4.613 | 4.613 | 3.685 | 2.606 | 2.556 | 2.556 | 2.556 | 2.606 | 3.685 | 4.613 | 4.613 | 4.613 |
| 4.613 | 4.613 | 4.613 | 3.685 | 2.606 | 2.556 | 2.556 | 2.556 | 2.606 | 3.685 | 4.613 | 4.613 | 4.613 |
| 4.613 | 4.613 | 4.613 | 4.148 | 2.656 | 2.556 | 2.556 | 2.556 | 2.656 | 4.148 | 4.613 | 4.613 | 4.613 |
| 4.613 | 4.613 | 4.613 | 4.613 | 3.221 | 2.708 | 2.656 | 2.708 | 3.221 | 4.613 | 4.613 | 4.613 | 4.613 |
| 4.613 | 4.613 | 4.613 | 4.613 | 4.613 | 3.282 | 3.221 | 3.282 | 4.613 | 4.613 | 4.613 | 4.613 | 4.613 |
| 2.621 | 2.621 | 2.621 | 2.621 | 2.621 | 2.621 | 2.621 | 2.621 | 2.621 | 2.621 | 2.621 | 2.621 | 2.621 |
| 2.621 | 2.62. | 2.621 | 2.621 | 2.621 | 2.621 | 2.621 | 2.621 | 2.621 | 2.621 | 2.621 | 2.621 | 2.621 |

r = R-L

θ = 0

$R$ = 25"

$L$ = 12.5"

$\theta_T$ = 51°

$r_p$ = 18.808"

$\theta_p$ = 25.5°

$R_B$ = 3.024"

$t_B$ = 1.952"

Pad dimensions - 50 In. O.D. x 25 in .I.D. 8 pad bearing

Figure A-12

PAD THICKNESS PROFILE

| r = R | | | | | | | | | | | | | |
|---|---|---|---|---|---|---|---|---|---|---|---|---|---|
| | 2.621 | 3.616 | 4.613 | 4.613 | 4.613 | 4.613 | 4.613 | 4.613 | 4.613 | 4.613 | 4.613 | 3.616 | 2.621 |
| | 2.621 | 4.114 | 4.613 | 4.613 | 4.613 | 4.613 | 4.613 | 4.613 | 4.613 | 4.613 | 4.613 | 4.114 | 2.621 |
| | 2.621 | 4.613 | 4.613 | 4.613 | 3.685 | 3.221 | 2.758 | 3.221 | 3.685 | 4.613 | 4.613 | 4.613 | 2.621 |
| | 3.119 | 4.613 | 4.613 | 3.685 | 2.708 | 2.606 | 2.556 | 2.606 | 2.708 | 3.685 | 4.613 | 4.613 | 3.119 |
| | 3.616 | 4.613 | 4.148 | 2.708 | 2.556 | 2.556 | 2.556 | 2.556 | 2.556 | 2.708 | 4.148 | 4.613 | 3.616 |
| | 4.114 | 4.613 | 4.685 | 2.656 | 2.556 | 2.556 | 2.556 | 2.556 | 2.556 | 2.656 | 3.685 | 4.613 | 4.114 |
| | 4.613 | 4.613 | 3.221 | 2.606 | 2.556 | 2.556 | 2.556 | 2.556 | 2.556 | 2.606 | 3.221 | 4.613 | 4.613 |
| | 4.613 | 4.613 | 3.685 | 2.656 | 2.556 | 2.556 | 2.556 | 2.556 | 2.556 | 2.656 | 3.685 | 4.613 | 4.613 |
| | 4.613 | 4.613 | 4.148 | 2.758 | 2.606 | 2.556 | 2.556 | 2.556 | 2.606 | 2.758 | 4.148 | 4.613 | 4.613 |
| | 4.613 | 4.613 | 4.613 | 4.148 | 2.758 | 2.708 | 2.708 | 2.708 | 2.758 | 4.148 | 4.613 | 4.613 | 4.613 |
| | 4.613 | 4.613 | 4.613 | 4.613 | 4.613 | 4.148 | 4.148 | 4.148 | 4.613 | 4.613 | 4.613 | 4.613 | 4.613 |
| | 2.621 | 2.621 | 2.621 | 2.621 | 2.621 | 2.621 | 2.621 | 2.621 | 2.621 | 2.621 | 2.621 | 2.621 | 2.621 |
| r = R-L | 2.621 | 2.621 | 2.621 | 2.621 | 2.621 | 2.621 | 2.621 | 2.621 | 2.621 | 2.621 | 2.621 | 2.621 | 2.621 |

θ = θ

R = 25"

L = 12.5"

$\theta_T$ = 38.25°

$r_p$ = 19.085"

$\theta_p$ = 19.125°

$R_B$ = 3.024"

$t_B$ = 1.952"

Pad dimensions - 50 in. O.D. x 25 in. I.D. 6 pad bearing.

Figure A-13

PAD THICKNESS PROFILE

r = R

| | | | | | | | | | | | | | |
|---|---|---|---|---|---|---|---|---|---|---|---|---|---|
| 2.621 | 3.616 | 4.613 | 4.613 | 4.613 | 4.613 | 4.613 | 4.613 | 4.613 | 4.613 | 4.613 | 3.616 | 2.621 |
| 2.621 | 4.115 | 4.613 | 4.613 | 4.613 | 4.613 | 4.148 | 4.613 | 4.613 | 4.613 | 4.613 | 4.115 | 2.621 |
| 2.621 | 4.613 | 4.613 | 3.221 | 3.221 | 2.758 | 2.708 | 2.758 | 3.221 | 3.221 | 4.613 | 4.613 | 2.621 |
| 3.119 | 4.613 | 4.148 | 2.758 | 2.656 | 2.556 | 2.556 | 2.556 | 2.656 | 2.758 | 4.148 | 4.613 | 3.119 |
| 3.616 | 4.613 | 2.758 | 2.606 | 2.556 | 2.556 | 2.556 | 2.556 | 2.556 | 2.606 | 2.758 | 4.613 | 3.616 |
| 4.115 | 3.685 | 2.708 | 2.556 | 2.556 | 2.556 | 2.556 | 2.556 | 2.556 | 2.556 | 2.708 | 3.685 | 4.115 |
| 4.613 | 3.685 | 2.708 | 2.556 | 2.556 | 2.556 | 2.556 | 2.556 | 2.556 | 2.556 | 2.708 | 3.685 | 4.613 |
| 4.613 | 3.685 | 2.758 | 2.556 | 2.556 | 2.556 | 2.556 | 2.556 | 2.556 | 2.556 | 2.758 | 3.685 | 4.613 |
| 4.613 | 4.613 | 3.221 | 2.708 | 2.606 | 2.056 | 2.556 | 2.556 | 2.606 | 2.708 | 3.221 | 4.613 | 4.613 |
| 4.613 | 4.613 | 4.613 | 3.685 | 2.758 | 2.758 | 21708 | 2.758 | 2.758 | 3.685 | 4.613 | 4.613 | 4.613 |
| 4.613 | 4.613 | 4.613 | 4.613 | 4.613 | 4.613 | 4.148 | 4.613 | 4.613 | 4.613 | 4.613 | 4.613 | 4.613 |
| 2.621 | 2.621 | 2.621 | 2.621 | 2.621 | 2.621 | 2.621 | 2.621 | 2.621 | 2.621 | 2.621 | 2.621 | 2.621 |
| 2.621 | 2.621 | 2.621 | 2.621 | 2.621 | 2.621 | 2.621 | 2.621 | 2.621 | 2.621 | 2.621 | 2.621 | 2.621 |

r = R-L

θ = 0

R = 25"

L = 12.5"

$\theta_T$ = 30.6°

$r_p$ = 19.215"

$\theta_p$ = 30.6°

$R_B$ = 3.024"

$t_B$ = 1.952"

Pad dimensions - 50 in. O.D. x 25 in.I.D.10 pad bearing

Figure A-14

PAD THICKNESS PROFILE

| r = R | | | | | | | | | | | | | |
|---|---|---|---|---|---|---|---|---|---|---|---|---|---|
| | 1.312 | 1.700 | 2.250 | 2.250 | 2.250 | 2.250 | 2.250 | 2.250 | 2.250 | 2.250 | 2.250 | 1.700 | 1.312 |
| | 1.312 | 1.875 | 2.200 | 2.250 | 2.250 | 2.200 | 2.030 | 2.200 | 2.250 | 2.250 | 2.250 | 1.875 | 1.312 |
| | 1.312 | 2.150 | 2.250 | 2.250 | 1.850 | 1.300 | 1.250 | 1.500 | 1.850 | 2.250 | 2.250 | 2.150 | 1.312 |
| | 1.400 | 2.250 | 2.250 | 1.850 | 1.250 | 1.250 | 1.250 | 1.250 | 1.250 | 1.850 | 2.250 | 2.250 | 1.400 |
| | 1.600 | 2.250 | 2.200 | 1.350 | 1.250 | 1.200 | 1.175 | 1.200 | 1.250 | 1.350 | 2.200 | 2.250 | 1.600 |
| | 1.875 | 2.250 | 1.950 | 1.250 | 1.250 | 1.137 | 0.906 | 1.137 | 1.250 | 1.250 | 1.950 | 2.250 | 1.875 |
| | 2.150 | 2.250 | 1.850 | 1.250 | 1.250 | 1.062 | 0.775 | 1.062 | 1.250 | 1.250 | 1.850 | 2.250 | 2.150 |
| | 2.250 | 2.250 | 1.950 | 1.250 | 1.250 | 1.175 | 1.062 | 1.175 | 1.250 | 1.250 | 1.950 | 2.250 | 2.250 |
| | 2.250 | 2.250 | 2.150 | 1.260 | 1.250 | 1.250 | 1.250 | 1.250 | 1.250 | 1.260 | 2.150 | 2.250 | 2.250 |
| | 2.250 | 2.250 | 2.250 | 1.850 | 1.250 | 1.250 | 1.250 | 1.250 | 1.250 | 1.850 | 2.250 | 2.250 | 2.250 |
| | 2.250 | 2.250 | 2.250 | 2.250 | 1.950 | 1.750 | 1.650 | 1.750 | 1.950 | 2.250 | 2.250 | 2.250 | 2.250 |
| | 1.885 | 1.885 | 1.885 | 1.885 | 1.885 | 1.885 | 1.885 | 1.885 | 1.885 | 1.885 | 1.885 | 1.885 | 1.885 |
| r = R-L | 0.937 | 0.937 | 0.937 | 0.937 | 0.937 | 0.937 | 0.937 | 0.937 | 0.937 | 0.937 | 0.937 | 0.937 | 0.937 |

θ =

R = 15.5"

L = 7.254"

$\theta_T$ = 38.25°

$r_p$ = 12"

$\theta_p$ = 19.125°

$R_B$ = 1.875"

$t_B$ = 1.210"

Pad dimensions - 31 in. O.D. x 16 1/2 in. I.D. Ahead Bearing of DD 933

Figure A-15

PAD THICKNESS PROFILE

| r = R | | | | | | | | | | | | | |
|---|---|---|---|---|---|---|---|---|---|---|---|---|---|
| | 0.688 | 1.250 | 1.438 | 1.438 | 1.438 | 1.438 | 1.438 | 1.438 | 1.438 | 1.438 | 1.438 | 1.250 | 0.688 |
| | 0.688 | 1.438 | 1.438 | 1.438 | 1.438 | 0.969 | 0.969 | 0.969 | 1.438 | 1.438 | 1.438 | 1.438 | 0.688 |
| | 0.688 | 1.438 | 1.438 | 1.438 | 0.813 | 0.813 | 0.797 | 0.813 | 0.813 | 1.438 | 1.438 | 1.438 | 0.688 |
| | 0.875 | 1.438 | 1.438 | 0.969 | 0.797 | 0.750 | 0.750 | 0.750 | 0.797 | 0.969 | 1.438 | 1.438 | 0.875 |
| | 1.063 | 1.438 | 1.282 | 0.813 | 0.766 | 0.750 | 0.750 | 0.750 | 0.766 | 0.813 | 1.282 | 1.438 | 1.063 |
| | 1.063 | 1.438 | 1.123 | 0.797 | 0.750 | 0.750 | 0.750 | 0.750 | 0.750 | 0.797 | 1.123 | 1.438 | 1.063 |
| | 1.250 | 1.438 | 1.123 | 0.782 | 0.750 | 0.750 | 0.750 | 0.750 | 0.750 | 0.782 | 1.123 | 1.438 | 1.250 |
| | 1.438 | 1.438 | 1.123 | 0.782 | 0.750 | 0.750 | 0.750 | 0.750 | 0.750 | 0.782 | 1.123 | 1.438 | 1.438 |
| | 1.438 | 1.438 | 1.123 | 0.797 | 0.750 | 0.750 | 0.750 | 0.750 | 0.750 | 0.797 | 1.123 | 1.438 | 1.438 |
| | 1.438 | 1.438 | 1.282 | 0.813 | 0.766 | 0.750 | 0.750 | 0.750 | 0.766 | 0.813 | 1.282 | 1.438 | 1.438 |
| | 1.438 | 1.438 | 1.438 | 1.123 | 0.813 | 0.797 | 0.766 | 0.797 | 0.813 | 1.123 | 1.438 | 1.438 | 1.438 |
| | 1.438 | 1.438 | 1.438 | 1.438 | 1.123 | 0.813 | 0.813 | 0.813 | 1.123 | 1.438 | 1.438 | 1.438 | 1.438 |
| r = R-L | 1.438 | 1.438 | 1.438 | 1.438 | 1.438 | 1.438 | 1.438 | 1.438 | 1.438 | 1.438 | 1.438 | 1.438 | 1.438 |

$\theta = \theta_T$

$R$ = 13"

$L$ = 4.25"

$\theta_T$ = 29°

$r_p$ = 10.875"

$\theta_p$ = 14.5°

$R_B$ = 1.715"

$t_B$ = 0.625"

Pad dimensions - 26 in. O.D. x 17 3/4 in. I.D. - Astern Bearing of DD 933

Figure A-16

PAD THICKNESS PROFILE

r = R

| | | | | | | | | | | | | |
|---|---|---|---|---|---|---|---|---|---|---|---|---|
| 1.324 | 1.827 | 2.331 | 2.331 | 2.331 | 2.331 | 2.331 | 2.331 | 2.331 | 2.331 | 2.331 | 1.827 | 1.324 |
| 1.324 | 2.079 | 2.331 | 2.331 | 2.331 | 2.331 | 2.331 | 2.331 | 2.331 | 2.331 | 2.331 | 2.079 | 1.324 |
| 1.324 | 2.331 | 2.331 | 2.331 | 1.862 | 1.628 | 1.394 | 1.628 | 1.862 | 2.331 | 2.331 | 2.331 | 1.324 |
| 1.576 | 2.331 | 2.331 | 1.862 | 1.368 | 1.317 | 1.292 | 1.317 | 1.368 | 1.862 | 2.331 | 2.331 | 1.576 |
| 1.827 | 2.331 | 2.096 | 1.368 | 1.292 | 1.292 | 1.292 | 1.292 | 1.292 | 1.368 | 2.096 | 2.331 | 1.827 |
| 2.079 | 2.331 | 1.862 | 1.342 | 1.292 | 1.292 | 1.292 | 1.292 | 1.292 | 1.342 | 1.862 | 2.331 | 2.079 |
| 2.331 | 2.331 | 1.628 | 1.317 | 1.292 | 1.292 | 1.292 | 1.292 | 1.292 | 1.317 | 1.628 | 2.331 | 2.331 |
| 2.331 | 2.331 | 1.862 | 1.342 | 1.292 | 1.292 | 1.292 | 1.292 | 1.292 | 1.342 | 1.862 | 2.331 | 2.331 |
| 2.331 | 2.331 | 2.096 | 1.394 | 1.317 | 1.317 | 1.292 | 1.317 | 1.317 | 1.394 | 2.096 | 2.331 | 2.331 |
| 2.331 | 2.331 | 2.331 | 2.096 | 1.394 | 1.368 | 1.292 | 1.394 | 1.394 | 2.096 | 2.331 | 2.331 | 2.331 |
| 2.331 | 2.331 | 2.331 | 2.331 | 2.331 | 2.096 | 2.096 | 2.096 | 2.331 | 2.331 | 2.331 | 2.331 | 2.331 |
| 1.324 | 1.324 | 1.324 | 1.324 | 1.324 | 1.324 | 1.324 | 1.324 | 1.324 | 1.324 | 1.324 | 1.324 | 1.324 |
| 1.324 | 1.324 | 1.324 | 1.324 | 1.324 | 1.324 | 1.324 | 1.324 | 1.324 | 1.324 | 1.324 | 1.324 | 1.324 |

r = R-L

θ =

R = 15.5"

L = 7.75"

$\theta_T$ = 38.25"

$r_p$ = 11.833"

$\theta_p$ = 19.125°

$R_B$ = 1.875"

$t_B$ = 1.020"

Pad dimensions - 31 in.O.D. x 15 1/2 in.I.D. - 8 pad bearing

Figure A-17

$\left(\frac{t}{t_{std}} = 0.7\right)$

PAD THICKNESS PROFILE

r = R

| | | | | | | | | | | | | |
|---|---|---|---|---|---|---|---|---|---|---|---|---|
| 1.982 | 2.735 | 3.489 | 3.489 | 3.489 | 3.489 | 3.489 | 3.489 | 3.489 | 3.489 | 3.489 | 2.735 | 1.982 |
| 1.982 | 3.112 | 3.489 | 3.489 | 3.489 | 3.489 | 3.489 | 3.489 | 3.489 | 3.489 | 3.489 | 3.112 | 1.982 |
| 1.982 | 3.489 | 3.489 | 3.489 | 2.788 | 2.436 | 2.086 | 2.436 | 2.788 | 3.489 | 3.489 | 3.489 | 1.982 |
| 2.359 | 3.489 | 3.489 | 2.788 | 2.048 | 1.972 | 1.934 | 1.972 | 2.048 | 2.788 | 3.489 | 3.489 | 2.359 |
| 2.735 | 3.489 | 3.138 | 2.048 | 1.934 | 1.934 | 1.934 | 1.934 | 1.934 | 2.048 | 3.138 | 3.489 | 2.735 |
| 3.112 | 3.489 | 2.788 | 2.009 | 1.934 | 1.934 | 1.934 | 1.934 | 1.934 | 2.009 | 2.788 | 3.489 | 3.112 |
| 3.489 | 3.489 | 2.436 | 1.972 | 1.934 | 1.934 | 1.934 | 1.934 | 1.934 | 1.972 | 2.436 | 3.489 | 3.489 |
| 3.489 | 3.489 | 2.788 | 2.009 | 1.934 | 1.934 | 1.934 | 1.934 | 1.934 | 2.009 | 2.788 | 3.489 | 3.489 |
| 3.489 | 3.489 | 3.138 | 2.086 | 1.972 | 1.934 | 1.934 | 1.934 | 1.972 | 2.086 | 3.138 | 3.489 | 3.489 |
| 3.489 | 3.489 | 3.489 | 3.138 | 2.086 | 2.048 | 2.048 | 2.048 | 2.086 | 3.138 | 3.489 | 3.489 | 3.489 |
| 3.489 | 3.489 | 3.489 | 3.489 | 3.489 | 3.138 | 3.138 | 3.138 | 3.489 | 3.489 | 3.489 | 3.489 | 3.489 |
| 1.982 | 1.982 | 1.982 | 1.982 | 1.982 | 1.982 | 1.982 | 1.982 | 1.982 | 1.982 | 1.982 | 1.982 | 1.982 |
| 1.982 | 1.982 | 1.982 | 1.982 | 1.982 | 1.982 | 1.982 | 1.982 | 1.982 | 1.982 | 1.982 | 1.982 | 1.982 |

r = R-L

$\theta = 0$

$R = 15.5"$

$L = 7.75"$

$\theta_T = 38.25^\circ$

$r_p = 11.833"$

$\theta_p = 19.125^\circ$

$R_B = 1.875"$

$t_B = 1.517"$

Pad dimensions - 31 in. O.D. x 15 1/2 in. I.D. 8 pad bearing

Figure A-18

$\left( \frac{t}{t_{std}} = 1.3 \right)$

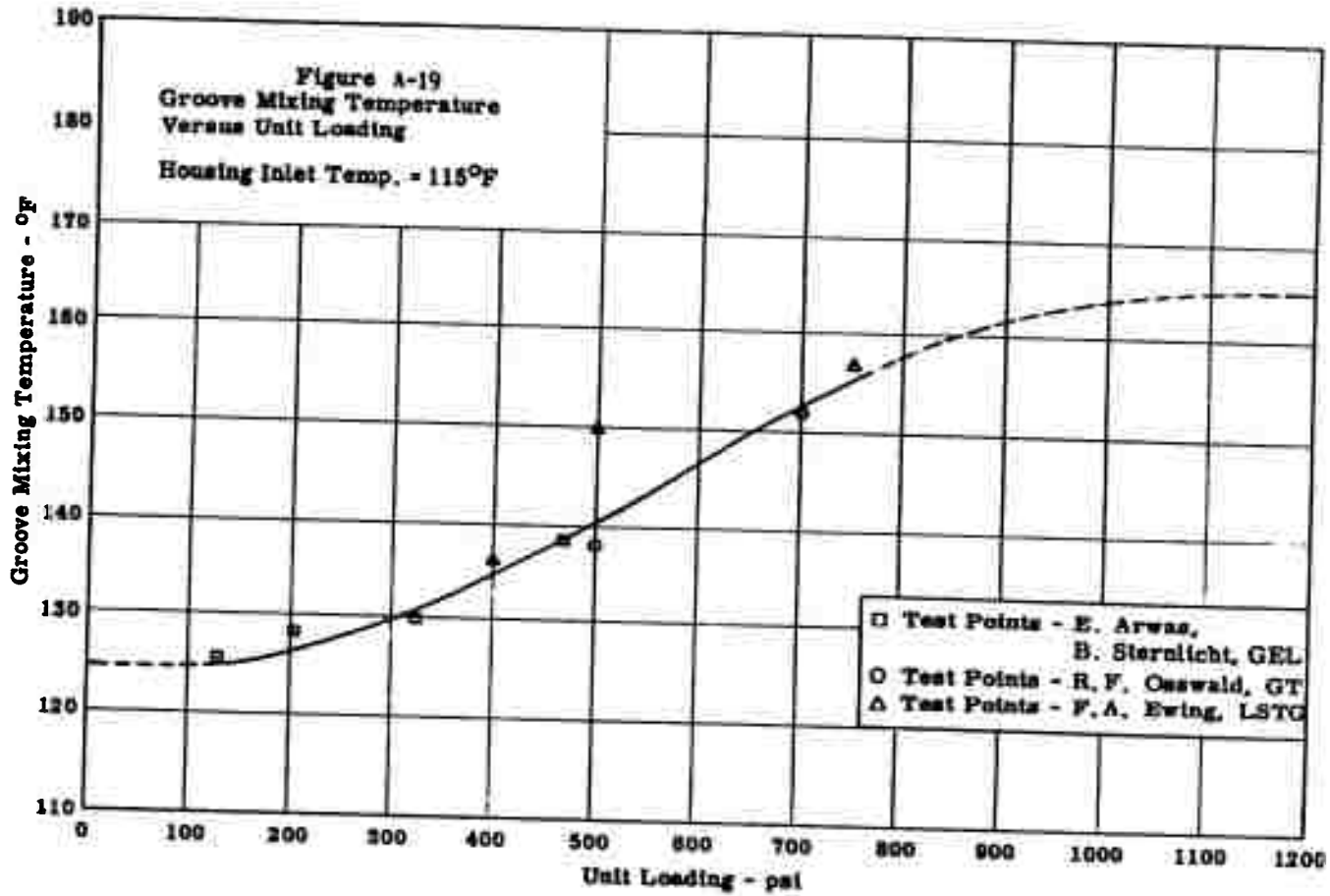
Figure A-19
Groove Mixing Temperature
Versus Unit Loading
Housing Inlet Temp. = 115°F
Groove Mixing Temperature - °F
190
180
170
160
150
140
130
120
110
0
100
200
300
400
500
600
700
800
900
1000
1100
1200
Unit Loading - psi
□ Test Points - E. Arwas, B. Sternlicht, GEL
○ Test Points - R. F. Oswald, GT
△ Test Points - F. A. Ewing, LSTG

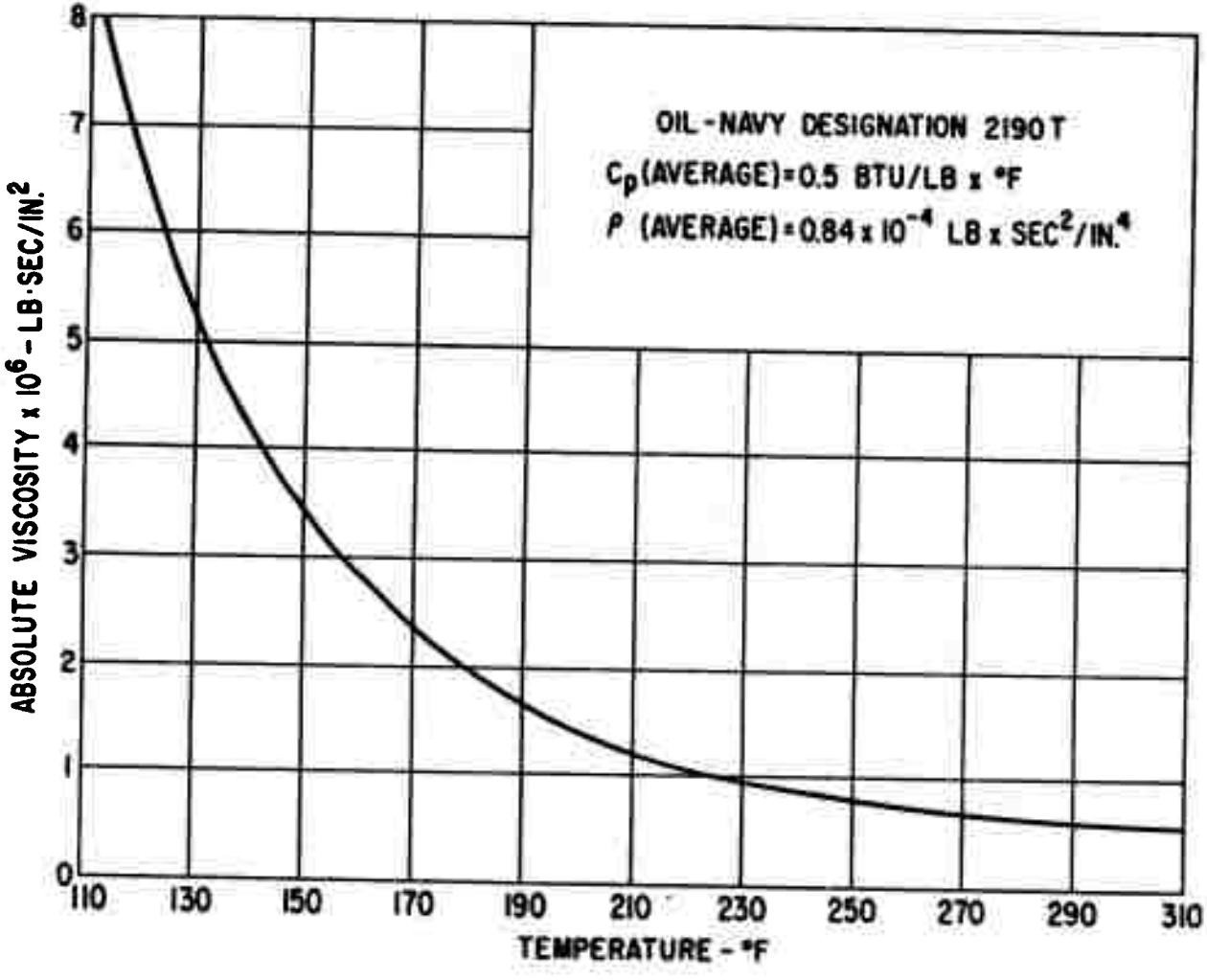


PROPERTIES OF 2190T OIL

## SYMBOLS

| | | |
|---|---|---|
| $A_i, A_j$ | Deflection coefficients (see Eqs. A-1, A-18) | inches |
| $B_{avg}$ | Average circumferential pad length = 1/2 (D-L)$\theta_{TOT}$ | inches |
| $C_p$ | Specific heat | BTU/lb.x$^{\circ}$F |
| D | Flexural rigidity = $\frac{Et^3}{12(1-\nu^2)}$ | lb. in. |
| E | Elastic modulus | psi |
| e | Deflection derivative (see Eq. A-11) | inches$^{-1}$ |
| f | Deflection functions (see Eqs. A-1, A-18, A-31) | |
| g | Deflection derivative (see Eq. A-10) | inches$^{-1}$ |
| h | Film thickness | inches |
| $h_{min}$ | Minimum film thickness | inches |
| $I_{i,j}, \bar{I}_{i,j}$ | Set of deflection coefficients comprising matrices | |
| J | Mechanical equivalent of thermal energy (=9339 in. lbs/BTU) | |
| $J_{i,j}$ | Inverse of $I_{i,j}$ matrix | |
| $K_j, \bar{K}_j$ | Set of deflection coefficients comprising matrices | |
| k | Deflection derivative (see Eq. A-12) | inches$^{-1}$ |
| L | Radial length of pad | inches |
| $M_x, M_y$ | Edge bending moments per unit length | in. lbs/in |
| m | Deflection modes (see e.g. Eq. A-4) | |
| $m_x, m_y$ | Internal bending moments per unit length | in. lbs/in |
| $m_\theta$ | circumferential inclination of pad | inches/inch |
| $m_r$ | radial inclination of pad | inches/inch |
| N | Speed of rotation | RPS |
| n | Deflection modes (see e.g. Eq. A-4) | |
| P | Pressure differential across pad | psi |
| p | Unit loading | psi |
| $p_{avg}$ | Average unit loading | psi |
| Q | Hydrodynamic oil flow per pad | gpm |
| $q_r$ | Surface temperature gradient, radially | $^{\circ}$F/inch |
| $q_\theta$ | Surface temperature gradient, circumferentially | $^{\circ}$F/radian |
| R | Outside radius of pad | inches |

## SYMBOLS - Cont'd.

| | | |
|---|---|---|
| $R_B$ | Radius of support ring | inches |
| $r$ | Radial coordinate | inches |
| $r_c$ | Radial coordinate (see Fig. A-1) | inches |
| $r_o$ | Radius of support pad (see Fig. A-1) | inches |
| $r_p$ | Radial coordinate of pivot | inches |
| $r_p\%$ | Radial coordinate of pivot = $100\left[r_p - (R-L)\right] / L$ | inches |
| $s$ | Deflection modes (see e.g. Eq. A-3) | |
| $T$ | Temperature | $^\circ F$ |
| $T_{avg}$ | Average film temperature | $^\circ F$ |
| $T_{GR}$ | Groove mixing temperature | $^\circ F$ |
| $T_{max}$ | Maximum film temperature | $^\circ F$ |
| $t$ | Pad thickness | inches |
| $t_B$ | Thickness of support ring | inches |
| $U_{avg}$ | Average surface velocity = $\pi(D-L)\,N$ | inches |
| $V$ | Energy of bending | lb. inches |
| $V_{sp}$ | Energy of bending of support plate | lb. inches |
| $V_p$ | Energy of bending of pad | lb. inches |
| $W$ | Potential energy associated with load | lb. inches |
| $W_p$ | Potential energy associated with pressure loading | lb. inches |
| $W_T$ | Potential energy associated with equivalent temperature loading | lb. inches |
| $w$ | Elastic deflection | inches |
| $w_o$ | Deflection of rim of support plate | inches |
| $\alpha$ | Linear coefficient of thermal expansion | $1/^\circ F$ |
| $\delta$ | Increment | |
| $\Delta T$ | Temperature difference across pad | $^\circ F$ |
| $\theta$ | Angular coordinate | radians |
| $\theta_p$ | Angular coordinate of pivot | radians |
| $\theta_p\%$ | Angular coordinate of pivot = $100\,(\theta_p/\theta_T)$ | radians |
| $\theta_{TOT}$ | Pad subtended angle | radians |
| $\mu$ | Absolute viscosity | lb. sec/in$^2$ |
| $\nu$ | Poisson's Ratio | |
| $\phi_c$ | Angular coordinate (see Fig. A-1) | radians |
| $\omega$ | Angular velocity | radians/sec. |

GENERAL ELECTRIC

**General Engineering Laboratory**

SCHENECTADY, NEW YORK

## TECHNICAL INFORMATION SERIES

| AUTHOR | SUBJECT CLASSIFICATION | NO. 60GL181 |
|---|---|---|
| E.B. Arwas<br>B. Sternlicht | Thrust Bearings | DATE 8/1/60 |

TITLE

Propeller Shaft Thrust Bearing Analysis - Phase II

ABSTRACT A new method of performance analysis of tilting pad thrust brgs. is presented in which the temperature distribution in the fluid film, & the pressure & temperature induced pad deflections are considered. The method consists of simultaneous, numerical integration of the Reynolds, Energy, & Elasticity Eqs. Calculation results and charts are presented covering the size & speed ranges of present propeller shaft practice. The influence of temperature and the effect of varying pad geometry are discussed.

| G.E. CLASS I | REPRODUCIBLE COPY FILED AT LIBRARY OF GENERAL ENGINEERING LABORATORY SCHENECTADY, NEW YORK | NO. PAGES 105 |
|---|---|---|
| GOV. CLASS. None | | |

CONCLUSIONS

1. Elastic deflections of tilting pads are several times the minimum film thickness. Thermal deflections are of the same order as those due to load. These deflections seriously affect bearing performance under heavy loads and should, therefore, be included in the analysis.

2. The maximum temperature reached in the lubricant film differs drastically from the average film and the average outlet temperatures. The slope of the maximum film temperature vs. unit load curve, rises sharply at high loads so that heavily loaded bearings have little margin of safety.

3. Accurate determination of minimum film thickness is theoretically possible from measurements of the maximum film and groove temperatures. This method offers greater accuracy than present direct film thickness indicators.

INFORMATION PREPARED FOR Medium Steam Turbine Generator and Gear Department

TESTS MADE BY

AUTHOR E.B. Arwas B. Sternlicht

COUNTERSIGNED

COMPONENT Bearing and Lubrication Engineering

GL-16-C